

Dissertation zur Erlangung des Doktorgrades  
der Fakultät für Chemie und Pharmazie der  
Ludwig-Maximilians-Universität München



## **Lipid-based delivery system for chemically modified mRNA**

Anita Jarzębińska

09.10.1989

aus Szczecin, Polen

2017

## Erklärung

Diese Dissertation wurde im Sinne von § 7 der Promotionsordnung vom 28. November 2011 von Herrn PD Dr. Carsten Rudolph betreut und von Herrn Prof. Dr. Ernst Wagner von der Fakultät für Chemie und Pharmazie vertreten.

## Eidesstattliche Versicherung

Diese Dissertation wurde eigenständig und ohne unerlaubte Hilfe erarbeitet.

München, 11.06.2017

.....

Anita Jarzębińska

Dissertation eingereicht am 03.03.2017

1. Gutachterin / 1. Gutachter: Prof. Dr. Ernst Wagner
2. Gutachterin / 2. Gutachter: PD Dr. Carsten Rudolph

Mündliche Prüfung am 16.05.2017

*“The mind is the most powerful weapon that I have.”*

Hanshi Zenpo Shimabukuro

## Table of contents

<b>1 Introduction</b>	<b>1</b>
1.1 Messenger RNA (mRNA)	1
1.2 Chemically modified mRNA and transcript therapies	2
1.3 Delivery challenge in transcript therapies	3
1.4 Cellular uptake and endosomal escape	3
1.5 mRNA delivery systems	4
1.5.1 Polymers	5
1.5.2 Lipids	7
1.6 Lipid nanoparticles as a multicomponent system	8
1.6.1 Cationic lipids	8
1.6.2 The role of helper lipids	10
1.6.3 PEG coating	11
1.6.4 Targeting ligands	12
1.7 Aim of the thesis	13
<b>2 Materials and Methods</b>	<b>15</b>
2.1 Materials	15
2.1.1 Solvents and chemicals	15
2.1.3 Lipids	15
2.1.4 Chemically modified mRNA	16
2.1.5 Cell culture	17
2.2 Methods	18
2.2.1 Synthesis of lipidoids	18
2.2.2 Complex formation and physicochemical characterization	18
2.2.3 <i>In vitro</i> methods	21
	I

2.2.4 Animal studies	25
2.2.5 Statistical analysis	26
<b>3 Results</b>	<b>27</b>
3.1 Lipidoids	27
3.1.1 Oligoalkylamine-based backbone	28
3.1.2 Oligoalkylamine-based dendrimers	37
3.1.3 Alkyl chain length of lipidoids	39
3.2 Helper lipids	40
3.2.1 Phospholipid type	40
3.2.2 Phospholipid alkyl chain length and saturation	42
3.2.3 Variations in the lipid composition	44
3.3 The importance of a PEG-lipid in lipoplex shielding	47
3.3.1 PEG lipid type and anchor chain saturation	47
3.3.2 Anchor chain length in a PEG-lipid	49
3.3.3 PEG length	50
3.3.4 PEG-lipid density	51
3.4 Coupled dependences between the lipids	56
3.4.1 Multicomponent system interactions	56
3.4.2 Nitrogen to phosphate ratio	62
3.5 Formulation conditions	63
3.5.1 Further condensation of mRNA by non-lipidic, cationic agents	63
3.5.2 Impact of formulation pH on the mRNA binding	64
3.6 mRNA release assay	65
3.7 Targeted delivery with folic acid	71
3.7.1 Folate targeting <i>in vitro</i>	72
3.7.2 Folate targeting <i>in vivo</i>	73

<b>4 Discussion</b>	<b>75</b>
4.1 Lipidoids	75
4.2 Helper lipids	78
4.3 The importance of a PEG-lipid in lipoplex shielding	79
4.4 Coupled dependences between the lipids	80
4.5 Formulation conditions	84
4.6 mRNA release assay	84
4.7 Targeted delivery with folic acid	85
<b>5 Summary</b>	<b>88</b>
<b>6 References</b>	<b>91</b>
<b>7 Appendix</b>	<b>97</b>
7.1 Abbreviations	97
7.2 List of lipid-based formulations	99
7.3 Publications	105
<b>8 Acknowledgements</b>	<b>106</b>

### 1 Introduction

According to the National Human Genome Research Institute,<sup>[1]</sup> there are known over 6000 disorders, e.g. cystic fibrosis, sickle-cell anemia, and Huntington's disease, which are classified as genetic diseases. On the example of cystic fibrosis, which is one of the most frequent fatal inherited diseases having its onset in childhood:<sup>[2]</sup> about 30 000 people in the United States suffer from the disease, caused by mutations in a single gene - the Cystic Fibrosis Transmembrane Regulator (CFTR) gene. Whereas most treatments still focus on alleviating the symptoms of a disease, the greatest hopes are pinned on gene therapies. Gene therapy is a treatment method working on a gene level: replacement of missing or defective genes with correct ones, inactivating a mutated gene, or introducing a new gene. Although in 2015 there were 167 gene therapy clinical trials approved worldwide,<sup>[3]</sup> the technique evokes many safety and efficiency concerns. Introducing genes to the cells is challenging and may bear risks for many reasons: DNA has to be transported into the nucleus; can integrate into the genome, causing insertional mutagenesis; and the resulting expression is enduring with only limited control.

#### 1.1 Messenger RNA (mRNA)

In the process of protein expression from a gene, an important role is played by an intermediate molecule, namely messenger RNA (mRNA). The information about certain genes (proteins) stored in DNA is replicated to a single-stranded mRNA in the transcription process. In eukaryotic cells, the transcript is produced by three different types of RNA polymerase<sup>[4]</sup> and, after processing including the addition of a 5' cap and poly-A tail at the 3' end as well as splicing, the mature, single-stranded transcript is transported to the cytoplasm. Then the biological protein synthesis takes place, using the information in mRNA as a template. This process (translation) occurs in molecular machineries called ribosomes with the participation of ribosomal RNA (rRNA) and transfer RNA (tRNA). When its role is fulfilled, mRNA is degraded, which allows the cells to control the protein synthesis level. Eukaryotic mRNAs' half-lives range from several minutes to several days.<sup>[5]</sup>

Influencing the protein production process from the transcript level opens a completely new possibility to treat gene disorders with benefits of: avoiding the risk of insertional mutagenesis, the necessity to deliver the nucleic acid to the cytoplasm only, and the transient translation of proteins produced in the patient's cells.

### 1.2 Chemically modified mRNA and transcript therapies

The greatest obstacles on the way from mRNA discovery to its therapeutic application have so far been the molecule's limited stability and strong immunogenicity.<sup>[6]</sup> As it has been described, these limits could be overcome by simple nucleoside modifications, which suppress the immune-stimulatory effects by decreased activation of the innate immune system sensors, e.g. Toll-like receptors, and immune cells, e.g. dendritic cells.<sup>[7]</sup> Moreover, chemical modifications such as replacement of uridine with pseudouridine can facilitate protein translation by diminishing activation of RNA-dependent protein kinase (PKR).<sup>[8]</sup> Further exploration of the chemically modified mRNA (cmRNA) showed that substitution of only 25% of uridine and cytidine with 2-thiouridine and 5-methyl-cytidine not only decreases activation of the immune system *in vivo* but also significantly escalates levels of reporter as well as physiologically functional protein.<sup>[9]</sup> With such improvements, mRNA-based therapeutics have many advantages: pharmaceutical safety, rapid and transient translation profile, *in situ* generation of proteins, and the possibility of repeated dosing. Overall, these mRNA characteristics create an opportunity of a wide range of medical applications. Starting from examples of metabolic diseases: it has been shown that mRNA coding for mouse erythropoietin (mEpo) led to increase in hematocrit in treated mice.<sup>[9]</sup> Another therapeutic potential of chemically modified mRNA lies in the treatment of genetic disorders and has been described in a model of a hereditary, lethal lung disease - congenital surfactant protein B (SP-B) deficiency. Repeated, aerosol application to the murine lungs restored 71% of the wild-type SP-B translation and prolonged the average life span of the animals.<sup>[9]</sup> A further possibility using mRNA is regenerative medicine, e.g. bone healing. Already two weeks after orthotopic administration of cmRNA coding for human bone morphogenetic protein 2 (hBMP-2), an accelerated bone regeneration in rat bone defects was observed.<sup>[10]</sup>



### 1.3 Delivery challenge in transcript therapies

The direct delivery of mRNA into cells is hampered by its highly anionic character that largely prevents a passage across cell membrane. To fulfil its function, the mRNA has to reach the cytosolic compartment of a cell. An additional barrier is represented by the ubiquitous presence of RNases. A potential solution could be local delivery to the target tissue by direct injection (e.g. intramuscular injection) but most organs are not easily accessible by this route of administration. For example, in order to treat metabolic liver diseases, mRNA must enter liver hepatocytes, which are only accessible from the blood stream. However, as any drug, mRNA introduced into the body via intravenous injection has to overcome numerous barriers on its route to the target cell: interaction with blood and serum components and cells of the immune system, among others. Unspecific interactions could lead to unwanted side effects such as e.g. blood coagulation and enhanced clearance. Furthermore, once the target tissue is reached, mRNA needs to cross the cellular membrane and enter the cytoplasm. To address all these challenges, a properly designed delivery system is necessary. It has to meet certain requirements such as efficient encapsulation of mRNA, protection from degradation and undesired interactions in the blood stream, delivery to the tissue of interest, possession of effective cell penetrating properties, the endosomal escape ability, and the final release of the mRNA into the cytoplasm.

### 1.4 Cellular uptake and endosomal escape

The cell membrane, consisting of a phospholipid bilayer with embedded proteins, is selectively permeable to small molecules. However, macromolecules cannot easily cross the membrane mostly due to their large size. In addition, mRNA is too hydrophilic and negatively charged to efficiently diffuse on its own across the cell membrane. Thus, an important barrier for an mRNA-carrier complex is association with the membrane and subsequent cellular uptake. The main mechanism of macromolecular drug complex internalization into the cells is the vesicular uptake by endocytosis.<sup>[11-13]</sup> So far, numerous mechanism of endocytosis have been described,<sup>[14,15]</sup> as schematically depicted in Figure 1.1.

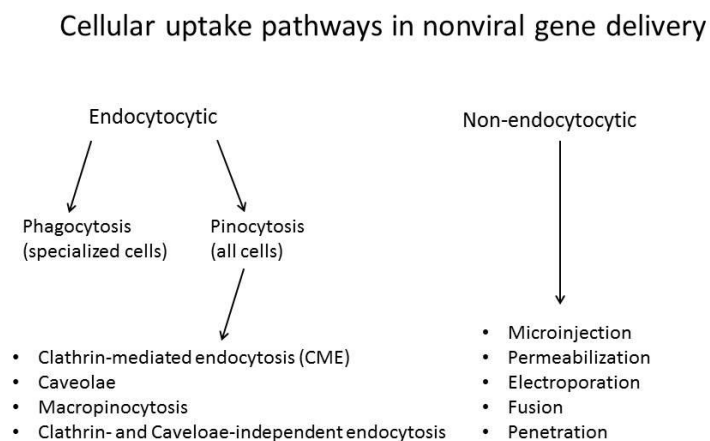


**Figure 1.1.** Different cellular uptake pathways in nonviral gene delivery.<sup>[1,3]</sup>

Once a complex enters the cell via endocytosis, it is trapped in intracellular vesicles. If it does not escape from endosome, it will be transported from early to late endosome and finally be degraded along the lysosomal pathway.<sup>[16]</sup> Endosomal escape requires membrane destabilization, which could be obtained e.g. in an acidification-dependent manner.<sup>[17]</sup> One hypothetical mechanism of endosomal escape of nonviral carriers is the proton sponge effect, firstly proposed by Jean-Paul Behr.<sup>[18]</sup> According to this theory, cationic vehicles, which are only partly protonated at neutral, extracellular pH and possessing substantial buffering capacity below physiological pH, may cause endosome swelling and rupture of the endosomal membrane through influx of chloride counterions and water.<sup>[19]</sup> Another assumed mechanism for cationic lipid-based complexes suggests rather disruption of the endosomal membrane by promoting the formation of nonbilayer lipid structures in combination with anionic phospholipids.<sup>[20]</sup> It has been reported that a  $pK_a$  value between 6.2-6.5 of cationic lipids exhibits a high correlation to their activity *in vivo*.<sup>[21]</sup> Finally, an efficient transfection process further requires dissociation of the mRNA from the carrier after reaching the cytoplasm.

### 1.5 mRNA delivery systems

In general, mRNA carriers can be divided into viral and nonviral vectors.<sup>[22,23]</sup> Despite some potential advantages of viral vectors, i.e. expression and replication of some RNA viruses localized in the cytoplasm and a capacity to express large amounts of protein in a broad range of different hosts,<sup>[24]</sup> a high risk of carcinogen-

esis, immune side effects, and difficulty of vector production limit the development of viral delivery systems.<sup>[25]</sup> A variety of promising nonviral carriers has been described for gene-based approaches, mostly lipoplexes and polyplexes. The basic principle in mRNA delivery involves the use of cationic polymers or lipids, resulting in complexation of the negatively charged nucleic acid via electrostatic interactions as well as further interactions with cell membranes.

### 1.5.1 Polymers

Based on experiments with widely used polymers for nucleic acid delivery, e.g. polyethylenimine (PEI) and poly(L-lysine) (PLL, see Figure 1.2a-b), it appeared that, specific to polymeric particles, binding strength between the mRNA and polymer is critical for translation efficiency.<sup>[26]</sup> Whereas transfection with PEI 25 kDa or PLL 54 kDa did not lead to any translation *in vitro*, smaller molecular weight polymers, 2 kDa and 3.4 kDa, significantly increased their activity in the presence of chloroquine, an agent of endosomolytic activity.

In comparison to PEI, polycations with histidine and polylysine residues (HIS RPCs) proved to enable efficient translation.<sup>[27]</sup> Transfection with histidine-rich RCPs mediated high levels of green fluorescent protein (GFP) in prostate cancer cells (PC-3), achieving as much as 97% positive cells in contrast to 33% transfected with PEI.

With a view toward delivery of mRNA-based vaccines, nanoparticles based on poly( $\beta$ -amino ester) and coated with a phospholipid bilayer were developed.<sup>[28]</sup> They led to successful transfection of dendritic cells *in vitro*, as well as reporter mRNA delivery after intranasal administration in mice. The design of described particles included surface binding of mRNA via electrostatic interactions, reduction of the toxicity by reduced interaction with the lipid bilayer and promotion of endosomal escape by pH-responsive poly( $\beta$ -amino ester).

In another study, the effect of PEGylation on the binding and transfection efficiency of polymers was investigated. Two types of polymers were analyzed, linear PEI and poly-N,N-dimethylaminoethyl methacrylate p(DMAEMA) (see Figure 1.2c), demonstrating that PEGylation improved mRNA binding, particle formation, and transfection efficiency as compared to their unmodified counterparts.<sup>[29]</sup> Additionally, enhanced endosomal release achieved by influenza-peptide 7 (an endolysosomal re-

lease peptide) further improved transfection efficiency. However, side-by-side comparisons of mRNA and pDNA complexes led to contradictory results, which is a proof that delivery systems require tailor-made design for each type of nucleic acid. Expanded knowledge about factors required for effective and safe delivery systems allowed to develop more complex carriers designed to enhance intracellular delivery of mRNA. Recently, triblock copolymers consisting of a cationic dimethylaminoethyl methacrylate (DMAEMA) mediating mRNA condensation, a hydrophilic poly(ethylene glycol) methyl ether methacrylate (PEGMA) which enhances complex stability and biocompatibility, and a pH-responsive endosomolytic copolymer of diethylaminoethyl methacrylate (DEAEMA) and butyl methacrylate (BMA) which facilitate cytosolic entry were described (see Figure 1.2d).<sup>[30]</sup> The order of these blocks as well as PEGMA length were varied to find the optimal combination for mRNA transfection efficiency. As a result, polyplexes of DMAEMA-PEGMA-DEAEMA-co-BMA exhibited the greatest stability and efficacy in two immune cell lines RAW264.7 macrophages and DC2.4 dendritic cells (77 and 50% of transfected cells, respectively).

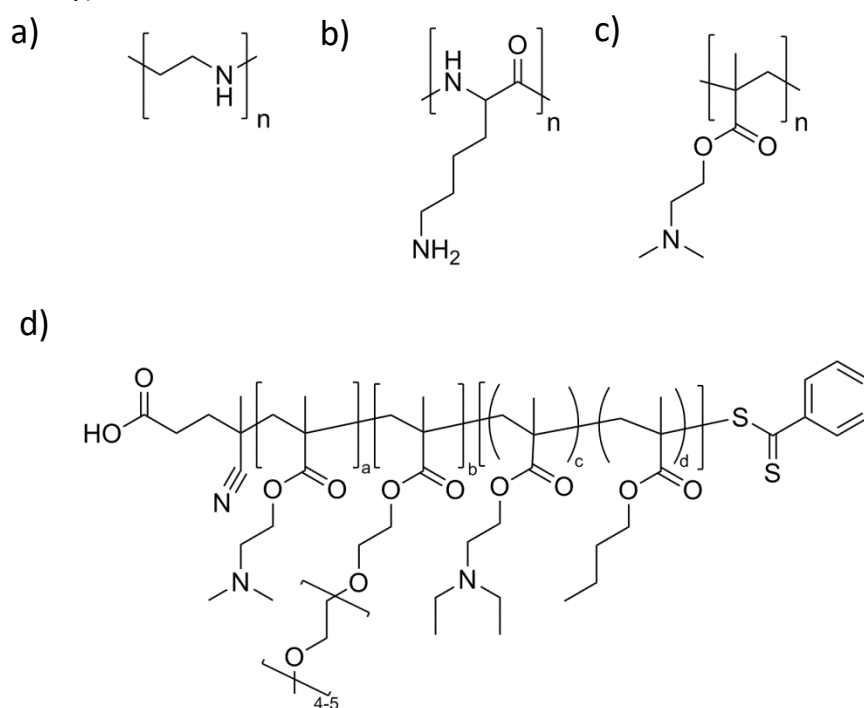


**Figure 1.2.** Chemical structures of polymers described for mRNA delivery: a) polyethylenimine (PEI), b) poly(L-lysine) (PLL), c) poly-N,N-dimethylaminoethyl methacrylate (p(DMAEMA)), and d) poly(DMAEMA-PEGMA-DEAEMA-co-BMA).

How even subtle changes in the carrier structure can influence transfection efficiency, was described in one example of N-substituted polyaspartamides with varied numbers of side chain aminoethylene repeats.<sup>[31]</sup> A clear correlation between the number of aminoethylene repeats and the translation level was found. Polyplexes with odd number of repeats (PA-Os) showed an increase in efficiency compared with those with even number of repeats (PA-Es). Thorough investigation of this effect revealed that two factors i) endosomal escaping capability and ii) stability in the cytoplasm play a critical role in the transfection process. Despite high endosomal escape efficacy of PA-Es, their insufficient cytoplasmic stability led to rapid mRNA degradation and, hence, lower transfection efficiency. In contrast, PA-Os stability overcame the limited endosomal escape capability, resulting in more sustainable translation. Interestingly, the same constructs comprising pDNA instead of mRNA showed the opposite pattern, which again indicate that each optimization and fine-tuning of the carrier needs to be tailored for the nucleic acid of interest.

### 1.5.2 Lipids

Since 1989, when a synthetic cationic lipid, N-[1-(2,3-dioleoyloxy)propyl]-N,N,N-trimethylammonium chloride (DOTMA) was reported to transfect human, rat, murine, *Xenopus* and *Drosophila* cells with mRNA coding for luciferase,<sup>[32]</sup> the field of lipid nanoparticles has gained a great interest in mRNA delivery. Despite the fact that its toxicity restricted the clinical development, DOTMA remained a common component of lipoplexes. Another widely used cationic lipid is DOTAP (1,2-dioleoyl-3-trimethylammonium-propane (chloride salt)), which is efficient in both *in vitro* and *in vivo* applications.<sup>[26,33,34]</sup> However, positively charged lipoplexes can be quickly removed from the systemic circulation, which strongly hampers their efficiency *in vivo*. To overcome this obstacle, it is common in nucleic acid delivery to coat lipid nanoparticles with poly(ethylene glycol) (PEG),<sup>[35,36]</sup> which improves carrier stability in blood and prevents aggregation.<sup>[37,38]</sup> On the other hand, the use of PEG may have undesirable effects such as interfering with the cellular uptake and following intracellular processes.<sup>[39,40]</sup>

Even though some lipid delivery systems for mRNA vaccination have been described and are currently in clinical testing,<sup>[41,42]</sup> no carriers for mRNA-based therapies exist

on the market so far. Since lipid-based carriers represent a potentially efficient delivery platform, their thorough development might warrant detailed investigation for future applications in transcript therapies.

### 1.6 Lipid nanoparticles as a multicomponent system

As mentioned in the previous chapters, mRNA binding as well as interactions with the cell membrane are achieved by the use of a cationic lipid or polymer. In addition, in order to increase complex stability in the blood circulation, a PEG-coating could be applied. To improve particles stability and transfection efficiency even further, additional components can be included in the lipoplex.

#### 1.6.1 Cationic lipids

Since cationic lipids represent the most critical part of lipoplexes for efficient nucleic acid delivery, the main emphasis is placed on finding the most effective and biocompatible structures both *in vitro* and *in vivo*. With the purpose of gene silencing via systemic delivery of siRNA, a novel synthetic approach was developed.<sup>[43]</sup> Previously, conventional lipid synthesis methods limited the ability to screen a high number of diverse structures. The rapid synthesis of a large library of over 1,200 lipid-like compounds (lipidoids) was enabled by performing reactions in the absence of solvent or catalysts, which eliminated the necessity of protection and deprotection steps or purification. Briefly, the library was generated by the conjugate addition of alkylacrylates or alkylacrylamides to low molecular weight oligoalkylamines comprising primary or secondary amines. After screening their ability to deliver siRNA *in vitro*, the top performing lipidoids were found to follow some structural rules which were important regarding delivery efficiency including most preferably an amide linkage, more than two alkyl tails, tail length in the range of 8–12 carbons, and one not fully modified, secondary amine. Resulting lipidoid formulations of potent silencing activity proved to be efficient in three distinct species, including non-human primates. Worth mentioning, the formulations contained, apart from lipidoid and siRNA, a PEG-lipid and cholesterol. This strategy created a foundation for new material development and was further improved regarding delivery efficacy. Another class of lipidoids, composed of polar head groups containing amines and

nonpolar hydrocarbon tails, was reported to facilitate gene silencing at significantly lower doses than any siRNA carriers before.<sup>[44]</sup> Similar as described above the synthesis method included a one-step reaction of epoxides with amines, required no purification and obtained lipids could be used directly for *in vitro* screening. An important conclusion from the study was that an optimized combination of amine group and tail length is required for nucleic acid delivery efficacy. For *in vivo* application, lipid formulations included additional distearoyl phosphatidylcholine (DSPC), cholesterol, and a PEG-lipid to increase particle stability. Importantly, no toxicity in mice was observed even several orders-of-magnitude above the efficacious dosage. The properties of a cationic lipid determining its high activity in the formulation were investigated with a large number of head group modifications to the lipids.<sup>[21]</sup> A clear correlation between the lipid pK<sub>a</sub> value and the silencing efficacy of the lipid-siRNA complex *in vivo* was found, with an optimal pK<sub>a</sub> range of 6.2–6.5. Previously, it has been noted that permanently charged quaternary amine moieties in the hydrophilic head group region were less effective *in vivo* as compared to ionizable lipids.<sup>[45]</sup> It has been proposed that neutral or close to neutral lipoplexes will exhibit minimal undesired interactions with proteins or blood cells after systemic administration, thus increasing the chances of reaching the liver tissue. On the other hand, positive surface charge enables interaction and destabilization of the endosomal membrane, resulting in endosomal escape of a complex. These two, seemingly contrary conditions, are fulfilled by ionizable lipids with pK<sub>a</sub> between 6.2 and 6.5, as they show minimum charge at physiological pH and maximum positive charge in the acidified endosomal compartment.<sup>[21]</sup> However, the presented data indicated that although an optimal pK<sub>a</sub> value is necessary, there are also other features such as the linker between the head group and the lipid tails, which can drastically affect the activity *in vivo*.

It has also been proposed that amino lipids with a small headgroup can adopt inverted, nonbilayer structures, which are hypothesized to destabilize the endosomal lumen, resulting in efficient release of nucleic acid cargo into the cytoplasm.<sup>[20,45]</sup> In addition to headgroup structures, other functional elements (alkyl chain, linker) can affect the properties of lipidic carriers.<sup>[45]</sup> In an attempt to define structure-function relationships, Whitehead *et al.* analyzed different criteria of degradable lipidoids

from a generated library and their correlation to siRNA delivery capability *in vivo*.<sup>[46]</sup> Based on the findings, a second-generation library was developed, designed towards potentially efficacious materials, following presumably critical structural rules. As a result, a set of four efficacy criteria predicting *in vivo* efficacy were established: appropriate tail length (alkyl-acrylate of 13 carbon chain length), alkylamine containing at least one tertiary amine, at least three substitution sites, and a pK<sub>a</sub> value above 5.4.

All of these discoveries contribute to the design of effective cationic lipids. This identified structure-function relationship represents a guideline for the design of future materials for nucleic acid delivery.

### 1.6.2 The role of helper lipids

The advanced lipid systems for siRNA delivery are usually composed of a cationic lipid/lipidoid, phospholipid, cholesterol, and a PEG-lipid. The knowledge about lipoplex structure could also help in understanding the exact role of helper lipids commonly used in the formulations. The classical model of lipid-nucleic acid complex (see Figure 1.3a) assumes a bilayer structure with a nucleic acid encapsulated in the aqueous interior.<sup>[47]</sup> However, recent cryo-transmission electron microscopy (cryo-TEM) studies revealed a presence of electron-dense cores<sup>[48]</sup> instead of less dense aqueous cores.<sup>[49]</sup> A thorough structure characterization using multiple biophysical assays combined with computer modeling showed that encapsulated nucleic acid is bound to cationic lipid in the internal core, which also contains phospholipid and cholesterol, whereas the outer layer consists of a homogeneous PEG-lipid coating (see Figure 1.3b).<sup>[50]</sup> The results also suggest that nucleic acid is immobilized in inverted micelles, fully protected from enzymatic degradation. Additionally, a role of phospholipid (phosphocholine) in the four lipid component formulation was proposed. Used in numerous lipid vehicles, it has been believed to contribute to particle stability. However, the obtained data suggested rather a role of charge mediator including forming ion pairs between the phosphate group of a lipid and the cationic lipid headgroup, whereas choline interacted with nucleic acid phosphates. Cholesterol is hypothesized to be distributed homogeneously in the core and surface, presumably facilitating the formation of the inverted hexagonal phase.



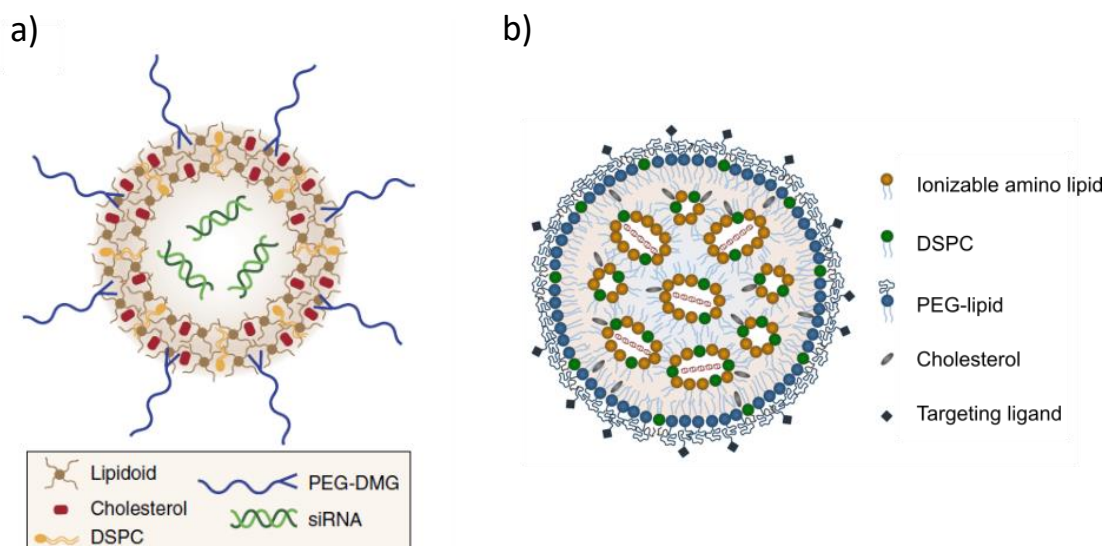


**Figure 1.3.** A scheme of a lipid nanoparticle (LNP) with encapsulated nucleic acid: a) classical model<sup>[46]</sup> and b) nano-structured core model.<sup>[51]</sup>

Cholesterol is a natural, essential component of lipid membranes, stabilizing their structure and maintaining fluidity. In some carriers developed for siRNA delivery it has been shown that by varying the ratio of cholesterol in the formulation different liver cell subpopulations can be targeted.<sup>[52]</sup>

### 1.6.3 PEG coating

In order to prevent aggregation and prolong circulation life time by creating stealth nanoparticles, a coating of a PEG-lipid is widely used in lipid-based delivery. However, the thoughtful choice of a PEG-lipid type has a huge impact on the carrier activity. For instance, it has been shown that the lipid anchor length determines how long the PEG-coating remains associated with the particle. Longer anchors in PEGylated ceramides need more time to be dissociated, which prevents interactions with cells and extends particles circulation time.<sup>[53]</sup> On the other hand, complexes comprising long acyl anchors (PEG-DSPE, 1,2-distearoyl-*sn*-glycero-3-phosphoethanolamine, C18 anchors) were rapidly removed after systemic administration as a consequence of an immune response to the PEG component.<sup>[54,55]</sup> This immunogenic response and resulting clearance can be avoided by using shorter anchors which rapidly dissociate from the complex (i.e. PEG-DMG, 1,2-dimyristoyl-*sn*-glycerol, C14 anchors).<sup>[51]</sup> The explanation behind these dependences is that a PEG-lipid is incorporated into a complex hydrophobically, and thus deshielding can be controlled relatively easy by changing its hydrophobic properties.<sup>[56]</sup>

### 1.6.4 Targeting ligands

Even without any external ligands conjugated to them, lipid nanoparticles can naturally target the liver via interactions with apolipoprotein (Apo) E, a natural serum protein.<sup>[57]</sup> The uptake of neutral lipoplexes by liver cells (hepatocytes) is enhanced by ApoE *in vivo*.<sup>[58]</sup> To target other tissues, the use of some exogenous ligands might be a necessity. Despite being efficient, ligands such as antibodies (or their fragments) and peptides have some disadvantages, with high costs and difficulties in manufacturing, among others. Consequently, small molecule ligands, which are relatively easy to synthesize and conjugate on the surface of lipid nanoparticle, represent a more promising approach for enhanced delivery to the target cells.<sup>[59,60]</sup> For example, to target the liver in an ApoE-independent manner, N-acetylgalactosamine (GalNAc), which binds with high affinity to the asialoglycoprotein receptor (ASGPR) present on the surface of hepatocytes, can be applied in the formulation.<sup>[59]</sup> Lung tumours and metastases can be targeted with a specific ligand such as anisamide, which interacts with sigma receptors.<sup>[61]</sup> Another described small molecule ligand, cardiac glycosides strophanthidin, stimulates endocytosis on binding to plasma membrane Na<sup>+</sup>/K<sup>+</sup> ATPase and enhances uptake in a variety of cell types derived from different tissues.<sup>[60]</sup>

### 1.7 Aim of the thesis

Transcript therapy based on chemically modified mRNA creates an opportunity to treat rare metabolic and/or genetic diseases that have had no cure until now, only options to alleviate the symptoms and improve the quality of patient's life. Moreover, the versatility of this nucleic acid provides numerous other potential applications, e.g. bone regeneration or cancer therapy. The major hurdle that must be overcome before achieving the final goal of clinical application is the delivery process. Despite some carriers described so far, the field is still in an early development stage. The complexity of the process is a challenge but in context with previous progress which has been made in the field of nucleic acid delivery, the critical factors that have to be taken into consideration in a design are continuously better defined. Importantly, even though delivery systems for other nucleic acids (pDNA, siRNA) have been investigated more thoroughly, mRNA vehicles need to be tailored to its unique molecular properties in context with the intended site of action.

In this thesis, a lipid-based system has been chosen because of its known capability to mediate efficient cellular uptake. A multicomponent system consisting of a lipidoid for mRNA binding and interaction with cells, helper lipids improving particle stability and enhancing transfection process, as well as a PEG-lipid prolonging blood circulation, preventing aggregation and undesired interactions has been adopted as a starting point. The aim of this thesis was the optimization of such a formulation in context with the needs of mRNA for *in vivo* applications. The ultimate goals were:

- formation of stable, monodisperse nanoparticles
- high transfection efficiency obtained by effective cellular uptake and endosomal escape
- low cytotoxicity
- ensuring tissue specificity by targeted delivery.

In order to attain these aims, more detailed objectives of the thesis were:

1. An attempt to explain and understand the role of each lipid component in context with delivery efficiency. This goal was to be achieved by synthesis and following screening of a small lipidoid library based on oligoalkylamines with determining critical structure-activity relationships, side-by-side com-

parison of the additional lipid components of the formulation, namely helper lipids and a PEG-lipid.

2. Defining the critical requirements for effective endosomal escape and protein translation through analysis of the cellular steps involved in the transfection process, i.e. cellular uptake in context with cell viability.
3. Better understanding of such multicomponent system by investigation of nonlipidic factors influencing the particle formation and physicochemical characterization of resulting nanoparticles.
4. Finally, *in vivo* testing as a proof of concept, both comparing different formulations in terms of their efficiency using a reporter mRNA sequence as well as testing functional protein translation by using mRNA coding for a toxin in a mouse tumour model.

## 2 Materials and Methods

### 2.1 Materials

#### 2.1.1 Solvents and chemicals

All chemicals and reagents were purchased in quality reagent grade or higher from commercial sources (Sigma-Aldrich (St. Louis, USA), EvoBlocks (Budapest, Hungary)) and used as received. Two kinds of water were used: water for injection (Aqua ad iniectabilia®, B. Braun (Melsungen, Germany)) and bidistilled water (Aqua bidest., Kerndl (Weissenfeld, Germany)). Anhydrous solvents were purchased from Carl Roth (Karlsruhe, Germany). A set of screened oligoalkylamines consisted of: (2-2): Diethylenetriamine, (3-3): N-(3-aminopropyl)-1,3-propanediamine, (2-2-2): Triethylenetetramine, (3-3-3): N,N'-Bis(3-aminopropyl)-1,3-propanediamine, (2-3-2): N,N'-Bis(2-aminoethyl)-1,3-propanediamine.

(2-3-2) dendrimers generations G1 and G2 were synthesized and supplied by SyMO-Chem (Eindhoven, the Netherlands).

#### 2.1.3 Lipids

**Table 2.1.** List of used lipids, their abbreviations and suppliers.

Abbreviation	Full name	Supplier
DOPE	1,2-dioleoyl- <i>sn</i> -glycero-3-phosphoethanolamine	Avanti Polar Lipids (Alabastar, USA)
DLPC	1,2-dilauroyl- <i>sn</i> -glycero-3-phosphocholine	Avanti Polar Lipids (Alabastar, USA)
DMPC	1,2-dimyristoyl- <i>sn</i> -glycero-3-phosphocholine	Avanti Polar Lipids (Alabastar, USA)
DPPC	1,2-dipalmitoyl- <i>sn</i> -glycero-3-phosphocholine	Avanti Polar Lipids (Alabastar, USA)
DSPC	1,2-distearoyl- <i>sn</i> -glycero-3-phosphocholine	Avanti Polar Lipids (Alabastar, USA)
DePC	1,2-di-O-hexadecyl- <i>sn</i> -glycero-3-phosphocholine	Avanti Polar Lipids (Alabastar, USA)
DOPC	1,2-dioleoyl- <i>sn</i> -glycero-3-phosphocholine	Avanti Polar Lipids (Alabastar, USA)

## 2 Materials and Methods

Cholesterol	Cholesterol, plant derived	Avanti Polar Lipids (Alabastar, USA)
DMPE-PEG2k	1,2-dimyristoyl- <i>sn</i> -glycero-3-phosphoethanolamine-N-methoxy(polyethylene glycol) (ammonium salt), 2000 Da	Avanti Polar Lipids (Alabastar, USA)
DMG-PEG2k/5k	1,2-Dimyristoyl- <i>sn</i> -glycerol-methoxy(polyethylene glycol), 2000/5000 Da	NOF America Corporation (White Plains, USA)
DPG-PEG2k/5k	1,2-Dipalmitoyl- <i>sn</i> -glycerol-methoxy(polyethylene glycol), 2000/5000 Da	NOF America Corporation (White Plains, USA)
DSG-PEG2k	1,2-Distearoyl- <i>sn</i> -glycerol-methoxy(polyethylene glycol), 2000 Da	NOF America Corporation (White Plains, USA)
DOPE-PEG2k	1,2-dioleoyl- <i>sn</i> -glycero-3-phosphoethanolamine-N-methoxy(polyethylene glycol) (ammonium salt), 2000 Da	Avanti Polar Lipids (Alabastar, USA)
Cholesterol-PEG2k	Cholesterol-polyethylene glycol, 2000 Da	NOF America Corporation (White Plains, USA)
DSPE-PEG2k	N-(Carbonyl-methoxy(polyethylene glycol))-1,2-distearoyl- <i>sn</i> -glycero-3-phosphoethanolamine, sodium salt, 2000 Da	NOF America Corporation (White Plains, USA)
DSPE-PEG2k-FA	DSPE-PEG-Folic acid, 2000 Da	Nanocs (New York, USA)
DOPS	1,2-dioleoyl- <i>sn</i> -glycero-3-phospho-L-serine (sodium salt)	Avanti Polar Lipids (Alabastar, USA)

### 2.1.4 Chemically modified mRNA

Chemically modified mRNAs (cmRNAs) coding for firefly luciferase, *Metridia* luciferase, A-chain abrin, and human erythropoietin were supplied by Ethris (Planegg, Germany). Genes of interest were cloned into plasmid vector pVAXA120, linearized by restriction digestion with *NotI*, and further purified by chloroform/ethanol and sodium acetate precipitation. Resulting linear DNA template was used for *in vitro* transcription (IVT) from ribonucleotide mixture containing adenosine-triphosphate (ATP), guanosine-triphosphate (GTP), uridine-triphosphate (UTP) and cytosine-triphosphate (CTP) as well as the chemically modified 5-methyl-CTP (25% of total CTP) and 2-thio-UTP (25% of total UTP) (Jena Bioscience GmbH, Jena, Germany). IVT was performed with RiboLock Rnase Inhibitor, Inorganic Pyrophosphatase, T7 RNA Polymerase, and DNase I (Thermo Fisher Scientific (Waltham, USA)). The obtained

cmRNA was subsequently subjected to the post-capping process in the presence of GTP, S-Methyladenosine, Vaccinia Virus Capping Enzyme, and mRNA Cap 2'-O-Methyltransferase (New England Biolabs (Ipswich, USA)). The final product was purified by ammonium acetate precipitation, and the resulting pellet was re-suspended in water for injection (WFI). cmRNA concentration and purity were determined with a NanoDrop 2000C spectrophotometer (Thermo Fisher Scientific (Waltham, USA)).

### 2.1.5 Cell culture

All cell culture consumables (flasks, plates) were purchased from Corning Incorporated (New York, USA). Growth media and additives (fetal bovine serum (FBS), penicillin/streptomycin (P/S)) were purchased from Gibco Life Technologies (Darmstadt, Germany). All cell lines were purchased from DSMZ (Braunschweig, Germany) or isolated at Ethris (Planegg, Germany). List of tested cell lines, according culture media as well as the provider's cell line number is presented in the table below:

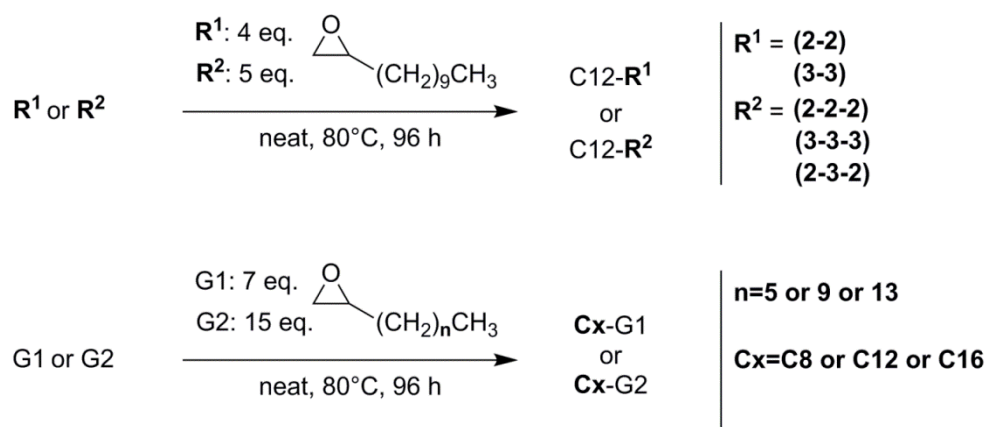
**Table 2.2.** List of tested cell lines, their providers and media.

Cell line	Description	Provider	Medium
NIH 3T3	murine fibroblasts	DSMZ – ACC 59	DMEM+ 10% FBS, 1% P/S
HepG2	human liver carcinoma cells	DSMZ – ACC 180	RPMI 1640 10% FBS, 1% P/S
AMSC	adipose mesenchymal stem cells	isolated from the fat tissue of a male rat, Ethris	DMEM+ 10% FBS, 1% P/S
A549	human alveolar type II like cells	DSMZ – ACC 107	MEM+ 10% FBS, 1% P/S
KB	human cervix carcinoma (derivative of HELA)	DSMZ – ACC 136	RPMI 1640 without folic acid 10% FBS, 1% P/S
KB for <i>in vivo</i>	human cervix carcinoma (derivative of HELA)	DSMZ – ACC 136	RPMI 1640 without folic acid 10% FBS

## 2.2 Methods

### 2.2.1 Synthesis of lipidoids

The lipidoids were synthesized in the reaction of selected oligoalkylamines with alkyl epoxide, as shown in Scheme 2.1. 100 mg of oligoalkylamine (corresponding to i.e. 0.623 mmol *N,N'*-Bis(2-aminoethyl)-1,3-propanediamine, (2-3-2)) was mixed with (N-1) equiv. of 1,2-epoxydodecane (corresponding to 575.07 mg, 3.12 mmol in the case of (2-3-2)), where N is defined as 2x number of primary amines plus number of secondary amines in one molecule of oligoalkylamine and stirred for 96 h at 80°C in a glass vial, as performed by Love *et al.*<sup>[44]</sup>



*Scheme 2.1. Synthesis of oligoalkylamine-based lipids.*

### 2.2.2 Complex formation and physicochemical characterization

#### 2.2.2.1 Lipoplex formation

Lipid particles were formulated from a lipidoid (Ethris), two helper lipids: a phospholipid and cholesterol (Avanti Polar Lipids) and a PEG-lipid (Avanti Polar Lipids or NOF America Corporation) at the molar ratios 8/5.29/4.41/0.88, if not stated differently. Proper volumes of lipid stock solutions in absolute ethanol of concentrations 50, 20, 20 and 20 mg/mL, respectively, were combined and adjusted to a total volume of 200 μL. Lipoplex formation was performed by a rapid solvent exchange; lipid mixture in ethanol was injected into 800 μL of mRNA in citrate buffer (10 mM citric acid, 150 mM NaCl, pH 4.5, if not stated differently). Final mRNA concentration was 200 μg/mL with N/P 17 or 8, if not stated differently. After 30 min of incubation at RT, lipoplexes were purified by overnight dialysis (in 7000 molecular weight cutoff



cassettes, Thermo Fisher Scientific (Waltham, USA)) against bidest. water. The concentration of mRNA in samples and encapsulation efficiency were determined by a modified RiboGreen assay (see below).

When higher concentration of lipoplexes was required for *in vivo* experiments, it was obtained by using Eppendorf Concentrator plus device (Eppendorf (Hamburg, Germany)) with heating (45°C) and vacuum for rapid evaporation of excessive volume. If samples had to be frozen, they were adjusted with 20% sucrose to obtain final desired concentration of mRNA in 2% sucrose and stored at -20°C.

### 2.2.2.2 RiboGreen Assay

To determine the mRNA concentration of lipoplex fractions, a standard curve of unpurified sample (concentration known and equal to 200 µg/mL) in the range of 0-4000 ng/mL for each composition was prepared. Samples were diluted 50 to 100-fold to obtain the expected concentration within that range. 150 µL of each calibration point and diluted sample was treated with 140 µL 2% Triton X-100 and 10 µL heparin (40 mg/mL) and incubated for 15 min at 70°C. After cooling to RT, 100 µL of each sample was transferred in duplicates into a black 96-well plate, followed by addition of 100 µL of 100-fold diluted RiboGreen (Quant-iT™ RiboGreen® RNA Assay Kit, Invitrogen (Carlsbad, USA)) reagent (solution in dimethyl sulfoxide) in 1x TE buffer (10 mM Tris-HCl, 1 mM EDTA, pH 7.5 in diethylpyrocarbonate (DEPC)-treated water) into each well and light-protected incubation for 5 min at RT. The fluorescence intensity was measured on a multilabel reader (1420 Multilabel Counter, Perkin Elmer (Waltham, USA)) at excitation/emission wavelength of 485/535 nm, respectively, with an untreated sample as control. The encapsulation efficiency was calculated from comparison of the signals of treated samples and untreated controls. It was assumed that the signal in untreated samples comes from untrapped mRNA, whereas in treated samples – from total mRNA.

### 2.2.2.3 Size and zeta potential determination

Hydrodynamic diameter of particles was measured by dynamic light scattering (DLS) using a Zetasizer Nano-ZS (Malvern Instruments, Worcestershire, UK) with an automatic attenuator and reported as intensity particle size distribution. Samples were

prepared by dilution of 10  $\mu\text{g}$  complexed mRNA in 1 mL PBS buffer/WFI and measured at 25°C. Zeta-potential was calculated from electrophoretic mobility.

### 2.2.2.4 Transmission electron microscopy (TEM)

To make carbon-formvar copper grids 300 mesh (Ted Pella, (Redding, USA)) hydrophilic, plasma cleaning was performed. 8  $\mu\text{L}$  of sample was applied to a carbon-formvar grid for 1 min and then the excess of sample was removed with a filter paper. Negative staining of the sample was performed with 7  $\mu\text{L}$  of a 1% uranyl acetate solution in water. Remaining uranyl acetate solution was removed with a filter paper. Grids were imaged with JEM 1011 (JEOL (Tokyo, Japan)) at 80 kV. TEM pictures were taken by Maximilian Utzinger, Ethris (Planegg, Germany) and Susanne Kempter, Department of Physics, LMU (Munich, Germany).

### 2.2.2.5 Buffering capacity

Prior to the potentiometric titration, 10  $\mu\text{moles}$  of lipidoids were dissolved in 1 mL ethanol and mixed with 2.5 mL 50 mM sodium chloride solution with the following pH adjustment to pH 2 with 0.5 M HCl. Experiments were performed on a potentiometric titrator Titrando (Metrohm (Herisau, Switzerland)) with an automated dosing. Measurements points were collected after each addition of defined volume of 50 mM sodium hydroxide and following pH determination. As a blank, 3.5 mL of 50 mM NaCl solution were titrated. The first detected pH value above 11 determined the end of titration. In order to calculate the volume of 50 mM NaOH required to reach certain, pH values between the real measurement points a linear regression between two nearest values was taken as an estimation. Buffering capacity was defined as a volume of 50 mM NaOH required to change pH by 0.1.

### 2.2.2.6 Agarose gel electrophoresis

The integrity of mRNA released from lipoplexes was determined by agarose gel electrophoresis. The samples were loaded on 1% (w/v) agarose (in TEA buffer (40 mM Tris, 20 mM acetic acid and 1 mM EDTA in distilled, deionised water; pH 8.5) with a fluorescent dye PeqGREEN (0.005% v/v (i.e. 75  $\mu\text{L}$  per 150 mL agarose gel), Peqlab (Erlangen, Germany)). The amount of mRNA varied between 500 and 700 ng depending on the sample concentration. Samples in the volume of 5  $\mu\text{L}$  were

treated with 3  $\mu\text{L}$  heparin (40 mg/mL) and 2  $\mu\text{L}$  Triton-X-100 (2%) and mixed with 10  $\mu\text{L}$  2x RNA loading dye to a total volume of 20  $\mu\text{L}$ . Next, samples were heated to 70°C for 15 min in order to denature mRNA. Samples were cooled down on ice for 2 min prior to loading on a gel. Electrophoresis was conducted at 150 V for 60 min and resulting gel imaging was performed with ChemiDoc XRS+ station (Bio-Rad (Hercules, USA)).

### 2.2.3 *In vitro* methods

#### 2.2.3.1 Cell transfection

Cells were cultured in appropriate medium (as listed in Table 2.3) at 37°C, 5% CO<sub>2</sub>. Cells were seeded at densities as showed in Table 2.3 in 100  $\mu\text{L}$  media in a 96-well plate (collagen-coated in the case of HepG2) 24 h prior to transfection. The appropriate amount of complexed mRNA was added in 20  $\mu\text{L}$ /well in triplicates after dilution series in PBS buffer starting from 500 ng/well if not stated differently. Plates were incubated for 24 h at 37°C, 5% CO<sub>2</sub>.

**Table 2.3.** Seeding conditions of tested cell lines.

Cell line	NIH 3T3	HepG2	AMSC	A549	KB
					RPMI 1640
	DMEM+	RPMI 1640	DMEM+	MEM+	without folic
<b>Medium</b>	10% FBS, 1%	10% FBS, 1%	10% FBS, 1%	10% FBS, 1%	acid
	P/S	P/S	P/S	P/S	10% FBS, 1%
					P/S
<b>Seeding cell</b>					
<b>density</b>	5000	20000	3000	20000	10000
<b>[cell/well]</b>					

Transfection with folate receptor targeting was performed stepwise. First step assured receptor saturation (with temperature inhibited uptake), where cells after 10 min preincubation on ice were treated with 20  $\mu\text{L}$  250 mg/mL sodium folate and incubated on ice for 15 min. Second step was the particle uptake, where transfection was conducted as described above with following 30 min incubation at 37°C, 5% CO<sub>2</sub>. Third step allowed reporter protein translation, where after media change cells were incubated for 24 h at 37°C, 5% CO<sub>2</sub>.

### 2.2.3.2 Firefly luciferase assay

After 24 h of incubation, medium was removed. Cells were lysed in 100  $\mu$ L of lysis buffer (25 mM Tris-HCl, 0.1 % TritonX-100, pH 7.8) and incubated on a plate shaker for 30 min at RT and 600 rpm. Next, 80  $\mu$ L cell lysate from each well was transferred to a 96-well plate and the activity of reporter protein firefly luciferase was measured by bioluminescence intensity on a multilabel reader (1420 Multilabel Counter, Perkin Elmer (Waltham, USA)) after addition of a luciferin buffer (0.47 mM D-luciferin, 0.27 mM Coenzyme A, 3.33 mM DTT, 0.53 mM ATP, 1.1 mM magnesium carbonate, 2.7 mM magnesium sulphate, 20 mM TRICINE, 0.1 mM EDTA). The luminescence at each well was measured for 1 s and expressed in relative light units (RLU).

### 2.2.3.3 Cytotoxicity studies

The effect of the lipoplexes on cell viability was determined by MTT Cell Proliferation Assay (TACS<sup>®</sup>, Trevigen (Gaithersburg, USA)) according to the manufacturer's protocol. Briefly, 24 h post transfection medium in each well was exchanged and 10  $\mu$ L MTT reagent added. After 2.5 h incubation (37°C, 5% CO<sub>2</sub>) 100  $\mu$ L detergent was added to each well and light-protected plates were incubated for 2 h at RT. Photometric measurement was performed at 570 nm on a multilabel reader (1420 Multilabel Counter, Perkin Elmer (Waltham, USA)). Cell viability was calculated as a relative value (in %) compared to the control, untransfected cells (100%).

### 2.2.3.4 Lipoplex uptake

Confluent NIH 3T3 cells were seeded in 6-well plates at 300,000 cells/well. 24 h after seeding, cells were transfected with 930 ng mRNA-MetLuc complexed in lipoplexes C12-(2-2), C12-(3-3), C12-(2-2-2), C12-(3-3-3) or C12-(2-3-2). After 0.5, 1, 2, and 4 h time points cells were washed with PBS and lysed with a lysis buffer (LBP, Macherey-Nagel (Düren, Germany)). The total RNA was isolated according to the manufacturer's protocol (NucleoSpin RNA plus kit, Macherey-Nagel (Düren, Germany)) and eluted in 40  $\mu$ L RNase-free water. The resulting concentration and purity were determined by spectrophotometry at 260 and 280 nm (NanoDrop 2000c, Thermo Fisher Scientific (Waltham, USA)). 1  $\mu$ g RNA of each sample was reversely

transcribed into cDNA with anchored-oligo(dT)<sub>18</sub> primer (Transcriptor First Strand cDNA Synthesis Kit, Roche (Basel, Switzerland)). mRNA-MetLuc amounts (for each construct, after each time point) were quantified by quantitative PCR (qPCR, Universal Probe Library, UPL #14, Roche (Basel, Switzerland)) in 100-fold diluted cDNA based on a standard curve of pure mRNA-MetLuc transcribed into cDNA (10<sup>2</sup>-10<sup>7</sup>-fold dilutions) on a LightCycler 96 System, Roche (Basel, Switzerland). qPCR mixture per sample contained: 3.5 µL water, 0.5 µL 20 µM forward DNA primer, 0.5 µL 20 µM reverse DNA primer, 0.5 µL UPL and 10 µL Master Mix (provided in a kit).

DNA primers were designed with an online tool available at <https://lifescience.roche.com/>. Primer sequences were synthesized by Eurofins Genomics (Ebersberg, Germany).

DNA primer sequences:

Forward: AACCTGGAAACCGACCTGT

Reverse: ATCGGCCTTGATCATCACTT

### 2.2.3.5 Bright microscopy

Bright imaging of transfected cells was performed with JuLI – smart fluorescent cell analyser (Ruskin Technology (Bridgend, UK) 24 h after transfection.

### 2.2.3.6 mRNA release assay

*Preparation of anionic liposomes (AL):* Stocks of 1,2-dioleoyl-sn-glycero-3-phospho-L-serine (sodium salt) (DOPS), 1,2-dioleoyl-sn-glycero-3-phosphocholine (DOPC) and 1,2-dioleoyl-sn-glycero-3-phosphoethanolamine (DOPE) in chloroform (20 mg/mL) were mixed in proper volumes to obtain molar ratios 1:1:2, respectively. Next, solvent was evaporated from the mixture under a stream of nitrogen and the resulting lipid film was subsequently resuspended by vortexing and sonication in PBS buffer pH 6 to obtain final DOPS concentration of 5 mg/mL.

*Sample treatment:* tested lipoplexes were mixed with murine plasma at equal volumes and incubated at 37°C for 20 min. Next, AL were added to the sample in a desired ratio of DOPS to C12-(2-3-2) and further incubated at 37°C for 15 min. As a plasma control served the sample with PBS buffer added instead of AL.

*mRNA release determination*: samples were diluted to obtain concentration in the range of RiboGreen linear response (0-4,000 ng/mL). The following procedure of mRNA quantification of total and encapsulated mRNA is described in Chapter 2.2.2.2 “RiboGreen Assay”. mRNA release was defined as percentage of mRNA amount detected in untreated sample in relation to total mRNA quantified in samples treated with Triton X-100 and heparin (100%).

*Relative mRNA release*: the value of relative mRNA release was determined as a ratio of mRNA release in samples treated with murine plasma and AL (in %, determined as described in “mRNA release determination”) to mRNA release in plasma control samples (PBS buffer instead of AL added to the sample), also expressed in %. The procedure of mRNA release assay is schematically presented in Figure 2.1.

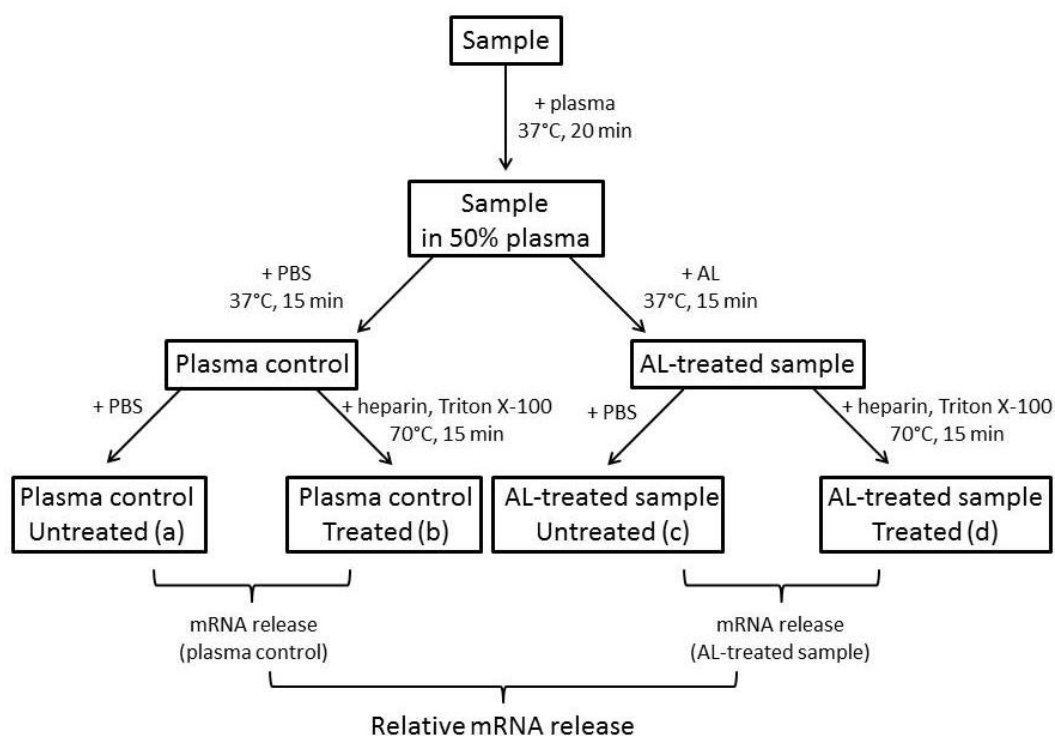


**Figure 2.1.** Scheme of sample treatment in mRNA release assay.

Relative mRNA release was calculated according to the equation below:

$$\begin{aligned}
 \text{Relative mRNA release} &= \frac{\text{mRNA release in AL treated sample}}{\text{mRNA release in plasma control}} \\
 &= \frac{\frac{\text{RiboGreen signal (c)}}{\text{RiboGreen signal (d)}} * 100\%}{\frac{\text{RiboGreen signal (a)}}{\text{RiboGreen signal (b)}} * 100\%}
 \end{aligned}$$

### 2.2.4 Animal studies

All experiments were performed according to German animal welfare law and were authorized by the local animal welfare authorities (Regierung von Oberbayern). Six to eight weeks old female Balb/c mice were obtained from Charles River Laboratories (Sulzfeld, Germany) and kept under specific pathogen-free conditions undergoing a 12 h/12 h light/dark cycle with free access to food and water. Animals were conceded an adaption time of at least 7 days prior to begin of experiments.

#### 2.2.4.1 Tail vein injection and luciferase activity

Tail vein injection experiments as well as luminescence imaging and quantification were performed by Dr. Tamara Pasewald, Ethris (Planegg, Germany).

The lipidic formulations in a volume of 140-150  $\mu$ L in PBS each, containing 18-20  $\mu$ g of mRNA-FLuc were injected into the tail vein (needles for injection: Microfine+ 1 mL, 0.33 mm (29G) x 12.7 mm (BD (Franklin Lakes, USA))) of a mouse fixed in a gadget. Luciferase activity was determined 6 h post administration. Mice were anesthetized through intraperitoneal injection of Medetomidin (0.5 mg/kg), Midazolam (5 mg/kg) and Fentanyl (0.05 mg/kg) followed by application of the substrate D-luciferin. Bioluminescence was measured 10 min later using a Xenogen IVIS In Vivo Imaging System 100 (Caliper Life Sciences (Waltham, USA) with an exposure time of 1 min. Quantification of a signal was performed with a software Living Image (Perkin Elmer (Waltham, USA)).

#### 2.2.4.2 Tumour culture and treatment

mRNA coding for the toxin abrin was produced and tested by Kristin Hirschberger, Ethris (Planegg, Germany). *In vivo* experiment was performed by Eva Kessel, Department of Pharmacy, LMU (Munich, Germany).

KB cells for *in vivo* experiment were cultivated in RPMI 1640 media without folic acid containing 10% FBS and no antibiotics at 37°C, 5% CO<sub>2</sub> in a humidified atmosphere for two weeks before harvesting. After harvesting cells were resuspended in cold PBS to a concentration of 5x10<sup>6</sup> cells/150  $\mu$ L. Until the subcutaneous injection into mice (strain RjOrl:NMRI-Foxn1nu /Foxn1nu; 6 weeks old females) on the same day, cells were stored on ice. As soon as tumours reached a sufficient size (around

250 mm<sup>3</sup>), lipoplexes were applied via intratumoral injection to anesthetized mice (inhalational anesthesia performed with isoflurane) three times a week. Injections were performed on the same day for all animals with a perceptible tumour with the injection volume of 50 µL containing 10 µg of mRNA and total injection number: six for toxin mRNA encapsulated in targeted lipoplexes, control mRNA in nontargeted lipoplexes, and 2% sucrose control or four in the case of control mRNA in targeted lipoplexes. Animals were examined daily with respect to inspections of the skin/fur, eyes, mucous membranes, respiratory and circulatory systems, somatomotoric activity, behaviour patterns and body weight. Tumour size were measured daily with a caliper using formula " $a \times b^2/2$ " with " $a$ " indicating the length of the tumour and " $b$ " the width. Tumour size and weight were also determined *ex vivo*. Blood samples were collected from the heart using EDTA tubes and analyzed by a Sysmex KX-21N system at Ethris GmbH to determine the following parameters: white blood cells, red blood cells, haemoglobin, haematocrit and platelets. Remaining blood samples were centrifuged at 2000 x g for 5 min at 4°C and the EDTA-containing supernatant were stored at -80°C until used for analysis. Cytokines (IL-10, IL-1β, IL-2, IP-10, IL-6, IFN-α, IFN-γ, IL-12p70, TNF-α and MCP-1) were measured according to the Ethris' protocols using ProcartaPlex™ Multiplex Immunoassay custom kits (eBioscience (San Diego, USA)) in combination with the Magpix instrument (Luminex Corporation (Austin, USA)). Mice were euthanized by cervical dislocation.

IVIS luminescence imaging was performed 24 h after intratumoral treatment. 100 µL of luciferin (60 mg luciferin/mL PBS) was administered intraperitoneally 15 min prior to imaging process.

### 2.2.5 Statistical analysis

Data are presented as means ± SEM. The significant differences between the groups were analyzed by one-way ANOVA, and a P value of <0.05 was considered significant.



### 3 Results

The subject of this thesis was the development and characterization of a lipid-based carrier for mRNA delivery *in vivo* that would fulfil criteria of high efficiency and stability without toxic side effects. Specifically, the ultimate goal was to target the liver via systemic administration. Since many metabolic processes are related to this organ, transcript therapy could enable treatments for a wide variety of genetic diseases. Similar to most nucleic acid based macromolecular drugs, extracellular stabilization and efficient intracellular transport represent the bottleneck in the development of an mRNA-therapeutic product. Since mRNA as a single stranded molecule has different physical properties than other nucleic acids, there is a high demand for the development of lipid-based vehicles tailored to the characteristics of mRNA.

Based on a literature search on nucleic acid delivery, a model system using mRNA coding for a reporter protein and four lipidic components (a lipidoid, two helper lipids and a PEG-lipid) was chosen. From this starting point, side-by-side comparisons of each presumably influencing factor, mostly in terms of transfection efficiency, were made in order to optimize formulations for mRNA delivery. The results are presented and described in the following chapters. Each experiment was performed using the same composition, nitrogen to phosphate (N/P) ratio, formulation conditions etc., unless stated differently. (A list of all formulations has been added to the appendix)

#### 3.1 Lipidoids

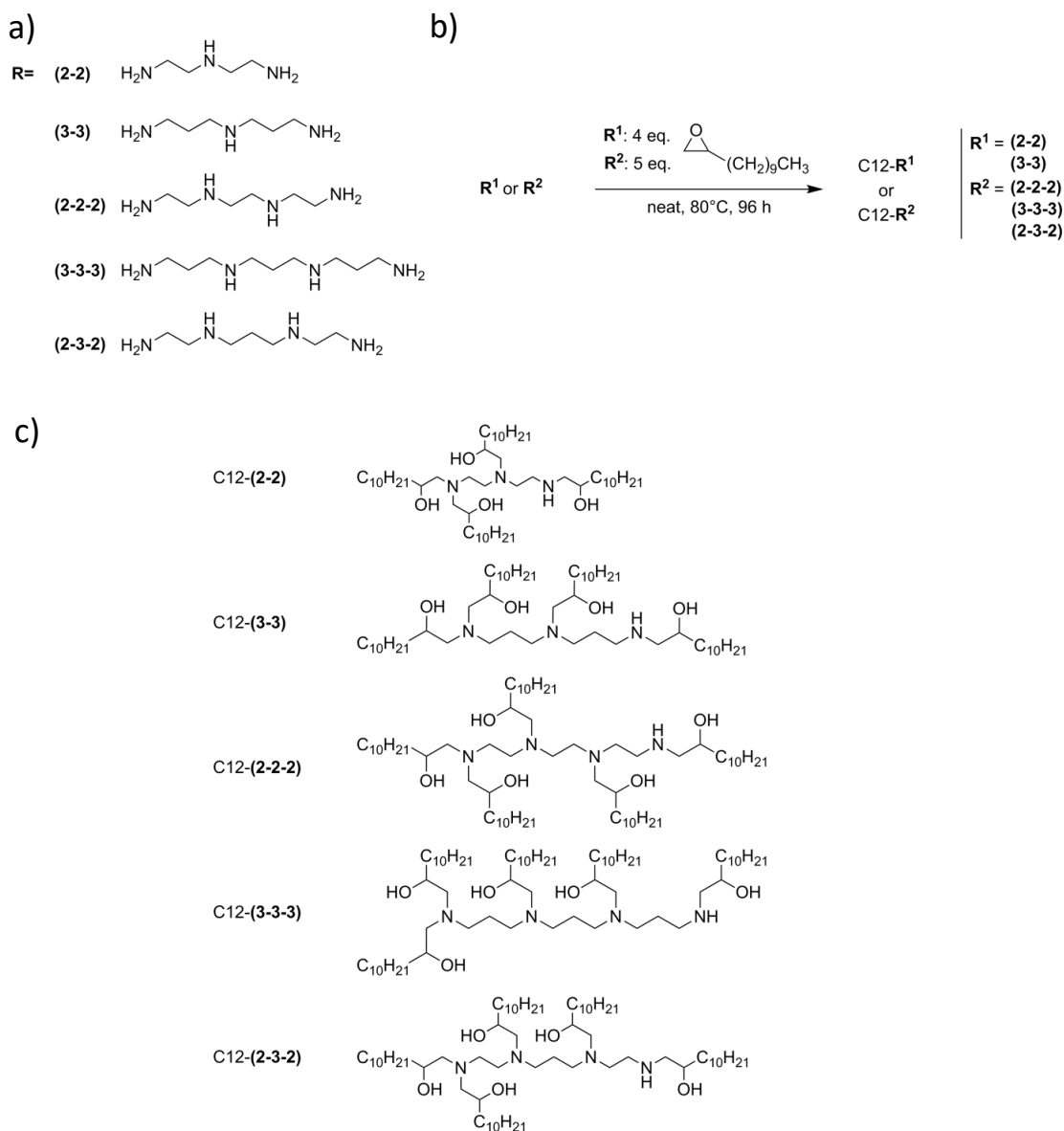
Lipidoids were chosen for the first component screening. A lipidoid enables encapsulation of a polyanionic biomolecule via electrostatic interactions and facilitates the cellular uptake as well as endosomal escape of a complex. The selected modification method, variations of a backbone and alkyl chain length are presented in the next chapter.

### 3.1.1 Oligoalkylamine-based backbone

This chapter has been partly adapted from:

Jarzębińska, A., Pasewald, T., Lambrecht, J., Mykhaylyk, O., Kümmerling, L., Beck, P., Hasenpusch, G., Rudolph, C., Plank, C. and Dohmen, C., 2016. A Single Methylene Group in Oligoalkylamine-Based Cationic Polymers and Lipids Promotes Enhanced mRNA Delivery. *Angewandte Chemie International Edition*, 55(33), pp.9591-9595.

As small oligoalkylamine structures are known for effective carriers of various nucleic acids, five lipidoids based on such scaffolds were synthesized as shown in Scheme 3.1a. A small set of tri- (2-2, 3-3) and tetramines bearing ethylene (2-2-2) and/or propylene spacers (2-3-2, 3-3-3) were modified with C12 alkyl chains by applying the method reported by Love *et al.*<sup>[44]</sup> Purification of the lipids was circumvented by performing a one-pot reaction with a ring-opening of CH<sub>3</sub>(CH<sub>2</sub>)<sub>9</sub>-epoxide (4 or 5 equivalents, no excess) by oligoalkylamines (reaction on Scheme 3.1b; resulting lipids are shown in Scheme 3.1c).



**Scheme 3.1.** a) Structures of oligoalkylamines. b) Synthesis of oligoalkylamine-based lipids. c) Structures of C12-decorated oligoalkylamines.

Resulting C12-oligoalkylamine lipidoids were subsequently screened for their buffering capacity, characterized in terms of physicochemical properties and transfection efficiency in lipid nanoparticles as described in the following chapters.

### Buffering capacity as a predictor of endosomal escape capability

The cellular uptake pathway of lipoplexes usually comprises endocytosis.<sup>[62]</sup> The transfection efficacy is dependent on complex release from the endosome into the cytosol to avoid lysosomal degradation. It is hypothesized that a key parameter which determines transfection efficiency of any nucleic acid delivery agent is an acid

dissociation constant, i.e. a  $pK_a$  value  $pK_a < 7$ . Optimal values are in a pH range of 6.2 to 6.5, which enhance endosomal escape of the carrier complex into the cytoplasm through membrane disruption by positively charged nanoparticle surface.<sup>[21]</sup> This step could be expected to be critical in the process of mRNA delivery as well and therefore, the buffering capacity for each structure was determined by potentiometric titration to predict their potency in mRNA delivery (Figure 3.1).

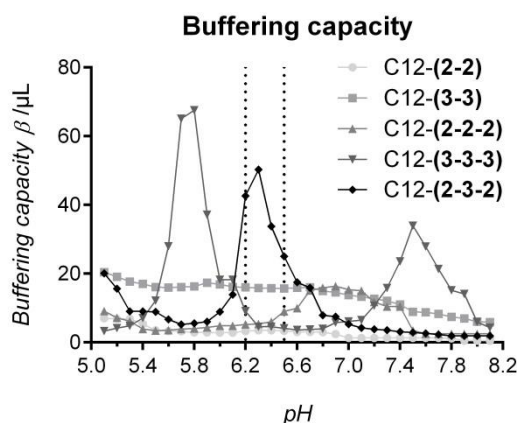


**Figure 3.1.** Plots of buffering capacities of C12-lipids with oligoalkylamine backbones. The area in between the dotted lines indicates the ideal buffering range for nucleic acid carriers, enhancing endosomal escape. Buffering capacity  $\beta$  was defined as volume of 50 mM NaOH added to the solution containing 10 mmoles lipid resulting in a pH change of 0.1.

Whereas the lipid-derivatized triamines (C12-(2-2) and C12-(3-3)) did not possess any increased buffering capability in the tested range (5.1 – 8.0), the tetramines exhibited clear maxima in different pH ranges. However, for C12-(3-3-3) and -(2-2-2), these were above and/or below pH 6.2 and 6.5. Only the C12-(2-3-2) displayed a peak buffering capacity in the desired range and, hence, was a promising candidate for further evaluation.

### Physicochemical properties of lipoplexes

Therapeutic nanoparticles have to fulfil some physicochemical requirements which play a critical role in drug stability, uptake, and efficiency *in vivo*. Therefore, this is the focus of the following chapter. In order to obtain nanoparticles, lipidoids were complexed with chemically modified mRNA together with two helper lipids and a PEG-lipid. Resulting lipoplexes were characterized in terms of their physicochemical properties, namely size, zeta potential, and encapsulation efficiency.

The summarized data is presented in Table 3.1 and Figure 3.2.

**Table 3.1.** Hydrodynamic diameter, zeta potential and encapsulation efficiency of lipoplexes.

Oligoalkylamine	Lipid C12-				
	(2-2)	(3-3)	(2-2-2)	(3-3-3)	(2-3-2)
Hydrodynamic diameter [nm]	61.0±0.9	56.1±0.7	68.8±0.9	54.0±0.3	59.7±0.7
Polydispersity (PDI)	0.227±0.012	0.189±0.005	0.143±0.004	0.154±0.003	0.162±0.002
Zeta potential [mV]	14.6±0.8	0.6±0.5	-1.5±0.1	-0.4±1.0	-0.9±0.4
Encapsulation efficiency [%]	96	100	90	98	97

Lipid-based nanoparticles were found to comprise uniform particles with hydrodynamic diameter between 54 and 61 nm and a neutral or slightly positive zeta potential. The process of mRNA complexation determined by RiboGreen was found to be efficient (>90% encapsulation efficiency, Table 3.1). However, some discrepancies could be observed: lipids with ethylene spacers led to lower encapsulation efficiency values compared to their counterparts with propylene spacers (96% for C12-(2-2) and 100% for C12-(3-3); 90% for C12-(2-2-2) and 98% for C12-(3-3-3)). The lipoplexes with the alternating structure lipid led to relatively high encapsulation efficiency as well (97%).

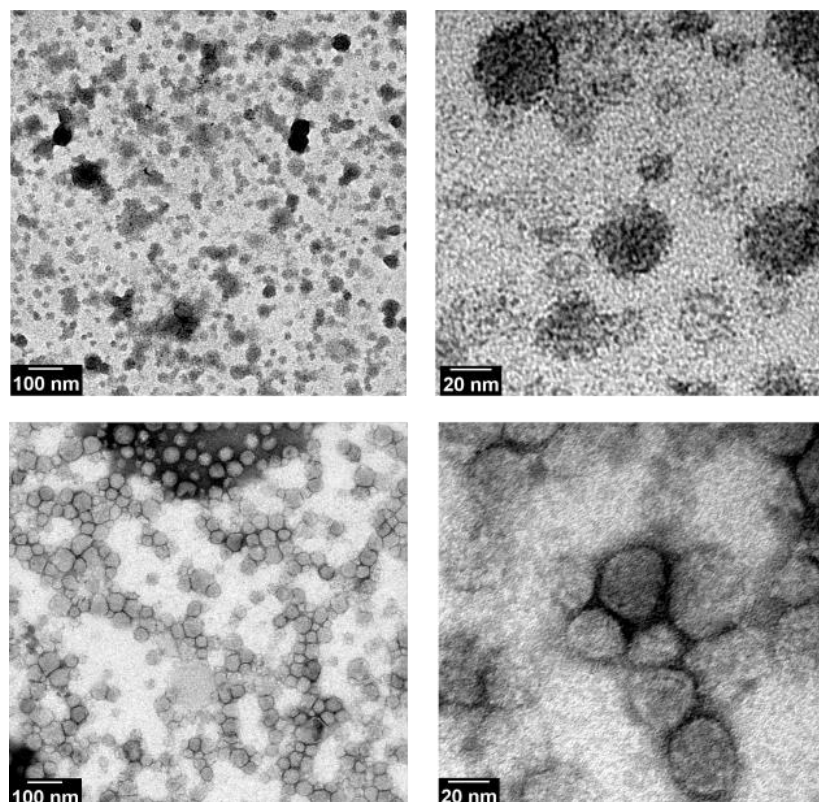


**Figure 3.2.** Transmission electron microscopic (TEM) images of C12-(2-3-2) lipoplexes.

Transmission electron microscopy images revealed the spherical shape of the resulting lipoplexes. Moreover, the observation from an agarose gel (Figure 3.3) proved that the encapsulated mRNA molecules remained intact.

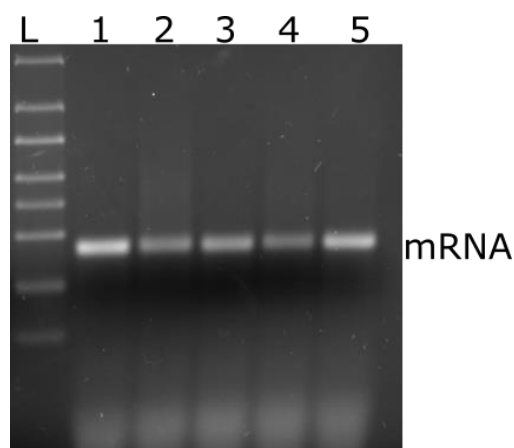


**Figure 3.3.** Agarose gel of C12-(2-2), -(3-3), -(2-2-2), -(3-3-3) and -(2-3-2) lipoplexes, (numbered 1-5, respectively), treated with heparin and Triton X-100. L=mRNA ladder.

All particles formed from tested lipidoids exhibited comparable physicochemical properties meeting the requirements of nucleic acid complexes.

### Cellular uptake

Since sufficient particle uptake is a prerequisite for high transfection efficiency, the efficacy of this process was determined for each tested lipidoid. Therefore, the amounts of reporter mRNA in NIH 3T3 cells treated with lipoplexes (in a dose of  $\sim 3$  pg mRNA per cell) were quantified via qPCR. Briefly, cells were incubated with lipoplexes varying in the type of lipidoid and after 0.5, 1, 2, or 4 h the amount of the reporter mRNA was evaluated based on a standard curve of pure mRNA of the same sequence (Figure 3.4).

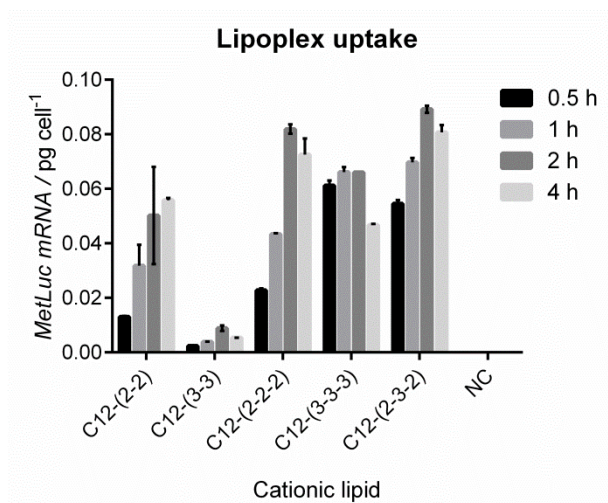


**Figure 3.4.** Levels of lipoplex uptake in NIH 3T3 cells after 0.5, 1, 2, and 4 h of incubation expressed as detected *Metridia luciferase* mRNA amount per cell. Complexes were applied at doses of 3.1 pg mRNA/cell. (NC = negative control, untreated cells)

Already 0.5 h after transfection, high levels of reporter mRNA in the cells were observed for C12-(3-3-3) and C12-(2-3-2). In the case of C12-(2-2-2), relatively steep increase with time could be noted, whereas for C12-(3-3-3) the values stayed at almost the same level, independently of the time point. In general, the lipoplex uptake in C12-(2-3-2), C12-(3-3-3), and C12-(2-2-2)-treated cells was in the comparable range. It was noticeably lower for C12-(2-2) and hardly any uptake could be observed for C12-(3-3).

### Cytotoxicity

One possible reason for varying protein levels could be differences in toxic effects caused by transfection with lipoplexes. To exclude this factor a cell viability assay was conducted in parallel with transfection experiments. Briefly, 24 h after transfection with lipoplexes from the oligoalkylamine lipid library, an MTT assay was per-

formed to evaluate metabolic activity of the cells, which correlates with their viability. The untreated cells were used as a reference (100% viable cells). Results are shown in Figure 3.5.

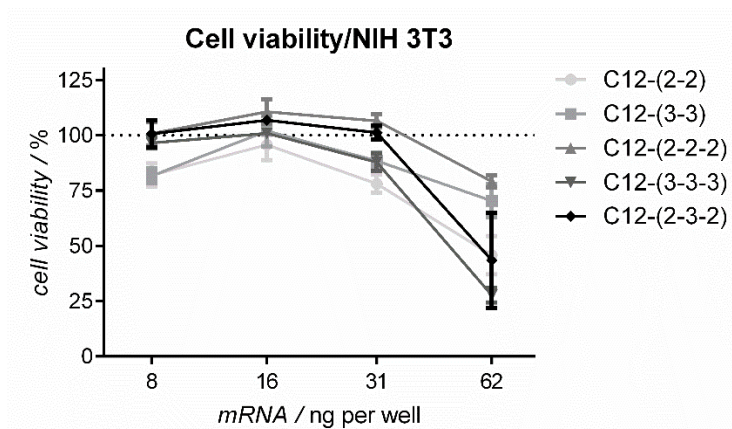


**Figure 3.5.** Influence of lipoplexes on cell viability of NIH 3T3 cells 24 h after transfection was evaluated using an MTT assay.

The lipidoid C12-(2-2-2) was the least toxic structure from all tested ones, whereas triamine-based lipids as well as C12-(3-3-3) were less well-tolerated. However, at doses of complexed mRNA lower than 62 ng/well, 100% cells were viable after treatment with C12-(2-3-2) (all values referred to the negative control, untransfected cells).

### Transfection efficiency

The most important characteristic of any potential drug is its functionality. In the case of mRNA-based therapeutic it is determined by the resulting protein level. Therefore, the set of oligoalkylamine-based lipidoids was screened *in vitro* on murine fibroblasts (NIH 3T3 cells) for their ability to transfect cells using chemically modified mRNA coding for firefly luciferase (mRNA-FLuc) as a reporter (Figure 3.6a) complexed additionally with of two helper lipids and a PEG-lipid. Since the lipoplexes were investigated with the aim of protein production in the liver after systemic administration, they were additionally tested on target tissue-derived, human liver carcinoma cells (HepG2, Figure 3.6b). Moreover, to learn more about structure-activity relationship, two other cell types were transfected: lung-derived human alveolar type II like cells A549 and rat adipose tissue-derived stem cells AMSC (Figure 3.6c-d).



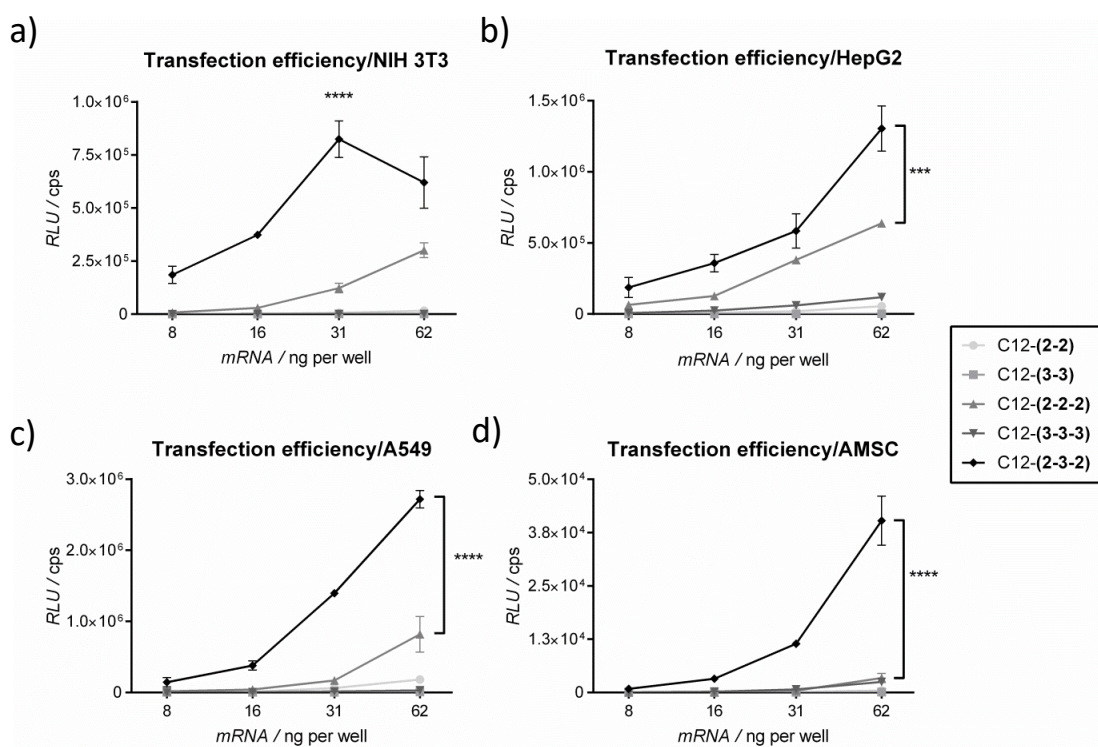


**Figure 3.6.** Transfection efficiency of lipoplexes carrying mRNA-FLuc on a) murine fibroblasts (NIH 3T3), b) target tissue-derived human liver carcinoma cells (HepG2), c) human alveolar type II like cells (A549), and d) adipose mesenchymal stem cells (AMSC). The protein level was determined 24 h post transfection by measuring bioluminescence expressed in counts per second (cps).

In all four tested cell lines triamine-based lipidoids exhibited only low levels of reporter enzyme activity. In contrast, the lipidoids C12-(2-3-2) and C12-(2-2-2) led to decent protein levels in NIH 3T3, HepG2 and A549. Interestingly, the best performing lipidoid proved to be C12-(2-3-2) with alternating oligoalkylamine structure, reaching nearly 7-fold increase compared to second best C12-(2-2-2) (NIH 3T3, 31 ng/well) and demonstrated high transfection efficiency even at low doses of mRNA. Importantly, the trend of superior efficiency of C12-(2-3-2) lipoplexes was independent of cell type, suggesting the existence of a more general structural rule.

#### ***In vivo* proof of concept**

With the goal of developing a carrier system suitable for intravenous application and enabling efficient protein translation *in vivo*, the potency of lipoplexes consisting of tetramine-based lipids to deliver mRNA was investigated in female Balb/c mice. Triamine-based lipids were excluded from the experiment due to their lack of functionality *in vitro*. Animals were treated with a dose of 1 mg/kg via tail vein injec-

tion. Bioluminescence images of the whole bodies, excised livers as well as quantification of bioluminescence intensity 6 h after treatment are shown in Figure 3.7.

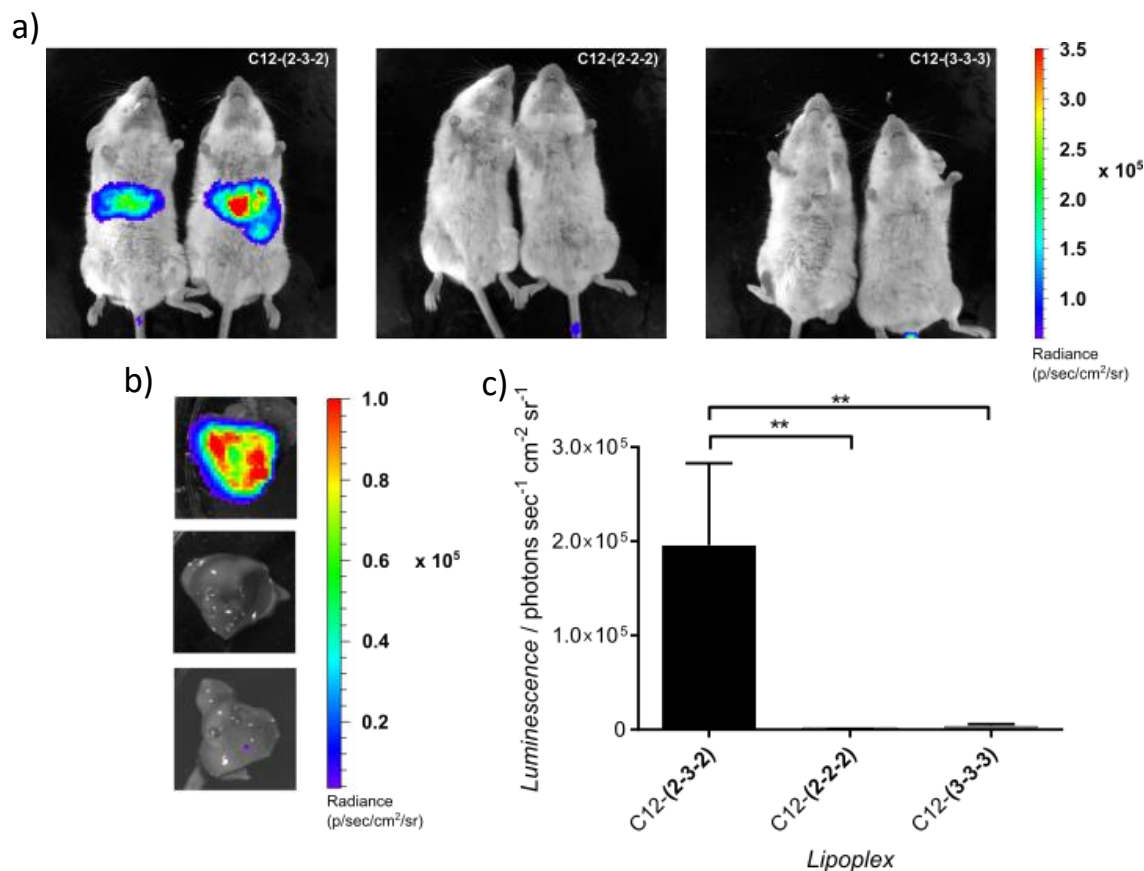


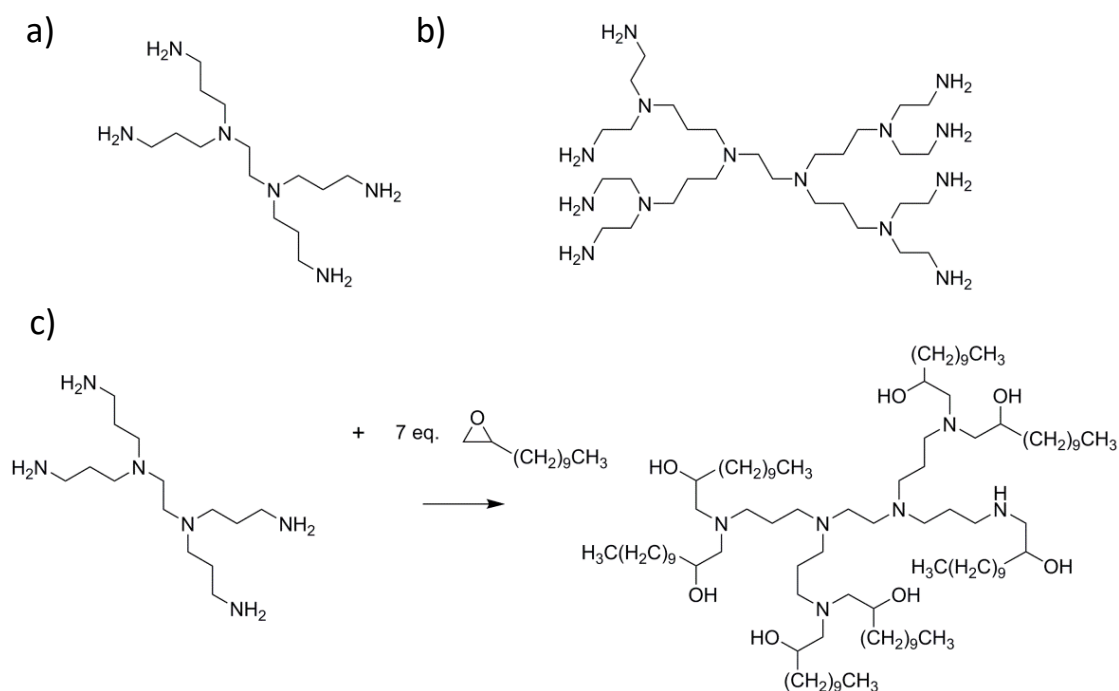
**Figure 3.7.** a) Exemplary bioluminescence images of mice treated intravenously with 18  $\mu$ g mRNA-FLuc complexed with C12-(2-3-2), C12-(2-2-2), and C12-(3-3-3). b) Exemplary bioluminescence images of excised livers. c) Quantification of bioluminescence intensity in treated mice (observed in a)).  $n=3$ . \*\* $p<0.01$ , \*\*\* $p<0.001$ , and \*\*\*\* $p<0.0001$ .

Bioluminescence in animals treated with lipidoids C12-(2-2-2) and C12-(3-3-3) was at the background level, whereas a strong signal in the liver of C12-(2-3-2)-treated mice was observed (Figure 3.7a-c). Results from cell culture experiments which indicated that the alternating structure is beneficial over the other oligoalkylamines was therefore confirmed also in an *in vivo* setting.

In conclusion, by screening a set of oligoalkylamines for efficient delivery of mRNA in nanoparticles, it was found that a tetramine with alternating ethyl–propyl–ethyl spacers modified with C12 alkyl chains exhibited a high ability to mediate robust levels of protein translation *in vitro* as well as *in vivo*.

### 3.1.2 Oligoalkylamine-based dendrimers

After finding that the motif based on (2-3-2) oligoalkylamine is successful in mRNA delivery in lipoplexes, the aim was to test if it may be modified to further improve mRNA delivery. Since the alternating structure proved to be critical for efficient translation of a nucleic acid, more complex, branched scaffolds based on it were investigated. For this purpose, (2-3-2)-dendrimers were chosen, as shown in Scheme 2. Lipid derivatives were synthesized from such scaffolds using the same method as described in Chapter 3.1.1. Two generations of (2-3-2)-dendrimers, G1 and G2 were modified with alkyl epoxides of C8, C12, and C16 chain lengths (resulting scaffolds are summarized in Table 3.2) and subsequently tested *in vitro* as well as *in vivo*.



**Scheme 3.2.** Structures of generations a) G1 and b) G2 of (2-3-2) dendrimers and c) synthesis of dendrimer scaffolds modified with alkyl epoxides of various carbon chain lengths on the example of G1 modified with C12-epoxide.

**Table 3.2.** A summary of generated (2-3-2) dendrimers modified with alkyl epoxides of C8, C12, and C16 chain lengths.

Dendrimers	Dendrimer generation	
	G1	G2
Alkyl epoxide length		
C8	C8-G1	C8-G2
C12	C12-G1	C12-G2
C16	C16-G1	C16-G2

All modified dendrimers were tested for their transfection efficiency *in vitro* in formulations containing helper lipids and a PEG-lipid at N/P 10, with dendrimers serving as lipidoids (see Figure 3.8, C12-(2-3-2) (C12-G0) added as a reference).

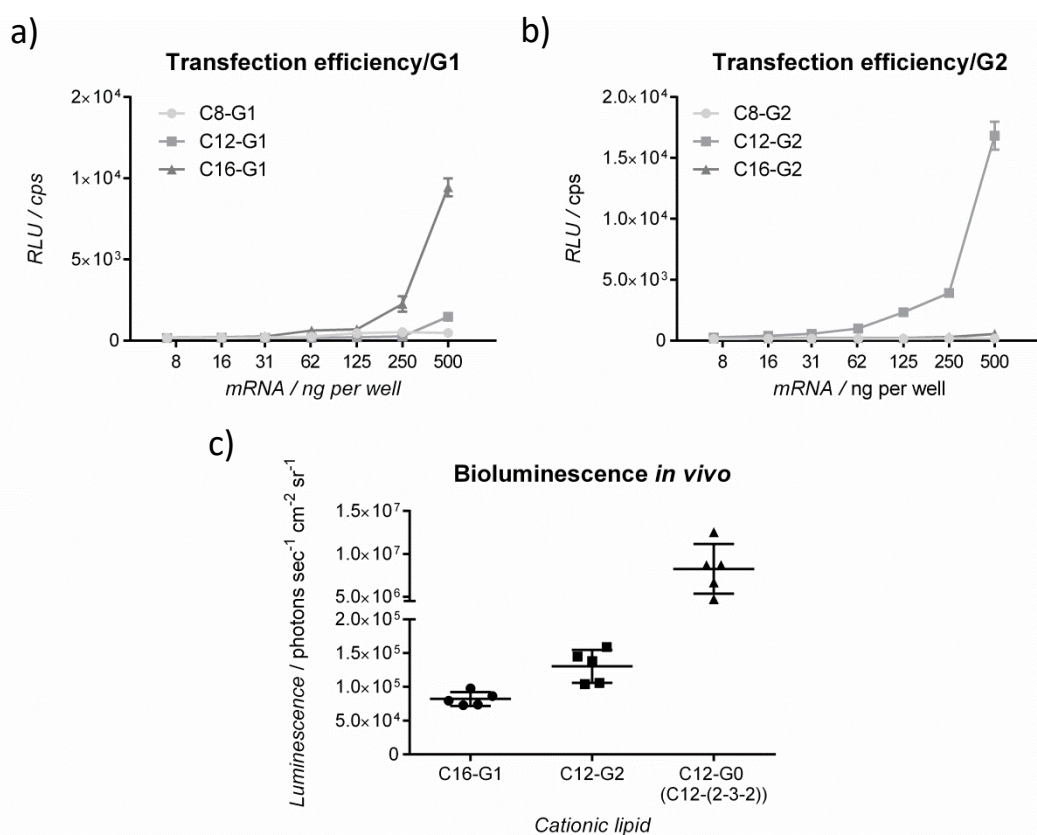


**Figure 3.8.** Transfection efficiency in murine fibroblasts (NIH 3T3) of a) G1 and b) G2 dendrimers modified with alkyl epoxides of various carbon chain lengths. c) Bioluminescence of *in vitro* best performers, C16-G1 and C12-G2, in comparison with previously tested C12-(2-3-2), C12-G0. Mice were treated intravenously with 20  $\mu$ g mRNA-FLuc complexed with corresponding lipidoid, helper lipids and a PEG-lipid.

The two most promising carriers were identified *in vitro*: one from G1 and one from G2 group. Interestingly, one was modified with C16 alkyl chain and the other with C12 (C16-G1 and C12-G2, respectively). Therefore, these two formulations were tested *in vivo* as well, leading to detectable luminescence values. Both constructs were almost at the same level: C12-G2 was not even 2-fold more efficient than C16-G1. However, in both cases bioluminescence was 100-fold lower than in the case of C12-(2-3-2) lipoplexes (corresponding formulation was added to Figure 3.8c as a reference, “C12-G0”). Worth noting, encapsulation efficiency yielded only 23% and 49% in C16-G1 and C12-G2, respectively.

In summary, the extended alternating motif of oligoalkylamine in the form of dendrimers was also able to deliver successfully mRNA into cells, both *in vitro* as well as *in vivo*. Nonetheless, the resulting mRNA translation did not reach the levels obtained with the original structure of (2-3-2).

### 3.1.3 Alkyl chain length of lipidoids

Initial modifications of oligoalkylamines with alkyl chains were performed with  $\text{CH}_3(\text{CH}_2)_9$ -epoxides, resulting in C12-lipids. In the next step the influence of alkyl chain length on the properties of a lipidic carrier was explored.

Therefore, a screening of (2-3-2) oligoalkylamine-based lipids modified with C5-C16 alkyl chains was conducted *in vitro* in terms of their transfection efficiencies (Figure 3.9). Lipoplexes were formed in the same composition with mRNA-FLuc as a reporter, varying only in the lipidoid.

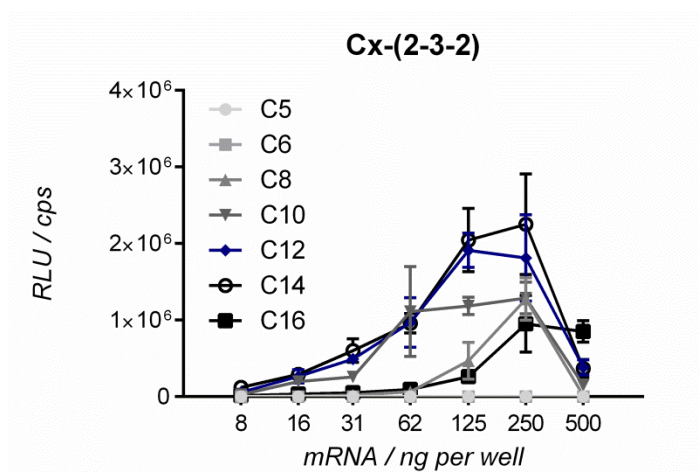


**Figure 3.9.** Transfection efficiency of lipoplexes consisting of (2-3-2) lipids with different alkyl chain lengths on murine fibroblasts (NIH 3T3). FLuc was used as a reporter mRNA and the protein level was determined 24 h post transfection by measuring bioluminescence expressed in counts per second (cps).

For all tested lipidoids a dose-dependent increase in reporter level could be observed, except the shortest alkyl chains C5 and C6-(2-3-2), which showed no transfection at all. The drop in efficiency at the highest dose, 500 ng/well, was presumably due to toxicity of the particles. In the non-toxic dose range, C12 and C14 led to the best results. The efficiency seemed to decrease with either lower alkyl lengths (C10 and C8) as well as higher alkyl length (C16).

Based on *in vitro* results, C5 and C6 lipidoids were excluded from the *in vivo* study. The other five were tested in mice treated with a dose of 1 mg/kg via tail vein injection, as shown in Figure 3.10.

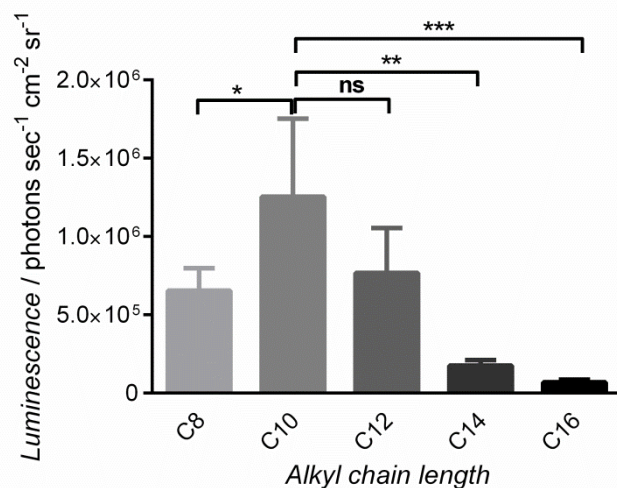


**Figure 3.10.** Quantification of bioluminescence intensity in mice treated with lipoplexes consisting of C8-, C10-, C12-, C14-, and C16-(2-3-2).

The results showed an alkyl chain length dependency with a maximal efficiency for C10-(2-3-2) and a decrease with both increasing and decreasing lengths. However, there was no significant difference between this alkyl chain and C12. Thus, both C10- and C12-(2-3-2) could be considered as the most promising lipidoids for mRNA delivery.

### 3.2 Helper lipids

The standard multicomponent lipoplex formulation described in this thesis contained two helper lipids: cholesterol and a phospholipid. Whereas the neutral helper lipid, cholesterol contributes to rigidity and stability of lipid nanoparticles,<sup>[63]</sup> the role of a phospholipid in lipoplexes covers additionally electrostatic interactions in mRNA-lipid complexes.<sup>[50]</sup> In this chapter, the importance of the latter was tested as well as the influence of variations in the composition.

#### 3.2.1 Phospholipid type

Since cholesterol seems to be a crucial component of lipid complexes, only the phospholipid type was tested in following experiments. As a starting point, 1,2-dioleoyl-sn-glycero-3-phosphoethanolamine (DOPE) was used in the formulation. At



first, the critical role of a phospholipid in general, a neutral lipid comprising two charges, was investigated by its replacement with cholesterol (Figure 3.11).

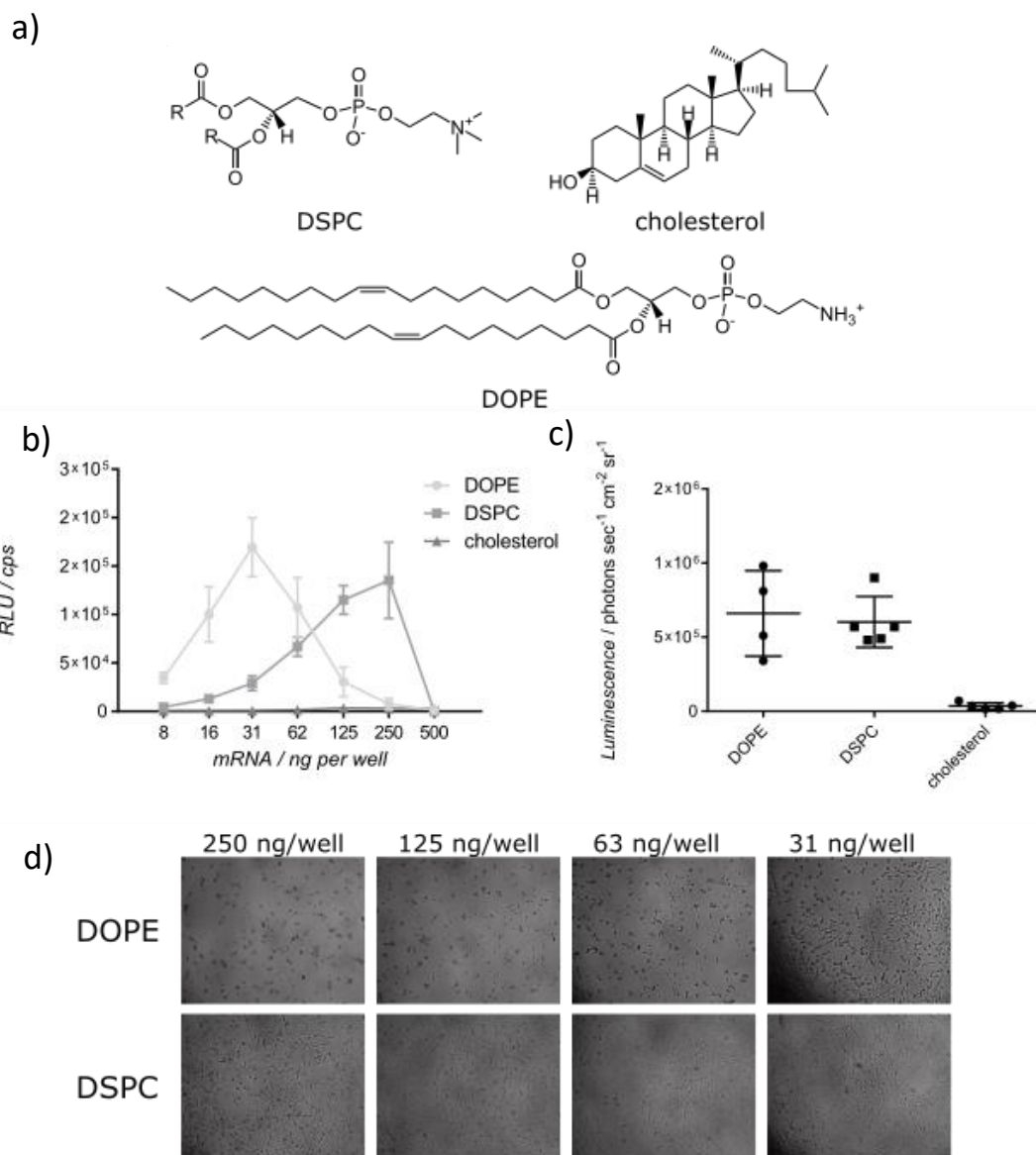


**Figure 3.11.** a) Structures of three compared helper lipids: DSPC ( $R=C18:0$ ), cholesterol and DOPE. b) Comparison of transfection efficiency in murine fibroblasts (NIH 3T3) and c) in mice of these helper lipids incorporated in lipoplexes with FLuc. d) Microscopic pictures of cells (NIH 3T3) 24 h after transfection with lipoplexes comprising helper lipids DOPE or DSPC.

How important the presence of a phospholipid is, was clearly observed when DOPE was completely replaced by cholesterol. As shown in Figure 3.11b-c, barely any transfection occurred, both *in vitro* as well as *in vivo* for a formulation comprising only cholesterol. On the other hand, when DOPE was exchanged to another type of phospholipid, 1,2-distearoyl-*sn*-glycero-3-phosphocholine (DSPC), the transfection peak appeared again, although shifted to higher mRNA doses *in vitro*. Such a result

could indicate possibly a better tolerability of phosphocholines in comparison with phosphoethanolamines. This hypothesis was investigated by analyzing microscopic pictures of the treated cells (Figure 3.11d). DOPE formulations led to toxic effect down to the dose of 31 ng mRNA/well as indicated by the changed appearance of cells (round and shrunken), whereas DSPC formulations were well tolerated at doses as high as 250 ng/well. The bioluminescence in mice (Figure 3.11c) after injection of lipoplexes comprising DOPE, DSPC, or cholesterol showed the same dependency as observed *in vitro*. A formulation without a phospholipid did not result in efficient mRNA translation. In addition, no significant difference between DOPE and DSPC could be noted *in vivo*.

In conclusion, it was found that the presence of a phospholipid in lipoplexes is critical for their functionality. Moreover, the phospholipid type showed to have an impact on both transfection efficiency and toxicity of a complex.

### 3.2.2 Phospholipid alkyl chain length and saturation

Due to better tolerability of phosphocholines (PCs) *in vitro*, this type of phospholipid became a subject of further studies. A series of different PCs varying between each other in alkyl chain length or its saturation were further tested both *in vitro* as well as *in vivo*. Three PCs with saturated alkyl chains: 16:0 (1,2-dipalmitoyl-sn-glycero-3-phosphocholine, DPPC), 14:0 (1,2-dimyristoyl-sn-glycero-3-phosphocholine, DMPC) and 12:0 (1,2-dilauroyl-sn-glycero-3-phosphocholine, DLPC) were chosen as well as one with unsaturated alkyl chain, corresponding to its counterpart among phosphoethanolamines (DOPE), 18:1 (1,2-dioleoyl-sn-glycero-3-phosphocholine, DOPC), and diether 16:0 (1,2-di-O-hexadecyl-sn-glycero-3-phosphocholine, DePC). DSPC (18:0) was excluded from further experiments as it was found to form unstable particles (precipitate occurred after some time). The comparisons of lipoplex size, zeta potential, the efficiency *in vitro* and *in vivo* are shown in Figure 3.12.



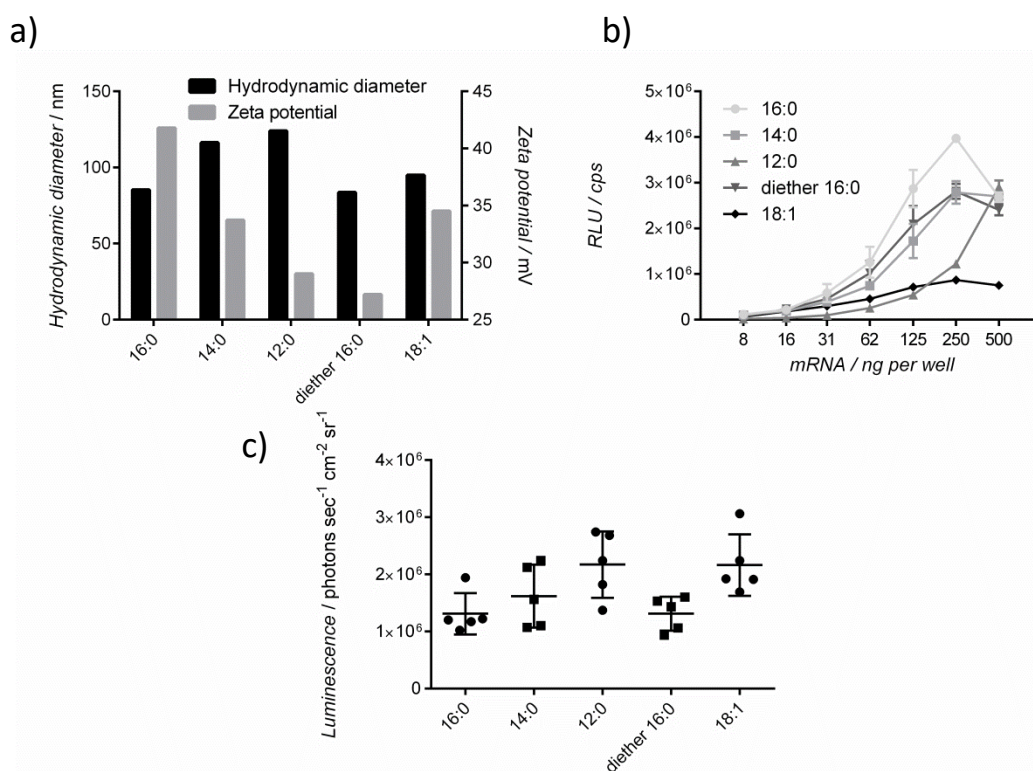


**Figure 3.12.** Comparison of a) size, zeta potential and transfection efficiency b) in murine fibroblasts (NIH 3T3) or c) mice of different phosphocholine-based helper lipids incorporated in lipoplexes with FLuc.

Even though no major differences in size between particles could be observed, their zeta potential decreased with shorter alkyl chain lengths (from 42 down to 29 mV, Figure 3.12a). The lowest zeta potential was noted for diether chains, whereas the 18:1 PC showed values comparable to 16:0 PC. The encapsulation efficiency of DOPC (18:1)-comprising lipoplexes was lower than of all others tested (87% compared to 95-98%, data not shown), which was reflected by the lowest transfection efficiency (Figure 3.12b). Despite similar transfection efficiency of DLPC (12:0) compared with the other formulations at high 500 ng/well, a sudden drop in efficiency was observed at lower doses. Whereas DMPC (14:0) and DePC (diether 16:0) showed similar transfection levels, DPPC (16:0) led to the highest recorded amounts of translated protein. In summary, it could be concluded from the *in vitro* experiment that: i) the efficiency decreased with shorter alkyl chain length of a PC; ii) alkyl chain was beneficial over its diether counterpart; iii) saturated alkyl chains were more efficient than unsaturated ones.

Interestingly, *in vivo* bioluminescence (Figure 3.12c) measurements showed the opposite trend with shorter saturated alkyl chains (16:0 < 14:0 < 12:0) leading to high-

er efficiency as compared with *in vitro* results. Moreover, no significant difference could be observed between 16:0 alkyl and diether 16:0 chains. It also seemed that the unsaturated alkyl chain PC (18:1, DOPC) was more active in mRNA delivery than some saturated alkyl chain PCs. In conclusion, a tendency towards DLPC (12:0) and DOPC (18:1) as the most efficient *in vivo* was observed.

### 3.2.3 Variations in the lipid composition

Not only variations in components themselves, but also in ratios between them can have an impact on lipoplex formation, stability, charge transfer, and, hence, transfection efficiency. As every single lipid plays a different role in mRNA delivery, it was important to determine how variation of the amounts of a single helper lipid (PEG-lipids are described in Chapter 3.3) would influence the ability to deliver mRNA into cells.

At first, the question about the effect of removing two or a single helper lipid was addressed. In this experiment (Table 3.3, 1<sup>st</sup> set), the amounts of a lipidoid C12-(2-3-2) and a PEG-lipid (DMG-PEG2k) were kept constant. One formulation contained no helper lipids at all; three formulations contained no phospholipid (DPPC), whereas cholesterol amount was either lower, equal, or higher than in the standard formulation. Three formulations contained no cholesterol, whereas DPPC amount was either lower, equal, or higher than in the standard formulation. The second set of experiments (Table 3.3, 2<sup>nd</sup> set) was performed to test the influence of varying amounts of one of the helper lipids when the second helper lipid is present but in only small, constant quantity (amounts of cholesterol higher, equal, or lower than standard, while DPPC amount constantly low and the opposite). The third set of experiments (Table 3.3, 3<sup>rd</sup> set) was designed in order to verify whether reduced PEG-shielding would alter the influence of a single helper lipid. Here, the second helper lipid was also kept at a constant, low ratio. The conditions of all three sets of experiments are summarized in Table 3.3; differences in relation to the standard amounts were marked red.

**Table 3.3.** Summary of molar ratios of the lipids in all three sets of experiments testing single lipid influence.

<b>1<sup>st</sup> set</b>	<b>C12-(2-3-2)</b>	<b>DPPC</b>	<b>Cholesterol</b>	<b>DMG-PEG2k</b>
<u>Standard formulation</u>	<u>8</u>	<u>5.29</u>	<u>4.41</u>	<u>0.88</u>
No helper lipids	8	0	0	0.88
Cholesterol low	8	0	2	0.88
Cholesterol mid	8	0	4.41	0.88
Cholesterol high	8	0	6	0.88
DPPC low	8	3	0	0.88
DPPC mid	8	5.29	0	0.88
DPPC high	8	7	0	0.88
<b>2<sup>nd</sup> set</b>				
Cholesterol low	8	0.8	2	0.88
Cholesterol mid	8	0.8	4.41	0.88
Cholesterol high	8	0.8	6	0.88
DPPC low	8	3	0.8	0.88
DPPC mid	8	5.29	0.8	0.88
DPPC high	8	7	0.8	0.88
<b>3<sup>rd</sup> set</b>				
Cholesterol low	8	2	0.8	0.24
Cholesterol mid	8	4.41	0.8	0.24
Cholesterol high	8	6	0.8	0.24
DPPC low	8	0.8	3	0.24
DPPC mid	8	0.8	5.29	0.24
DPPC high	8	0.8	7	0.24

All described formulations were characterized in terms of their physicochemical properties (size, zeta potential) and transfection efficiency *in vitro* (see Figure 3.13).

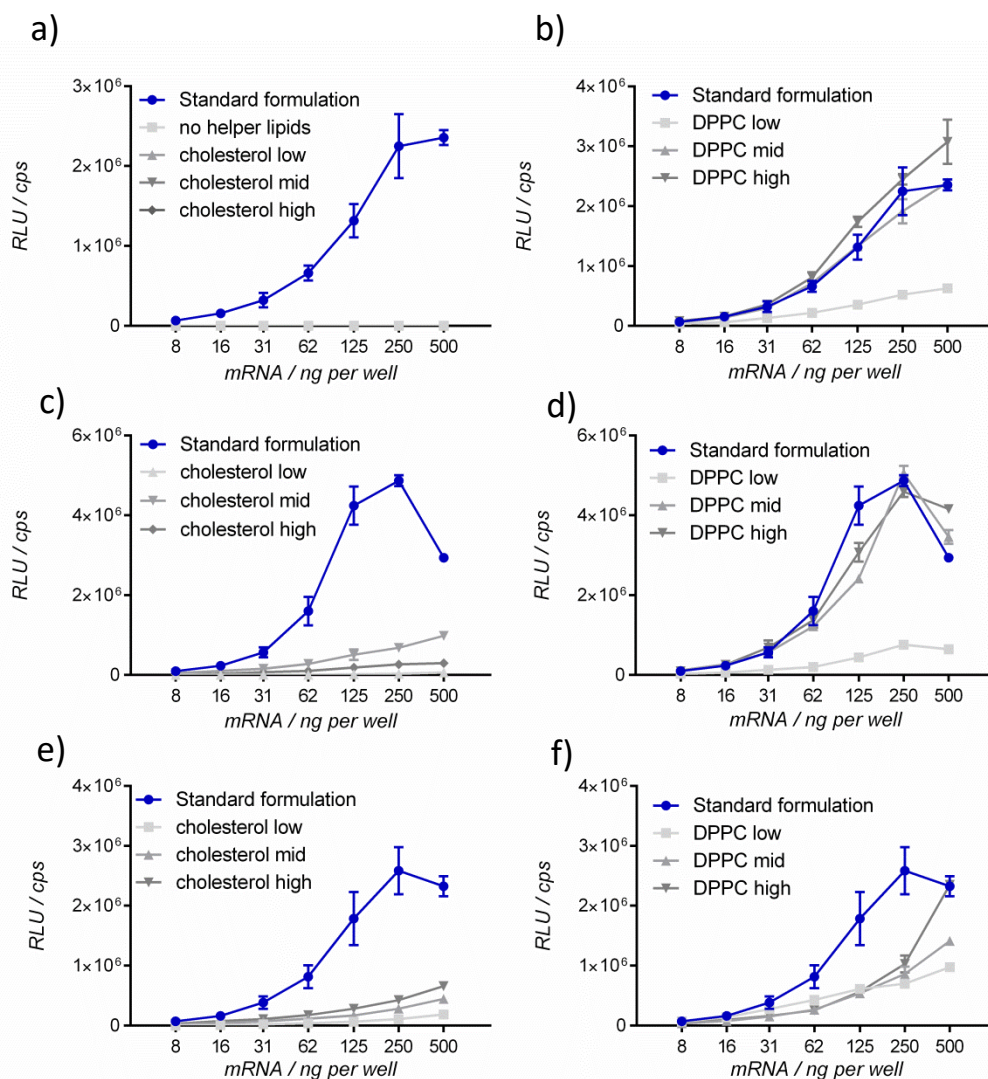


**Figure 3.13.** The influence of a single helper lipid on transfection efficiency in murine fibroblasts (NIH 3T3). In lipoplexes in a) and b) one or both of the helper lipids were completely removed, whereas the amounts of the second were varied; in c) and d) the amount of one of the helper lipids was kept constant, whereas the amounts of the second were varied; in e) and f) the amount of one of the helper lipids was kept constant and the amount of the PEG-lipid was reduced, whereas the amounts of the second helper lipid were varied.

The first set of experiments revealed that the formulations without DPPC were non-functional, independently of cholesterol content (Figure 3.13a). In addition, a positive correlation between the phospholipid quantity and particle activity was observed, despite lack of cholesterol in the formulation (Figure 3.13b). The efficiency of standard lipoplexes (marked blue in the graph) was even exceeded when more DPPC was incorporated in the formulation. In the second set of experiments a tendency to enhanced transfection efficiency with higher amounts of DPPC was further confirmed (Figure 3.13d). On the contrary to the phospholipid, the variation in cholesterol amount did not show a strong influence on the efficacy of protein produc-

tion (Figure 3.13c). In the case of reduced PEG-shielding (third set of experiments), the trend was not as pronounced as observed for formulations with a higher PEG amount (first and second set), but still showing a strong correlation between high transfection efficiency and increased amount of a phospholipid. As shown in Figure 3.13e, a slight increase in activity was observed with higher cholesterol content. Yet, the values were much lower in comparison with the standard formulation (blue curve). Similarly, for the formulation with varying DPPC amounts at lower PEG content, transfection rates were below the level of standard lipoplexes (Figure 3.13f). However, the efficiencies showed an increase compared to cholesterol formulations and additionally a dependence on the DPPC amount. On the other hand, a general decrease resulting from lowered PEG-shielding should be noted.

In all sets of experiments, no correlation between size, polydispersity or zeta potential of the particles and variation in the single lipid amounts was found.

The presented results showed that the presence of a phospholipid in a formulation is essential for its functionality and indicated a strong correlation between the phospholipid amount and transfection efficiency. The effect of the second helper lipid, cholesterol, was less significant. In addition, the reduction in PEG-coating minimized the influence of a phospholipid and led to decreased efficacy.

### 3.3 The importance of a PEG-lipid in lipoplex shielding

A PEG-lipid plays a critical role in lipoplex composition as a shielding agent, enabling prolonged circulation in the blood and preventing undesirable interactions. There are a couple of variables in a PEG-lipid, which could have an influence on complex stability and transfection efficiency: i) a PEG lipid type (i.e. glycerolipid vs. glycerophospholipid), anchor length and ii) if saturated or unsaturated, iii) as well as polyethylene glycol length. Some selected comparisons of these are presented in the following chapter.

#### 3.3.1 PEG lipid type and anchor chain saturation

As a starting point in the lipid formulation included 1,2-dimyristoyl-*sn*-glycero-3-phosphoethanolamine-N-[methoxy(polyethylene glycol)-2000] (ammonium salt) (DMPE-PEG2k), a PEG-lipid with two compensating charges in the backbone. The

first aim was to compare it with a neutral PEG-lipid widely used in nucleic acid delivery, 1,2-dimyristoyl-*sn*-glycerol, methoxypolyethylene glycol (DMG-PEG2k). Therefore, lipoplexes varying in one PEG-lipid type only, were tested for their transfection efficiency *in vitro* as well as *in vivo* (see Figure 3.14).

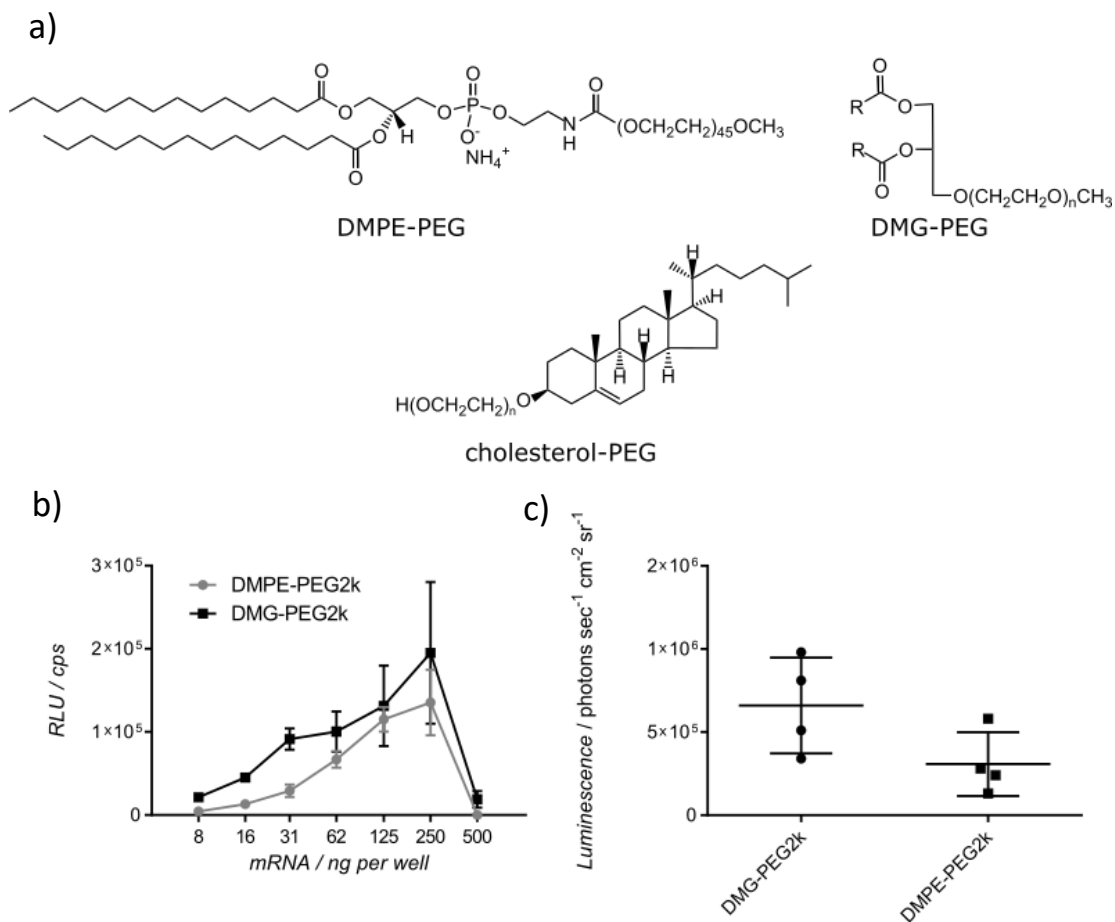


**Figure 3.14.** a) Chemical structures of DMPE-PEG2k and DMG-PEG2k ( $R=C14:0$ ). Comparison of transfection efficiency of lipoplexes comprising DMPE-PEG2k and DMG-PEG2k b) in murine fibroblasts (NIH 3T3) and c) quantification of bioluminescence intensity in treated mice.

As a result, DMG-PEG2k yielded in both cases higher reporter protein levels (Figure 3.14b-c), although its advantages over DMPE-PEG2k became significant only at low doses of (<62 ng/well) *in vitro* and showed just a tendency towards increased translation levels *in vivo*.

Next, the study was extended to comparisons between: i) two neutral lipid types (glycerolipid and cholesterol; see Figure 15a) and ii) two different anchor chains of the same lipid type (glycero-3-phosphoethanolamine backbone) either saturated and short (C14:0) or unsaturated and long (C18:1) (see Figure 3.15b) *in vitro*.

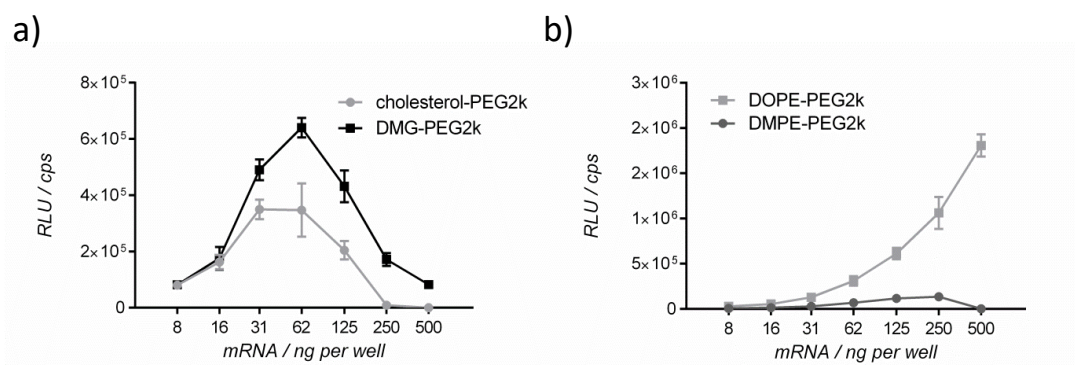


**Figure 3.15.** Comparison of transfection efficiency in murine fibroblasts (NIH 3T3) of lipoplexes comprising a) cholesterol-PEG2k and DMG-PEG2k in the formulation comprising C12-(2-3-2) and helper lipids cholesterol and DOPE, b) DOPE-PEG2k, DMPE-PEG2k, and DMG-PEG2k in the formulation comprising C12-(2-3-2) and helper lipids cholesterol and DSPC.

As a result, PEGylated cholesterol did not show any benefits over DMG-PEG2k in the entire tested dose range (Figure 3.15a). The superior properties of DMG-PEG2k suggest a significant impact of a PEG-lipid headgroup on transfection efficiency. In the second comparison the unsaturated anchor chain (C18:1) in 1,2-dioleoyl-*sn*-glycero-3-phosphoethanolamine-N-[methoxy(polyethylene glycol)-2000] (ammonium salt) (DOPE-PEG2k) led to substantially higher efficiency than saturated and shorter anchor chains (C14:0) in PEGylated glycerol-3-phosphoethanolamine (Figure 3.15b), which in turn shows the importance of the anchor chain length and saturation.

### 3.3.2 Anchor chain length in a PEG-lipid

As the next parameter, which could have an impact on lipoplex shielding, anchor chain length was varied. For this purpose, three saturated chains with glycerolipid backbone were chosen. DMG-PEG2k (R=C14:0 in Figure 3.14a) was compared with 1,2-dipalmitoyl-*sn*-glycerol, methoxypolyethylene glycol (DPG-PEG2k, R=C16:0 in Figure 3.14a) and 1,2-distearoyl-*sn*-glycerol, methoxypolyethylene glycol (DSG-PEG2k, R=C18:0 in Figure 3.14a) in the lipoplexes of the same composition for mRNA delivery as shown in Figure 3.16.

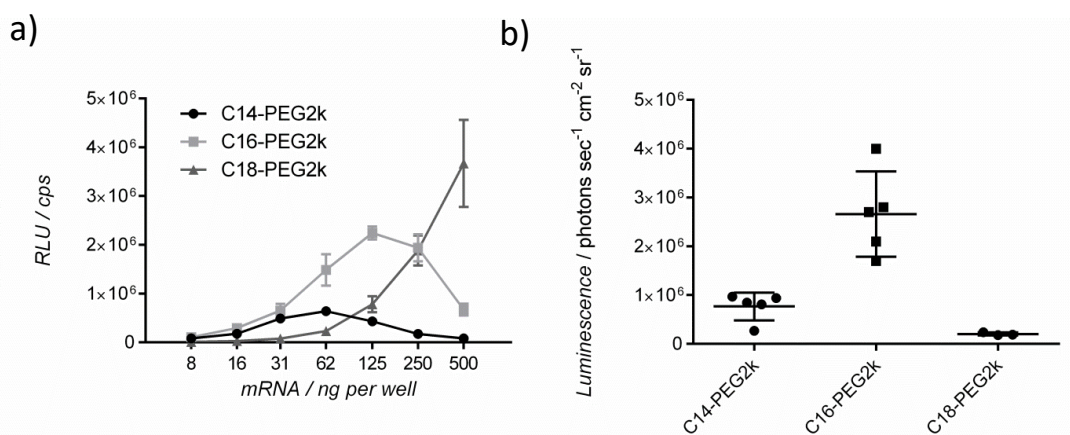


**Figure 3.16.** Comparison of transfection efficiency in a) murine fibroblasts (NIH 3T3) and b) mice after i.v. injection of lipoplexes comprising PEGylated glycerolipid with C14, C16, and C18 saturated anchor chains.

Interestingly, a change in only 2 carbon atoms led to a markedly different transfection pattern. C16-PEG transfected cells more efficiently than C14-PEG over the entire dose range, whereas C18-PEG showed high reporter protein levels only at the high doses with a steep drop transfection efficiency in the lower dose range as shown in Figure 3.16a. *In vivo*, six hours after i.v. injection, DPG-PEG2k showed a 4-fold increase compared to the second best DMG-PEG2k (Figure 3.16b). The longer anchor chain (C18) was less efficient in mRNA delivery.

### 3.3.3 PEG length

Another parameter, which had to be taken into consideration, was the polyethylene glycol length in a PEG-lipid. It is known that the PEG chain length can have a significant influence on biological activity. It has been shown that binding and uptake of nanoparticles by cells is affected by the PEG chain length<sup>[64]</sup>

To understand how the PEG chain length affects mRNA delivery of lipid formulations, two PEG molecular weights of 2,000 Da and 5,000 Da were compared in PEGylated glycerolipid of C14 and C16 anchor chains, DMG-PEG and DPG-PEG, respectively, as shown in Figure 3.17.



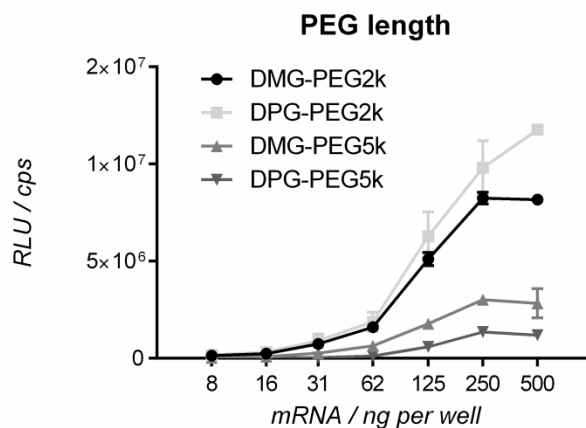


**Figure 3.17.** Comparison of transfection efficiency in murine fibroblasts (NIH 3T3) of lipoplexes comprising DMG-PEG or DPG-PEG of different molecular weights, 2000 Da or 5000 Da.

Although in both types of the PEG-lipids, increased PEG length inhibited cell transfection, the difference between DMG-PEG 2,000 Da and 5,000 Da was not as pronounced as between corresponding DPG-PEG lipids.

In summary, the presented data show that each of the PEG-lipid characteristics, i.e. i) PEG-lipid type, ii) anchor length with saturated or unsaturated alkyl chains, iii) as well as PEG length has an impact on lipoplex activity. Taken together, this series of experiments allowed to identify an optimal PEG lipid anchor length and PEG molecular weight.

### 3.3.4 PEG-lipid density

The shielding of the lipid complex is determined not only by the type of PEG-lipid and PEG-length but also by the ratio of PEGylated lipid to the other components of the formulation, i.e. by its total amount in the nanoparticle formulation. Increased PEG density was shown to affect the particle zeta potential as well as its interaction with cells or proteins.<sup>[65]</sup>

In order to investigate the impact of PEG-shielding on the lipoplex properties and potency in mRNA delivery, a series of experiments were performed. In a first step, different molar percentages of DMG-PEG2k were incorporated into complexes during the production process of either standard one-step assembling (all lipids assembled at the same time) or post-assembling of excessive (in relation to the standard amount, 5% molar) PEG-lipid (two-step assembling: excessive PEG-lipid added to preassembled particles). These two mixing techniques were chosen to evaluate

whether coating of preassembled particles with additional PEG has an impact on their physicochemical properties and shielding density compared to single-step assembling. The method of DMG-PEG2k post-assembling was described for siRNA delivery by Kumar *et al.*<sup>[65]</sup> The size, PDI, and zeta potential of resulting complexes are summarized in Table 3.4.

**Table 3.4.** Hydrodynamic diameter, PDI, and zeta potential of lipoplexes with varying DMG-PEG amount and method of assembling.

<b>DMG-PEG2k molar percentage</b>	<b>Single-step assembling</b>			<b>Post-assembling</b>		
	<b>5%</b>	<b>10%</b>	<b>20%</b>	<b>5%</b>	<b>10%</b>	<b>20%</b>
<b>Hydrodynamic diameter [nm]</b>	161.2	127.8	113.9	89.8	106.4	146.6
<b>PDI</b>	0.144	0.221	0.236	0.195	0.240	0.162
<b>Zeta potential in water [mV]</b>	22.5	24.9	26.3	27.3	44.2	43.1
<b>Zeta potential in PBS [mV]</b>	-5.52	0.447	-3.1	-2.24	-3.39	-2.47

For the single-step assembly process, increased PEG-lipid amounts did not affect zeta potential. On the other hand, a trend towards decreased size was observed, whereas polydispersity of the nanoparticles slightly increased. In the case of post-assembled formulations, the shielding decreased at high amounts of DMG-PEG2k as demonstrated by the increased zeta potential (at least measured in water). Particles also became larger but without changes in polydispersity.

All six complexes were tested in terms of transfection efficiency as well (see Figure 3.18).

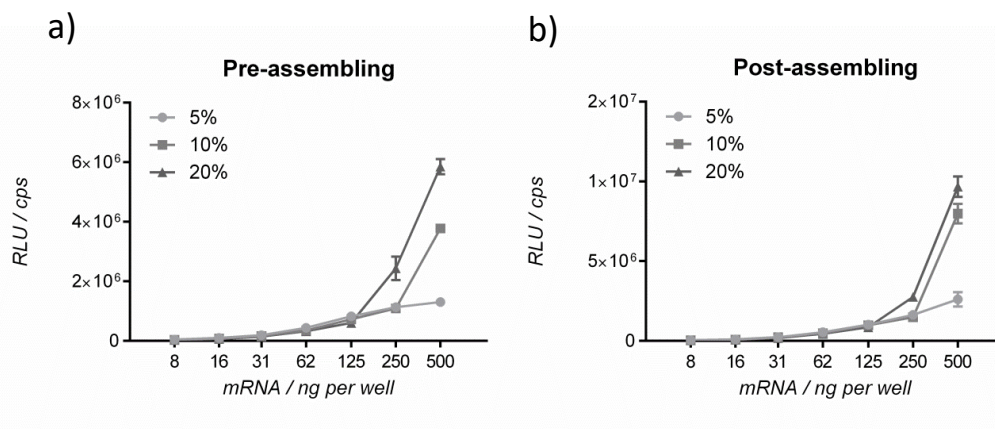


**Figure 3.18.** Transfection efficiency in murine fibroblasts (NIH 3T3) of lipoplexes with varying DMG-PEG amount and method of assembling; a) pre-assembled excessive PEG-lipid amount, b) post-assembled excessive PEG-lipid amount.

Higher percentage of incorporated DMG-PEG2k enhanced the detected protein level (Figure 3.18a) and the process of post-assembling increased this effect even further (Figure 3.18b). Interestingly, this phenomenon was observed only for the high doses of mRNA.

As the effect of PEG-shielding on particle activity may become most apparent *in vivo*, a comparison of 5% and 20% DMG-PEG2k (both pre-assembled) was performed after i.v. injection in mice (Figure 3.19).

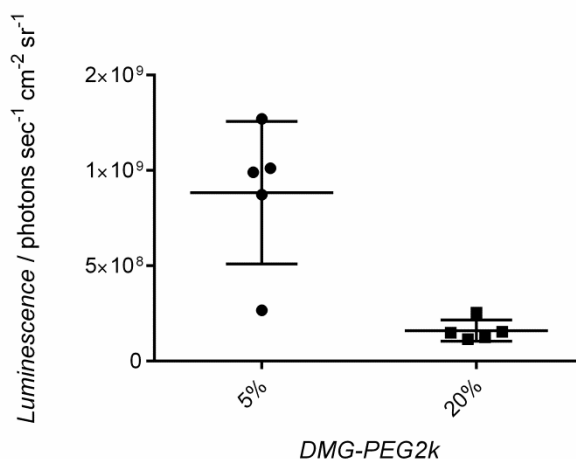


**Figure 3.19.** Comparison of transfection efficiency in mice of lipoplexes comprising of 5% or 20% molar DMG-PEG2k.

The results from the *in vivo* experiment (Figure 3.19) showed that lipoplexes with 5% content of DMG-PEG2k were almost 6-fold more efficient than lipoplexes with 20% of DMG-PEG2k.

In the second step, the PEG-lipid amount was further increased and, additionally, DPG-PEG2k was included in the experiment in order to examine if the observed trends are independent on a PEGylated glycerolipid type (Figure 3.20).

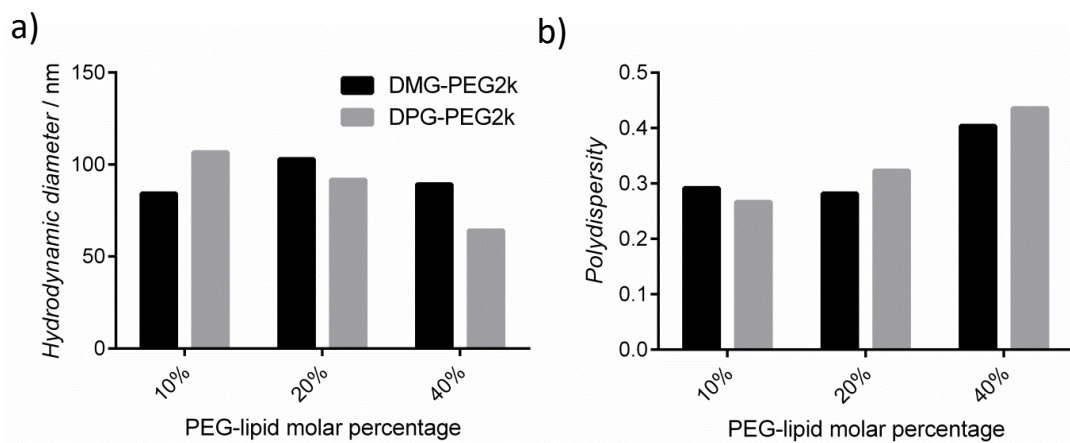


**Figure 3.20.** a) Hydrodynamic diameter and b) polydispersity of lipoplexes comprising DMG-PEG2k or DPG-PEG2k in a varying molar amounts.

A trend towards decreasing size (Figure 3.20a) and increasing PDI (Figure 3.20b) with increasing PEG-lipid amount was observed for DPG-PEG2k. In the case of DMG-PEG, although the tendencies were not as evident, a notable increase in PDI for 40% of a lipid was observed.

The observed tendencies in size and PDI were followed by appearance of a second peak population in the size distribution graphs, as seen in Figure 3.21. A potential explanation for this observation might be the existence of a subpopulation of ~20 nm particles resulting from excessive PEG-lipid which could not be incorporated into complexes anymore. This would possibly lead to the formation of PEG-lipid micelles, which should be smaller than the major particle population comprising the encapsulated mRNA. To prove this hypothesis, pure DMG-PEG2k micelles were formed by mixing ethanol solution of the lipid with the citric buffer (just as for lipid nanoparticles but without mRNA) and dialyzed. Resulting particles were compared in terms of their size with the size distribution of lipoplexes formed with an excess of DMG-PEG2k (Figure 3.21; PEG-micelles in a dashed line).

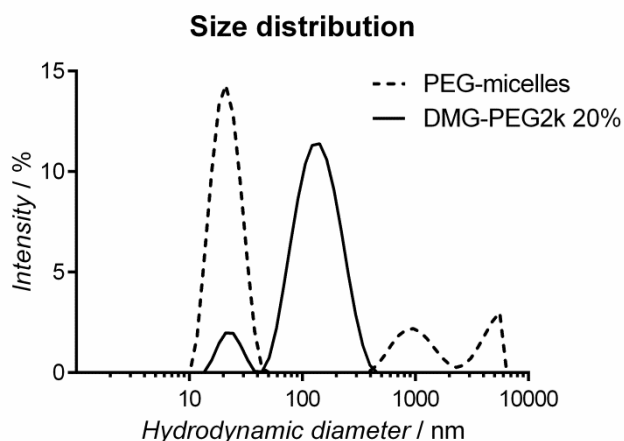


**Figure 3.21.** Size distribution graphs by intensity of scattered light of lipoplexes comprising 20% molar DMG-PEG2k (solid line) and pure DMG-PEG2k micelles (dashed line).

As the main peak from PEG-lipid micelles (Figure 3.21) appeared at the size of the particle subpopulation in the sample with lipoplexes comprising 20% molar DMG-PEG2k, it was confirmed that above a certain ratio of a PEG-lipid, the excessive amounts of PEG-lipid are not incorporated into lipid particles anymore.

The presence of PEG-lipid micelles could also be the reason for the observed cell transfection pattern (see Figure 3.18). In order to confirm this, pure DMG-PEG2k micelles were added to the wells of cells transfected with a standard formulation (containing 5% DMG-PEG2k) to a final amount of 20% DMG-PEG2k (15% in a form of PEG-lipid micelles). The results are presented in Figure 3.22.

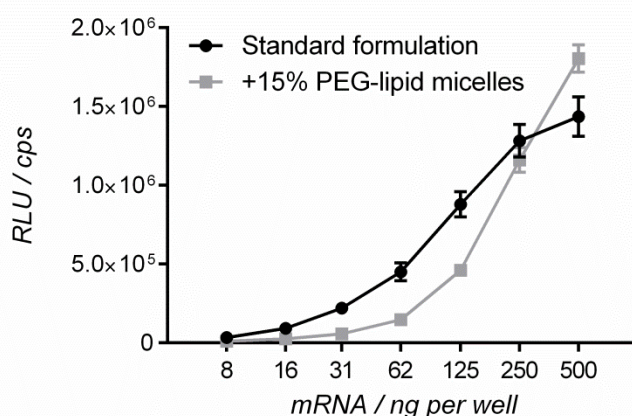


**Figure 3.22.** Transfection efficiency in murine fibroblasts (NIH 3T3) of lipoplexes with 5% DMG-PEG2k compared with the same lipoplexes after addition of DMG-PEG2k micelles.

As observed in Figure 3.22, the pattern of augmented reporter enzyme activity at higher doses was similar compared to the transfection with formulations with higher PEG-lipid amount.

In conclusion, PEG-lipid content above 5% did not lead to increase in shielding since the results suggest that it could not be properly incorporated in the particle anymore.

### 3.4 Coupled dependences between the lipids

The side by side comparisons of lipid nanoparticles varying in only one component (e.g. oligoalkylamine headgroup) or factor (e.g. lipidoid alkyl chain length) help to understand the multicomponent system of lipid-mRNA complexes. However, more complex interactions, i.e. coupled dependences between two or more lipid components, must not be omitted when optimizing lipoplex formulation.

#### 3.4.1 Multicomponent system interactions

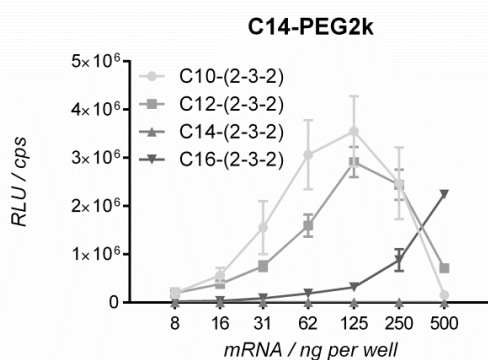
As it became apparent that transfection efficiency of a formulation comprising a certain individual lipid can be largely affected by the remaining lipids of the formulation and their ratios (see Chapter 3.2.3 Variations in the composition), it would be helpful to better understand mutual interactions between the lipids in order to generate more general rules or trends for the design of optimized formulations.

Since the effect of alkyl chain length was investigated in the case of lipidoids, helper lipids as well as PEG-lipids, the coupled interactions between alkyl chain lengths of different lipidic components were first analysed. For this purpose, the combinations of varying alkyl chains simultaneously in both (2-3-2)-based lipidoids and PEGylated glycerolipid were tested *in vitro* for their transfection efficiency, as shown in Figure 3.23. A list of tested combinations (all contained cholesterol) is presented in Table 3.5.

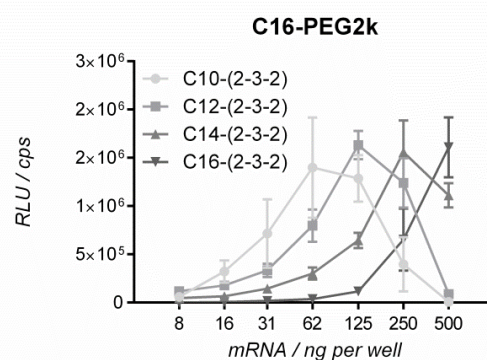
**Table 3.5.** A summary of formulation combinations with varying alkyl chains simultaneously in both (2-3-2)-based lipidoids and PEGylated glycerolipid. All formulations contained cholesterol.

(2-3-2)-based lipidoid	PC helper lipid	PEGylated glycerolipid
C10	C16	C14
C12	C16	C14
C14	C16	C14
C16	C16	C14
C10	C16	C16
C12	C16	C16
C14	C16	C16
C16	C16	C16
C10	C16	C18
C12	C16	C18
C14	C16	C18
C16	C16	C18

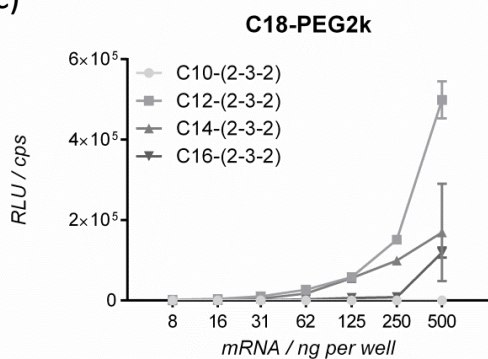
a)



b)



c)



d)

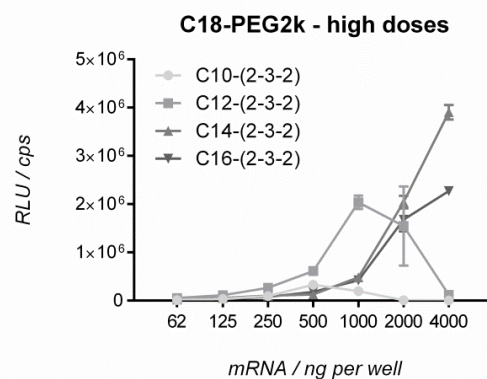


**Figure 3.23.** Transfection efficiency of lipoplexes with varying alkyl chain length in both lipidoid and PEG-lipid.

The effect of alkyl chain in lipidoid (C10-, C12-, C14, or C16-(2-3-2)) varied in the presence of different alkyl chain length in PEG-lipids (C14-, C16-, or C18-PEG-lipid, DMG-, DPG-, and DPG-PEG2k, respectively). When combined with C14-PEG, the highest transfection efficiency in the tested dose range was observed for C10- and C12-(2-3-2), although high levels of protein translation were also observed at the highest dose of the C16 lipidoid formulation. With C16-PEG in the formulation, maximum transfection efficiencies shifted towards higher doses with increasing alkyl chain length of the lipidoids. In the case of C18-PEG these maxima were shifted even further, to 1 µg mRNA/well and higher, as seen in Figure 3.23c-d. Interestingly, here the efficiency of C10-(2-3-2) was much lower than for the other tested lipidoids with longer alkyl chains.

It could be expected that a similar effect of mutual interactions of the alkyl chain lengths of the lipidoid and a phospholipid may occur, respectively. Thus, the combinations of previously described C12, C14, and C16 PCs with C8-, C10-, C12-, and C16-(2-3-2) were tested *in vitro* (see Figure 3.24). A list of tested combinations (all contained cholesterol) is presented in Table 3.6.

**Table 3.6.** A summary of formulation combinations with varying alkyl chains simultaneously in both (2-3-2)-based lipidoids and helper lipids phosphocholines. All formulations contained cholesterol.

(2-3-2)-based lipidoid	PC helper lipid	PEGylated glycerolipid
C8	C12	C14
C8	C14	C14
C8	C16	C14
C10	C12	C14
C10	C14	C14
C10	C16	C14
C12	C12	C14
C12	C14	C14
C12	C16	C14
C16	C12	C14
C16	C14	C14
C16	C16	C14



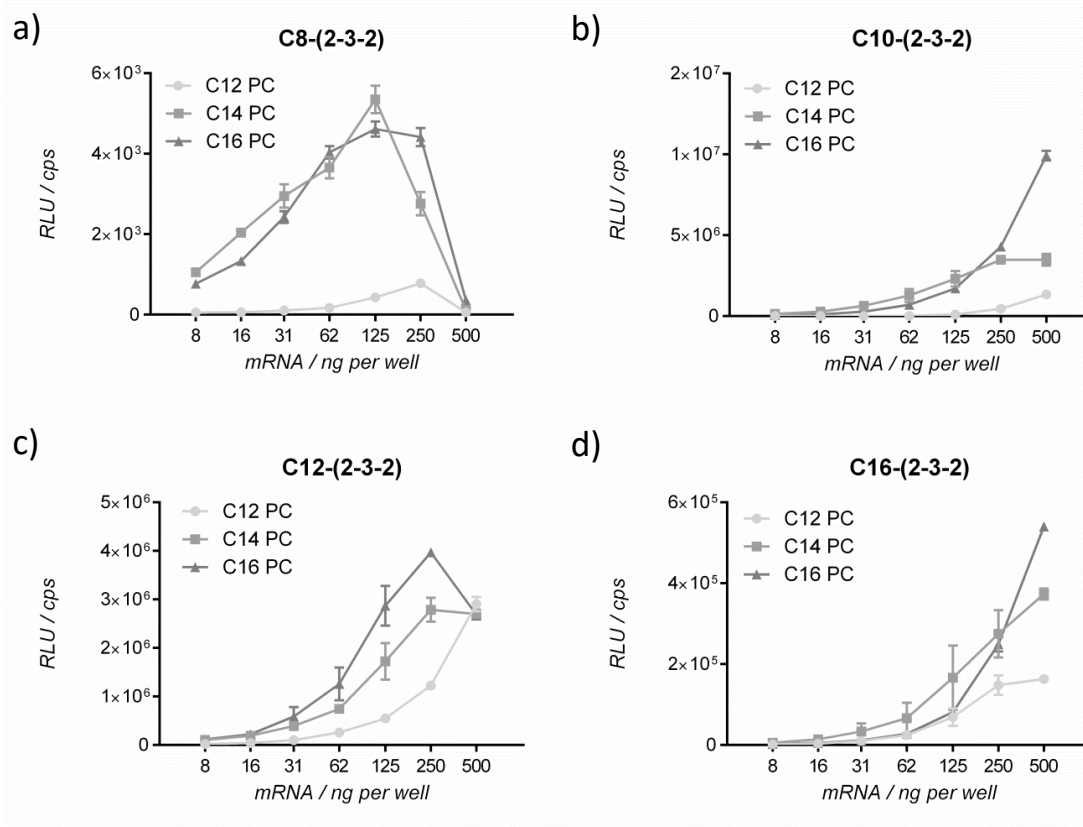


**Figure 3.24.** Transfection efficiency of lipoplexes with varying alkyl chain length in both lipidoid and a phospholipid (phosphocholine).

Here, in all four sets of tested combinations the lowest chain length of phosphocholine showed low transfection efficiency independently of the lipidoid. The advantage of C16 PC was obvious in combination with C12-(2-3-2), as shown already in Chapter 3.2.1.3, but became disputable in the case of lipidoids of shorter or longer chain lengths. To make this comparison more transparent from the perspective of a helper lipid, the curves of transfection efficiency of DPPC in combination with lipidoids of different alkyl chain length are summarized in Figure 3.25.

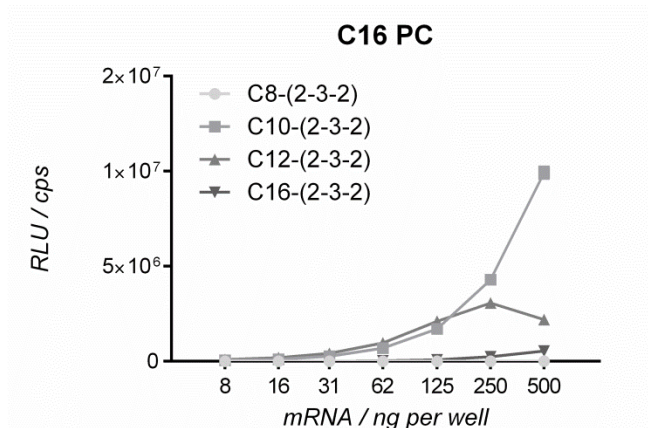


**Figure 3.25.** Transfection efficiency of lipoplexes comprising DPPC (C16 PC) as a helper lipid with varying alkyl chain lengths of a lipidoid.

Whereas in this composition C8- and C16-(2-3-2) transfect less efficient, C10- and C12-(2-3-2) seem to be of similar activity at lower dose range, whereas C10-(2-3-2) exhibited a steep increase at the two highest doses tested.

In the previous experiments the alkyl chain lengths of helper lipid (DPPC) or PEG-lipid (DMG-PEG2k) were kept constant in the formulation. However, it would be more desirable to understand the interactions between all three lipid components of the formulation, i.e. lipidoid, helper lipid, and PEG-lipid at the same time. Therefore, two lipidoids (C10- and C12-(2-3-2)) were combined with two helper lipids (C14 and C16 PCs, DMPC and DPPC) and two PEG-lipids (C14 and C16-PEG, DMG-PEG2k and DPG-PEG2k). The list of tested combinations is summarized in Table 3.7 and their transfection efficiency *in vitro* is shown in Figure 3.26.

**Table 3.7.** A summary of formulation combinations with varying alkyl chains simultaneously in (2-3-2)-based lipidoids, helper lipids phosphocholines, and PEGylated glycerolipid. 10-14-14 = C10-(2-3-2)/DMPC/DMG-PEG2k; 10-16-14 = C10-(2-3-2)/DPPC/DMG-PEG2k etc. All formulations contained cholesterol.

Combination abbreviation	(2-3-2)-based lipidoid	PC helper lipid	PEGylated glycerolipid
10-14-14	C10	C14	C14
10-16-14	C10	C16	C14
10-14-16	C10	C14	C16
10-16-16	C10	C16	C16
12-14-14	C12	C14	C14
12-16-14	C12	C16	C14
12-14-16	C12	C14	C16
12-16-16	C12	C16	C16

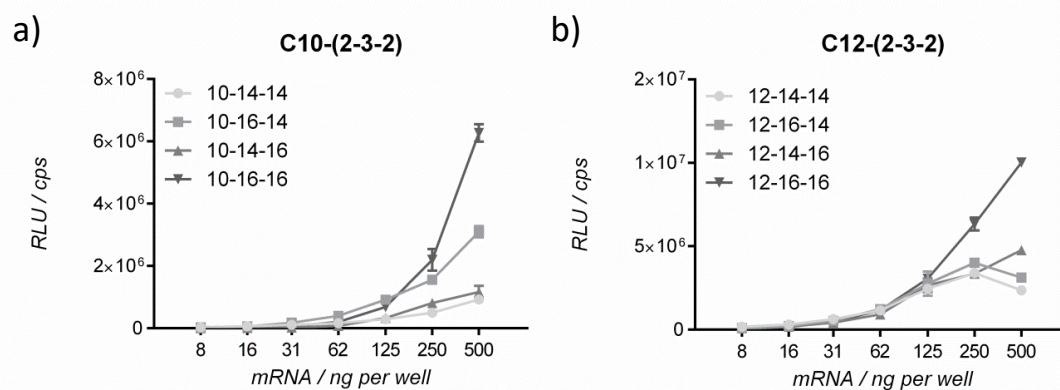


**Figure 3.26.** Transfection efficiency of all variations of two lipidoids (C10- and C12-(2-3-2)), two helper lipids (DMPC and DPPC) and two PEG-lipids (DMG-PEG2k and DPG-PEG2k). 10-14-14 = C10-(2-3-2)/DMPC/DMG-PEG2k; 10-16-14 = C10-(2-3-2)/DPPC/DMG-PEG2k etc. All lipoplexes contained cholesterol.

Interestingly, the optimal composition for both lipidoids was the one with C16 alkyl chains in the helper and PEG lipid, respectively. It also seemed that in the case of C10-(2-3-2) there was no difference between DMPC/DMG-PEG2k (C14 PC/C14-PEG) and DMPC/DPG-PEG2k (C14 PC/C16-PEG), which suggests a smaller impact of the PEG-lipid on translation efficiency. On the contrary, formulations containing C12-(2-3-2) and either DMPC/DMG-PEG2k (C14 PC/C14-PEG) or DPPC/DMG-PEG2k (C16 PC/C14-PEG) were more comparable, which suggest a greater impact of the PEG-lipid in this case.

Summarizing this chapter, a series of experiments testing some combinations of varying chain lengths in a lipidoid, phospholipid, and a PEG-lipid revealed mutual

interactions between the lipids affecting the activity of the resulting lipoplexes. The data showed that a choice of the most effective component is mostly dependent on the other lipids used in the formulation.

### 3.4.2 Nitrogen to phosphate ratio

One of the reported critical factors which determines the complexation of mRNA and delivery capability of a cationic carrier is the nitrogen to phosphate ratio (N/P) which is a measure for the ratio of positive charge of the cationic carrier to negative charge of the nucleic acid. If the molar ratios between all four lipids of the formulation are kept constant variation of the N/P ratio results in a change in total lipid to mRNA ratio.

A starting point in this research was N/P 17, exhibiting high efficiency both *in vitro* as well as *in vivo*. However, the goal was to reduce this ratio as much as possible without any loss in resulting protein translation levels in order to minimize the total amount of lipid which would need to be applied. At first, an experiment was performed in which the effect of the N/P ratio dependent on the mRNA dose was performed (Figure 3.27).

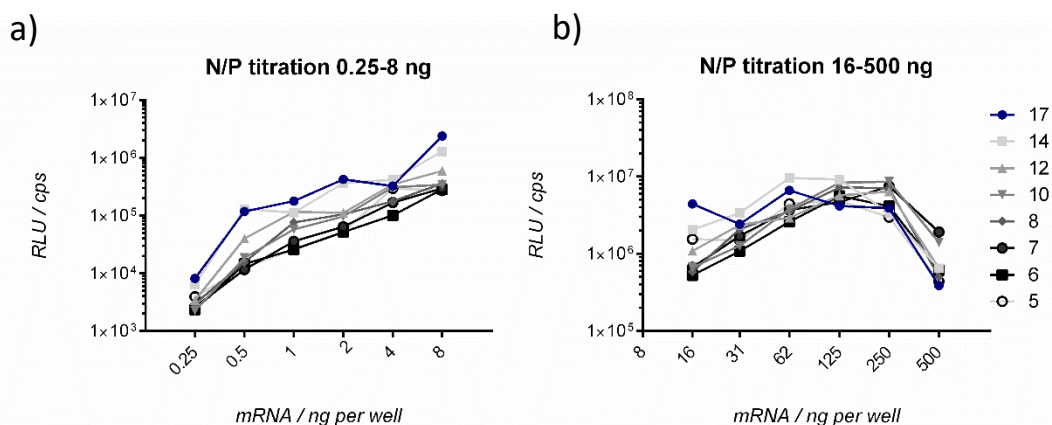


**Figure 3.27.** N/P titration on murine fibroblasts (NIH 3T3) from N/P 17 to 5 in doses of a) 0.25-8 ng/well and b) 16-500 ng/well.

The observation from the titration experiment was that higher N/P ratios exhibited lower transfection efficiencies at high doses, while higher transfection efficiency was observed at low doses (Figure 3.27a-b).

The goal of the following *in vivo* experiment (Figure 3.28a) was to test whether reduction of N/P from 17 to 4 (a more than 4-fold decrease in lipid amount in relation

to mRNA) would allow to keep the efficiency while minimizing the dose of the carrier (Figure 3.28).

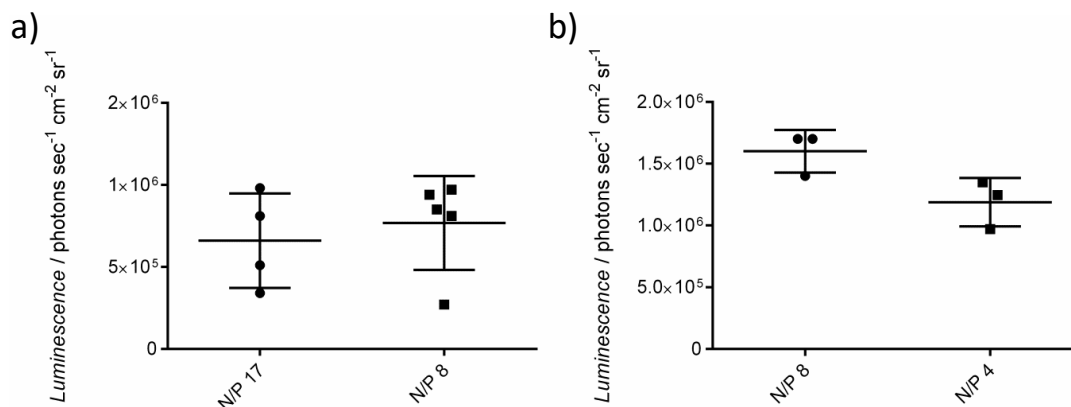


**Figure 3.28.** Bioluminescence in mice treated with a) formulations of N/P 17 or 8, and b) formulations of N/P 8 or 4. Formulations in a) and b) differed in a phospholipid type.

Surprisingly, when N/P ratio was halved from the starting point of 17 to 8, the reporter enzyme activity *in vivo* showed a slight increase which, however, was not significant. On the other hand, further reduction to N/P 4 resulted in lower activity of the complex which was, however, also not significant.

The presented data proved that it was possible to reduce N/P ratio of the lipid formulation remarkably without any losses in its activity *in vitro* or *in vivo*.

### 3.5 Formulation conditions

#### 3.5.1 Further condensation of mRNA by non-lipidic, cationic agents

Another possibility to decrease the N/P ratio without a drop in efficiency could be incorporation of a positively charged non-lipidic component in a formulation, which would help to further complex mRNA. It has been described that i.e. Ca<sup>2+</sup> enhances the transfection efficiency of DNA-cationic liposome complexes<sup>[66]</sup> and even millimolar Mg<sup>2+</sup> concentrations are able to stabilize RNA tertiary structures.<sup>[67]</sup>

In this chapter, Mg<sup>2+</sup> was chosen to test the influence of an inorganic cation on mRNA delivery using the above described lipid system. For this purpose, magnesium chloride (MgCl<sub>2</sub>) was included in the aqueous mRNA solution of the formulation. Different N/P ratios (8, 6, 4, or 2) were tested for their transfection efficiency and characterized in terms of physicochemical properties of resulting particles (see Figure 3.29).

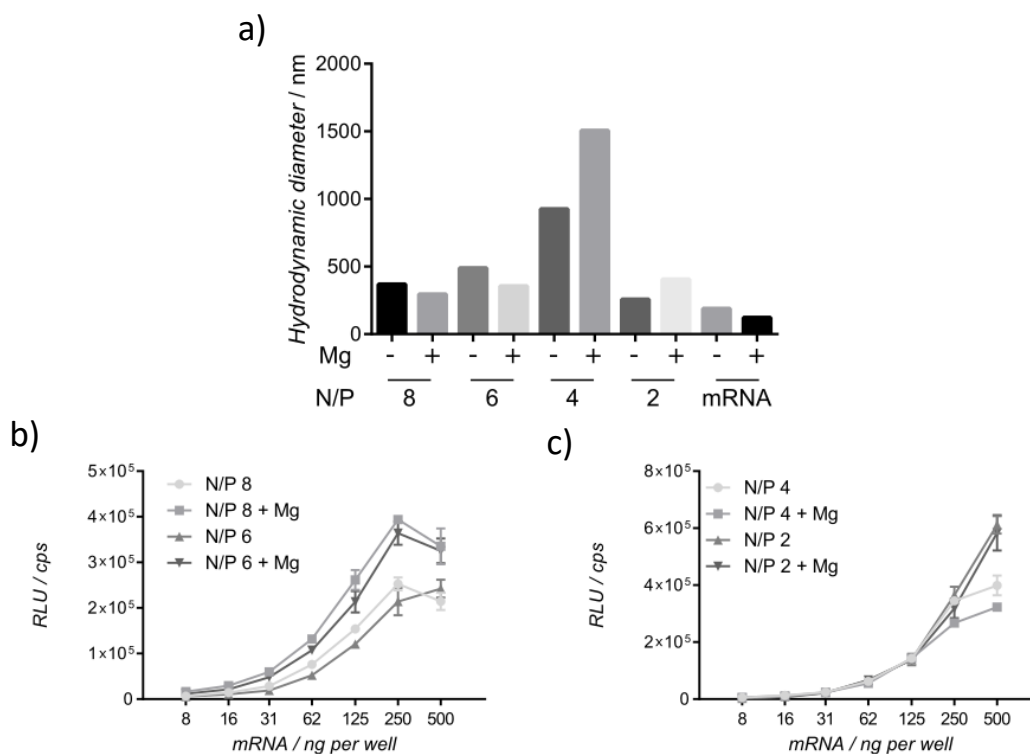


**Figure 3.29.** Comparisons of lipoplexes of N/P 8, 6, 4, or 2 with and without  $Mg^{2+}$  in a) their ability to complex mRNA and b), c) their ability to deliver reporter mRNA to the NIH 3T3 cells.

Particles of N/P 8 or 6 formed in the presence of  $Mg^{2+}$  showed a tendency towards a decrease in size compared to those formed without any addition of  $Mg^{2+}$  cation (Figure 3.29a). Additionally, they were able to enhance transfection efficiency *in vitro* (Figure 3.29b). In contrast, when the N/P was lower (4 or 2), particles became larger and slightly less effective in mRNA delivery (Figure 3.29a and c). The ability of  $Mg^{2+}$  itself to interact with mRNA would be suggested by DLS measurements of reporter mRNA (“mRNA” in Figure 3.29a) compared to the same mRNA mixed with  $MgCl_2$  solution (“mRNA + Mg” in Figure 3.29a) as the diameter of the mRNA slightly decreases (35%).

### 3.5.2 Impact of formulation pH on the mRNA binding

The process of mRNA binding of the lipodic formulation is based on electrostatic interaction between the negatively charged nucleic acid and the cationic lipid. Therefore, it could be expected that the protonation level of the lipidoid and the mRNA may have a great impact on entrapment of mRNA, particle formation, and, hence, the performance of the mRNA-lipid complex. The initial assumption was that the aqueous mRNA solution should have rather an acidic pH to enable sufficient

attraction in the lipoplex. Therefore, the citric buffer of pH 4.5 was used in each experiment. In order to test this theory, lipoplexes were formed in citric buffers of pH i) lower than used for the standard formulation (pH 2 and 3), ii) equal to one of the  $pK_a$ 's of the lipidoid (pH 5.2), iii) and higher than used for the standard formulation (pH 6 and 7), and subsequently characterized for their size and PDI as well as tested *in vitro* (see Figure 3.30). Since it is known that mRNA is not stable in alkaline solutions<sup>[68]</sup>, pH above 7 was not tested.

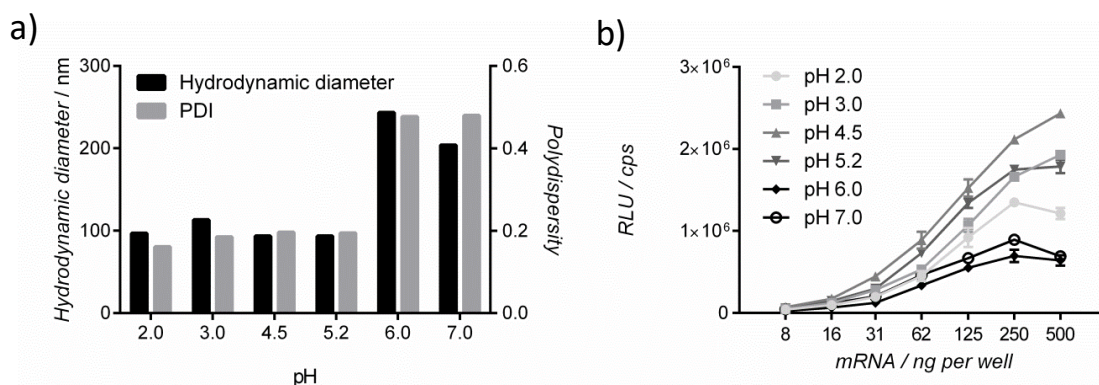


**Figure 3.30.** Comparison of lipoplexes formulated in the citric buffer of pH 2, 3, 4.5, 5.2, 6, or 7 in their a) hydrodynamic diameter and polydispersity and b) transfection efficiency on murine fibroblasts (NIH 3T3).

As seen in Figure 3.30a, the complexation process is affected at pH higher than 5.2 (6 and 7) as the particle size and polydispersity increased. The physicochemical properties resulted in reduced transfection efficiency *in vitro* as well (Figure 3.30b). Interestingly, lipoplexes prepared at pH 2 also led to lower reporter protein levels despite proper particle size and polydispersity. The highest enzyme activity was observed for the pH 4.5.

No substantial differences could be observed in encapsulation efficiency determined by RiboGreen assay or in mRNA band intensity on agarose gel.

In summary, these results showed that the optimization of formulation conditions, e.g. inclusion of inorganic ions such  $Mg^{2+}$  or pH of the mixing solution is critical for the mRNA complexation process and, hence, can affect the properties of lipid nanoparticles.

### 3.6 mRNA release assay

The fate of a particle after intravenous injection is a series of complex interactions with the environment that is difficult to mimic under *in vitro* conditions. A typical



transfection procedure is helpful in judging whether the mRNA is able to enter the cell and how well it is tolerated but does not provide any information about e.g. stability in the blood. Therefore, a more detailed *in vitro* method was proposed. Based on a model described by Zhang *et al.*<sup>[69]</sup>, in which the final release of siRNA from LNP was found to correlate with efficiency *in vivo*, a sequence of *in vitro* treatments was introduced for mRNA-lipid complexes as well. As shown in the Figure 3.31, the mRNA release assay included steps mimicking circulation in the blood, when a PEG-lipid is disassociated from a lipoplex, and an interaction with the anionic lipids of endosomes in the slightly acidic pH, resulting in lipoplex disruption and mRNA release. The amount of released mRNA was quantified by RiboGreen assay.

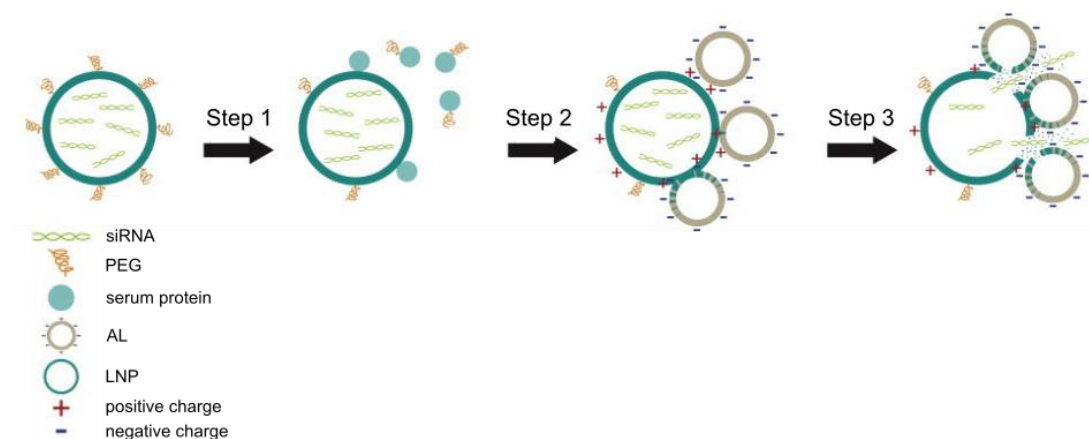


**Figure 3.31.** A proposed model for the release of siRNA from LNP (Zhang *et al.*).<sup>[69]</sup> Step 1: incubation of LNP with serum at 37°C under physiological pH; PEG-lipid diffuses from LNP; Step 2: LNP-serum mixture treated with anionic liposomes at pH 6.0; cationic lipids are protonated and electrostatically interact and exchange lipids with anionic liposomes; Step 3: LNP membrane disruption and release of siRNA from LNP.

At first, the optimal ratio of anionic liposomes (AL) to lipidoids in the lipoplexes was examined. Thus, a lipoplex comprising mRNA-FLuc was incubated with murine plasma at 37°C for 20 min and consequently, increasing amounts of AL comprising DOPS (1,2-dioleoyl-sn-glycero-3-phospho-L-serine (sodium salt))/DOPC (1,2-dioleoyl-sn-glycero-3-phosphocholine)/DOPE were added. After 15 min of incubation at 37°C, mRNA release was quantified as a percentage of nucleic acid outside of the complex compared to the total amount. The resulting mRNA release dependence on anionic lipids to lipidoid ratio (DOPS(-)/C12-(2-3-2)(+)) is presented in Figure 3.32.



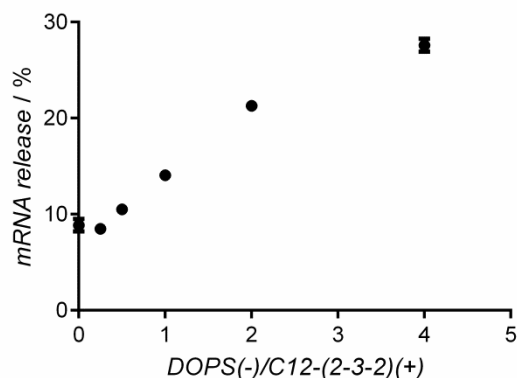


**Figure 3.32.** mRNA release after treatment in plasma at 37°C in the presence of anionic liposomes of different DOPS to C12-(2-3-2) ratios. mRNA release was expressed as the percentage of nucleic acid outside of the complex compared to the total amount.

As seen in Figure 3.32, the release seemed to reach a plateau at DOPS to C12-(2-3-2) ratio of 4, which means that from this point on a saturation of AL mimicking endosomes occurred. In order to record an artificial endosomal escape as close to the cellular process as possible, an excessive amount of anionic lipids is unnecessary. On the other hand, the observed release effect should be noticeable. Therefore, for further experiments the chosen ratio of AL to lipidoid was 2.

In order to find if such an assay is reliable, most of investigated particles were further tested *in vivo*. Firstly, lipoplexes varying in the phospholipid (DPPC) amount described in Chapter 3.2.3 (“Variations in the composition”, see Figure 3.13f) with additionally included complex of different than standard molar ratios (named “varied ratios”) as described by Love *et al.*<sup>[44]</sup> for siRNA delivery were compared (Figure 3.33).

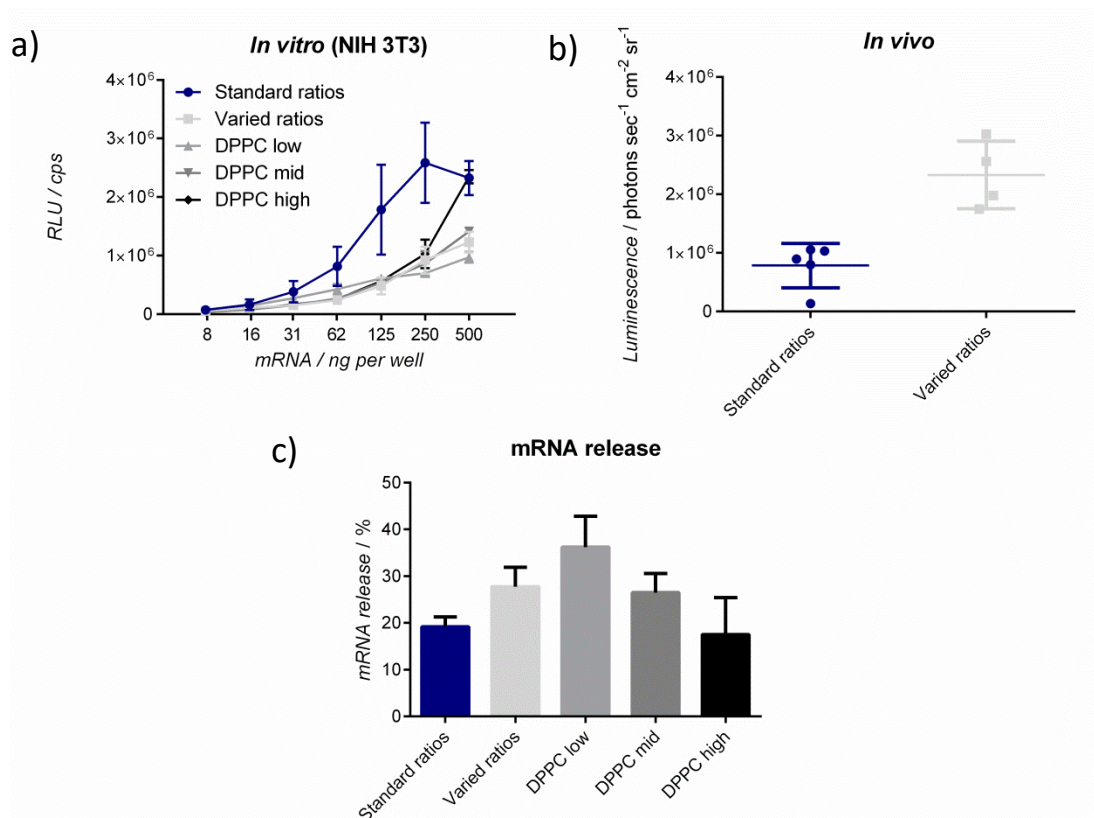


**Figure 3.33.** Comparison of lipoplexes with standard lipid ratios, ratios described by Love et al.<sup>[44]</sup> (“Varied ratios”) and with varying DPPC/cholesterol ratios a) *in vitro* in murine fibroblasts (NIH 3T3), b) *in vivo* in mice after intravenous injection, and c) in mRNA release assay.

Although the formulation with the standard ratio of lipid components performed most efficient *in vitro* (Figure 3.33a), it showed lower mRNA release than the formulation with “varied” ratios (Figure 3.33c). Interestingly, the upward trend in luciferase activity with increasing DPPC amounts observed *in vitro* was completely reversed in the mRNA release assay. The “DPPC low” formulation leading to the highest mRNA release in the artificial endosome did not show any benefits in transfection efficiency *in vitro*. Two of the tested lipoplexes, with standard and “varied” ratios were investigated in mice. Surprisingly, “varied” ratios led to 3-fold higher bioluminescence and showed correlation in trend rather with mRNA release assay than with transfection *in vitro*.

Next, the same set of experiments was applied to lipoplexes with different helper lipids in the place of the phospholipid DPPC (see Figure 3.34).

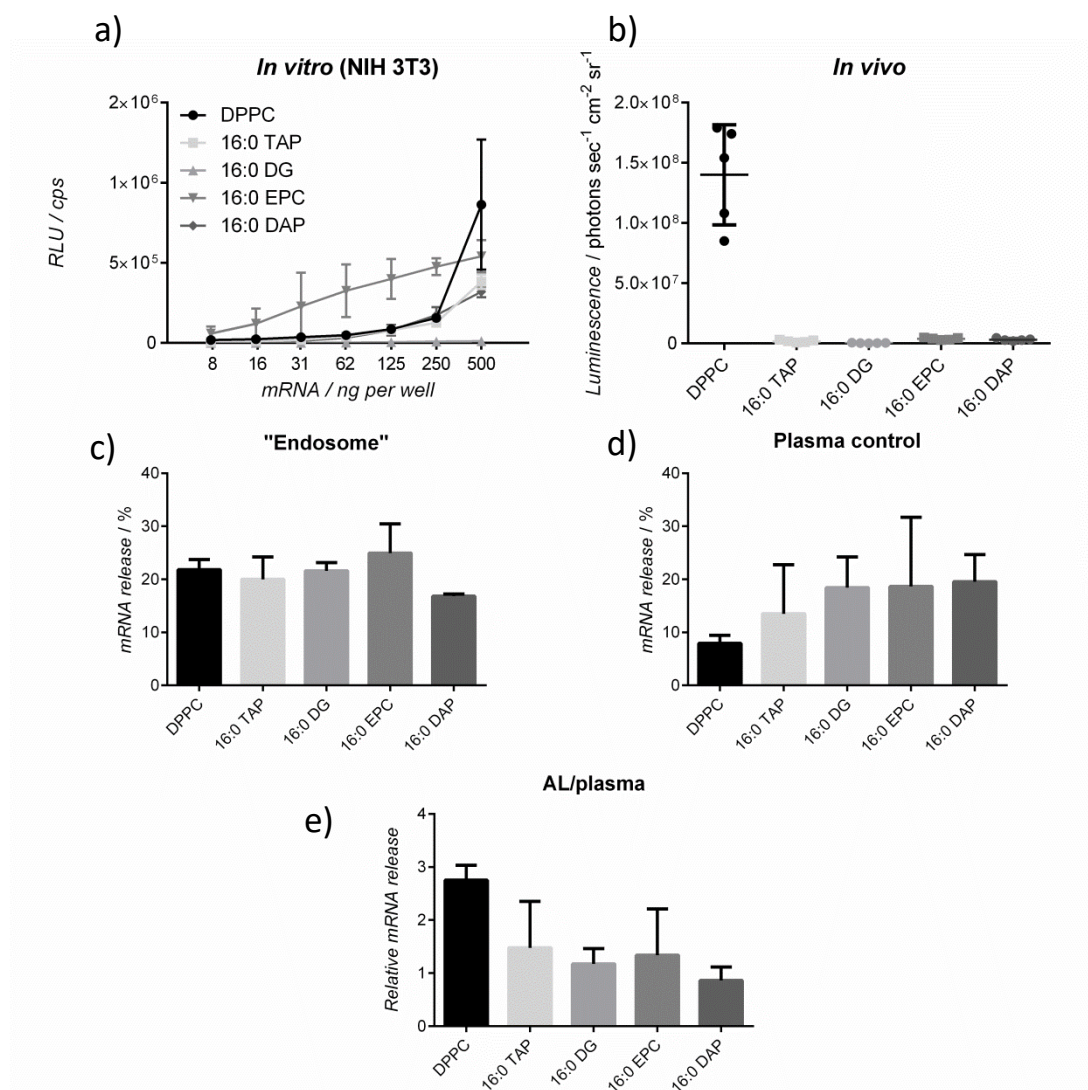


**Figure 3.34.** a) *In vitro* and b) *in vivo* luminescence of lipoplexes comprising DPPC or other helper lipids. mRNA release from these particles in c) artificial endosome, d) plasma only, and e) relative mRNA release defined as ratio of values from c) and d).

In this case, no correlation between mRNA release in artificial endosomes (in the presence of AL) (Figure 3.34c) and *in vivo* results (Figure 3.34b) was observed. Also, *in vivo* data did not reflect *in vitro* pattern (Figure 3.34a). Therefore, an additional control was added to the release assay. Released mRNA was quantified in samples treated with plasma without addition of AL as in the Step 1 of the model depicted in Figure 3.31 ("Plasma control" in Figure 3.34d). Next, the ratio of mRNA release in artificial endosome (in the presence of AL) to mRNA release in plasma control (without AL) was calculated ("AL/plasma", Figure 3.34e). This ratio was assumed to mimic the *in vivo* situation more reliably than simple mRNA release in the presence of AL. The plasma control would provide the information of mRNA amount released in the blood, whereas treatment with AL should indicate how much mRNA is re-

leased later in the cell. Ratio of these two values, named “relative mRNA release” showed a correlation with bioluminescence in mice (Figure 3.34b and e).

In the next release assay experiment two comparisons were made. Three different phosphocholines (16:1(cis)PC, 16:1(trans)PC, and 18:2(cis)PC) were tested in the lipoplexes comprising FLuc as well as three cationic lipids (C12-(2-3-2), C12-200, and MC3) were compared with each other in lipoplexes comprising mRNA coding for human erythropoietin (hEpo) As previously, the relative mRNA release was evaluated and compared with protein translation *in vivo* (Figure 3.35).

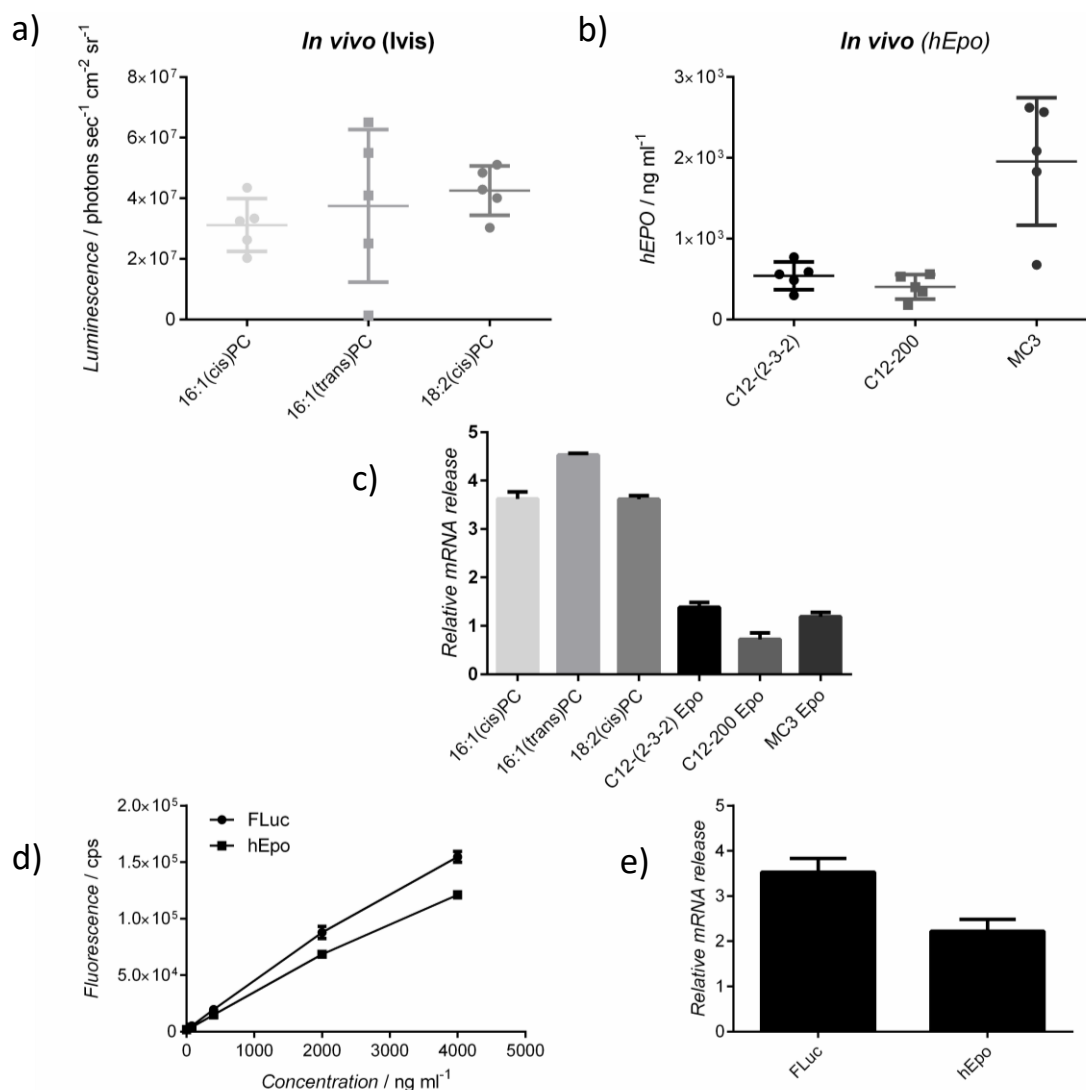


**Figure 3.35.** a) Bioluminescence in mice treated with lipoplexes comprising FLuc. b) hEpo levels in mice treated with lipoplexes comprising hEpo. c) Relative mRNA release of lipoplexes comprising FLuc and three different phosphocholines as well as lipoplexes comprising hEpo and three different lipidoids. d) Standard curves of fluorescence of FLuc and hEpo mRNA evaluated by RiboGreen assay. e) Relative mRNA release of two lipoplexes with the same lipidic composition but different mRNA (FLuc or hEpo).

Both relative mRNA-FLuc release and a relative mRNA-hEpo release (Figure 3.35c) showed a correlation with bioluminescence and hEpo levels in mice, respectively (Figure 3.35a and b). However, if all complexes were compared to each other in mRNA release assay, one conclusion would be that in general mRNA-hEpo complexes were less efficient than mRNA-FLuc. In order to compare signals of different mRNAs obtained in the release assay, two additional tests were performed. Firstly, the standard curves of fluorescence for these two mRNAs were performed (Figure 3.35d). Secondly, a side by side comparison of lipoplexes with the same lipid composition but comprising diverse mRNA sequences (mRNA-FLuc vs. mRNA-hEpo) in terms of mRNA release values was conducted (Figure 3.35e). FLuc led to higher fluorescent signal and relative mRNA release ratio than hEpo. The observed discrepancies proved that lipoplexes comprising different mRNA transcripts cannot be compared with each other in described assay.

In summary, the presented mRNA release assay proved to be an effective indicator for formulation delivery efficiencies *in vivo*. The ratio of mRNA released in artificial endosomes to mRNA released in plasma (“relative mRNA release”) showed a positive correlation to reporter enzyme activity detected in mice after i.v. administration.

### 3.7 Targeted delivery with folic acid

With the goal of treating a variety of diseases with mRNA-based drugs, it is important to reach a target tissue exclusively with minimized translation in other organs. Targeted delivery would be especially critical in the case of anti-cancer treatment using mRNA coding for toxin described in the following chapter. For the purpose of tumour growth inhibition a plant toxin isolated from *Abrus precatorius*, abrin, was chosen. Abrin is a highly potent member of the family of type II ribosome inactivating proteins (RIPs)<sup>[70,71]</sup> and has already shown promising anti-tumour effects in preclinical studies.<sup>[72]</sup> Folate receptor (FR) is overexpressed on the surface of many cancer types, which makes folic acid (FA) a desirable small molecule for anti-cancer targeted conjugates. In the case of lipoplexes, in order to ensure that FA is present on the surface of lipoplex and, hence, available for the cellular receptors, it

was conjugated to a PEG-lipid (N-(Carbonyl-methoxy(polyethylene glycol))-1,2-distearoyl-*sn*-glycero-3-phosphoethanolamine, sodium salt, 2,000 Da; DSPE-PEG2k).

### 3.7.1 Folate targeting *in vitro*

As an *in vitro* model for an FA-expressing tumour, KB cells were chosen, whereas NIH 3T3 served as a control. To prove that the targeted nanoparticles are taken up by the FR in KB cells, the transfection procedure was split into three steps: binding to the receptors (on ice), uptake (30 min at 37°C), and translation (24 h at 37°C after media change), which is described in more detail in Materials and Methods. Additionally, transfection with formulation comprising FA was performed in the presence of free FA in media for a competitive binding to the receptors. Furthermore, two controls for the targeted lipoplexes (comprising DSPE-PEG2k-FA) were included: DMG-PEG2k (standard) and DSPE-PEG2k formulation. The result of the transfection efficiency in both cell lines is presented in Figure 3.36.

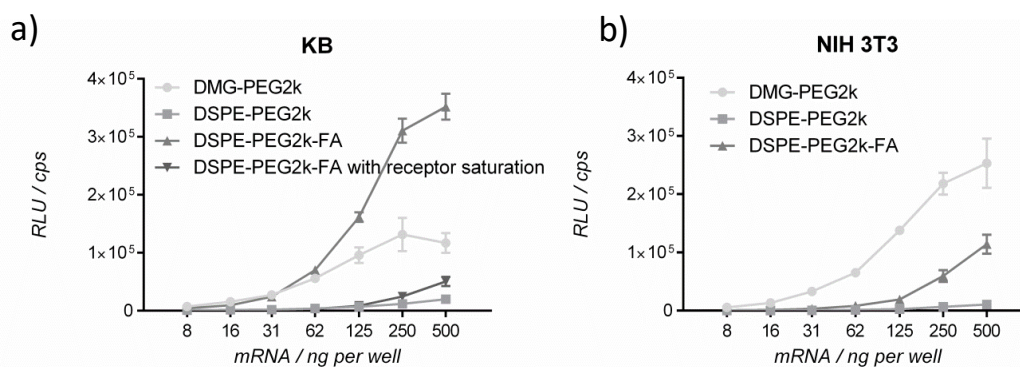


**Figure 3.36.** Folate targeting with lipoplexes shown on a) KB cells and b) NIH 3T3 as a control.

As shown in Figure 3.36a, transfection efficiency of FA-conjugated lipidic carriers was drastically reduced by free FA. On the other hand, its non-targeted counterpart, DSPE-PEG2k formulation, hardly led to any reporter protein translation at all. Together these results suggest that transfection was largely driven by a folate-mediated process. A control formulation which was tested in previous chapters, DMG-PEG2k, showed higher transfection efficiency than DSPE-PEG2k without a targeting moiety, which confirmed that FA is not essential for mRNA delivery into KB cells. However, DMG-PEG2k lipoplexes were not even nearly as effective as DSPE-PEG2k with FA, which demonstrated advantages of receptor-mediated uptake. Transfection of NIH 3T3 was performed with media change after 30 min incubation

and proved benefits of standard DMG-PEG2k over FA conjugates (Figure 3.36b). All in all, the *in vitro* experiments showed promising results of FA targeted lipoplexes as they transfected cells which express the FR mostly by receptor-mediated uptake.

### 3.7.2 Folate targeting *in vivo*

To prove the concept of FA targeting *in vivo* as well, KB cells were injected into immunodeficient mice. Once tumours reached an appropriate size they were treated with FA-targeted lipoplexes carrying mRNA coding for A-chain of the toxin abrin (AA). Abrin belongs to the family of AB-toxins, which consist of a B subunit specifically binding to target cells and enabling cellular entry of the catalytic A subunit.<sup>[73]</sup> For the mRNA production only the A chain is used. The tumour growth during the treatment with a comparison to sucrose-treated group is shown in Figure 3.37.

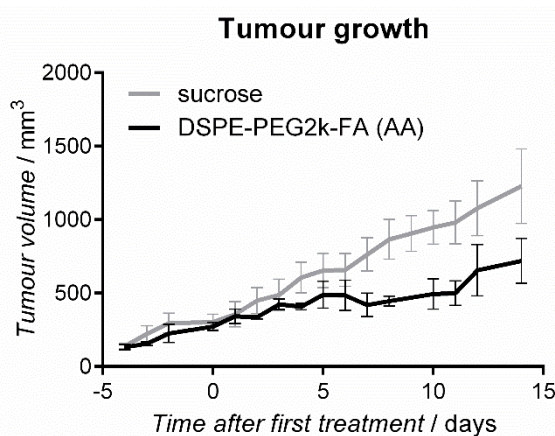


**Figure 3.37.** Tumour growth during treatment with FA-lipoplexes comprising mRNA coding for toxin abrin (DSPE-PEG2k-FA (AA)) with a sucrose-treated control.

When the tumours reached the appropriate size (250 mm<sup>3</sup>), FA-targeted lipoplexes were injected directly into cancer tissue every 2-3 days. Compared to sucrose control, a trend of inhibited tumour growth was observed.

With the purpose of *in vivo* targeting, formulations of DSPE-PEG2k-FA and DSPE-PEG2k were compared in their ability to deliver reporter mRNA-FLuc to KB tumour bearing mice (see Figure 3.38).

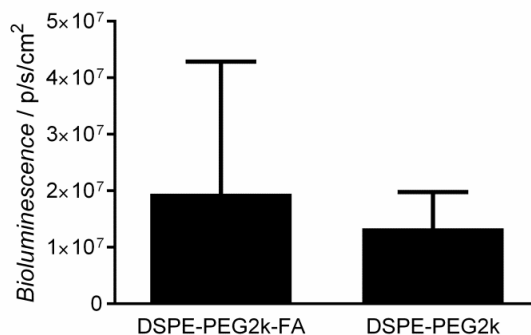


**Figure 3.38.** Bioluminescence in KB tumours in mice treated with targeted DSPE-PEG2k-FA and non-targeted DSPE-PEG2k lipoplexes.

Although there was no significant difference between these two groups (most likely due to the low number of animals), the average bioluminescence in tumours of mice treated with FA-targeted carriers was higher.

In summary, these data suggest that targeted delivery with folic acid as a ligand is remarkably efficient *in vitro* by showing a receptor-mediated transfection process. Although the benefits of using targeted formulation *in vivo* were not significant, a trend towards increased bioluminescence in mice treated with FA-targeted lipoplexes was observed. Moreover, the lipid nanoparticles successfully delivered the therapeutic mRNA to the tumour tissue.



## 4 Discussion

The aim of this thesis was the optimization of a multicomponent lipid-based delivery system for chemically modified mRNA. The experiments were designed to tailor the formulation towards the needs of mRNA and help to understand the delivery process with this system in more detail. The following chapter contains conclusions drawn from the results of the experiments and possible explanations for the observations. The contribution to the knowledge of aspects crucial for transfection process enables further development of transcript therapies.

### 4.1 Lipidoids

A cationic lipid plays a crucial role in mRNA delivery in lipid-based systems, fulfilling more than just one function. Not only encapsulation of a polyanionic nucleic acid via electrostatic interactions, but also cellular uptake as well as endosomal escape of a complex are among them. Cationic particles can bind to anionic functional groups on a cell surface and undergo a clathrin-mediated uptake.<sup>[74]</sup> After endocytosis, cationic lipids are presumed to interact with anionic phospholipids in the endosomal membrane, forming ion pairs that adopt nonbilayer structures such as hexagonal phase (see Figure 4.2) and, hence, disrupt membranes.<sup>[20,45]</sup>

At first, the lipidoid headgroup became the subject of the studies. A small set of oligoalkylamines (tri- (2-2, 3-3) and tetramines bearing ethylene (2-2-2) and/or propylene spacers (2-3-2, 3-3-3)) were modified with C12 alkyl chains and screened for their buffering capacity. High buffering capacity in a pH range 6.2-6.5 is hypothesized to enhance endosomal escape of the mRNA-carrier complex into the cytosolic compartment. The assumption was based on a discovery of a strong correlation between carrier's  $pK_a$  in above mentioned range and *in vivo* siRNA activity.<sup>[21]</sup> Since the results showed that only C12-(2-3-2) displayed a clear peak in the desired range, this tetramine was expected to deliver mRNA to the cells efficiently. All tested structures, when complexed together with mRNA and three other lipids (two helper lipids and a PEG-lipid), formed monodisperse, spherical particles in the nanosize range of neutral or slightly positive zeta potential. Moreover, the encapsulation

efficiency was high in each case (>90%) and mRNA was shown to be intact. In conclusion, all nanoparticles fulfilled the physicochemical requirements of complexes suitable for *in vivo* applications. However, a careful analysis of the agarose gel (Figure 3.3) reveals that the mRNA band intensities of complexes with lipidoids bearing propylene spacers only (C12-(3-3) and -(3-3-3)) were slightly weaker than in other cases. Such an observation could indicate a very strong binding of these lipidoids to the nucleic acid, which is undesired and can hamper the translation process as it has been shown for some polymeric carriers.<sup>[26]</sup> Next, as a prerequisite for any further cellular processes, the particle uptake of lipoplexes was evaluated. Even though some differences in the kinetics of the process were observed, in general the uptake driven by tetramine-based lipids was on a comparable level, whereas triamine-based lipids led to poor reporter mRNA levels in the cells. If the cellular uptake of lipoplexes was a limiting step of the transfection process, it should result in a similar transfection efficiency order like the observed uptake levels. However, the recorded protein translation values differed from expectations (e.g. poor transfection efficiency in the case of C12-(3-3-3) despite effective uptake), which excludes the cellular uptake as the most crucial factor. Nevertheless, it could be assumed that a certain threshold needs to be exceeded. Since the good tolerability of the carriers is one of the most important requirements of their characteristics, the cell viability of the cells treated with each screened lipidoid in lipoplexes was tested. The results demonstrated that C12-(2-2-2) is the least toxic. However, the differences in cell viability also exhibited no correlation with transfection efficiency. The following screening for efficient delivery of mRNA in nanoparticles showed that a tetramine with alternating ethyl–propyl–ethyl spacers (C12-(2-3-2)) exhibited a high ability to mediate robust levels of protein translation *in vitro* in four different cell lines, derived from different species and tissues, although the oligoalkylamines within the tested carriers hardly varied. The beneficial delivery capability of the (2-3-2)-based lipid was further confirmed in mice. Importantly, no direct correlation between augmented protein levels driven by C12-(2-3-2) and particles properties, cellular uptake or viability was found. The main influencing parameter seems to be the buffering capacity in the pH range 6.2-6.5, as it was described for siRNA delivery.<sup>[21]</sup> The transfection with lipoplexes comprised of carriers with low buffering capacity in

the endosomal pH range exhibited only low levels of reporter enzyme activity in murine fibroblasts. In contrast, the lipidoid C12-(2-3-2), showing high buffering capacity in the pH range 6.2-6.5, exhibited superior activity compared to the other tested lipids. Such a result confirms the importance of protonation in the endosomal escape and, hence, carrier efficiency.

The observation of a clear advantage of the alternating oligoalkylamine-bearing lipid *in vitro*, independent of cell type, as well as *in vivo* indicates the existence of a general structural trend. The lack of functionality of triamine-based carriers could be hypothetically explained by the odd-even effect described by Uchida *et al.*<sup>[31]</sup> They have shown that polyplexes with odd number of repeats displayed an increase in efficiency compared with those with even number of repeats (PA-Es). The scaffolds with even number of repeats were unstable in the cytoplasm, which disabled them to transfect the cells efficiently. One hypothesis explaining the effect of the alternating structure would be that it combines good buffering capacity with sufficient, but also not too strong, complex stability. As a consequence, endosomal release of (2-3-2) tetramine is facilitated and the intact complex is able to enter the cytosol. These surprising findings reveal that even subtle changes in the structure of carriers hold high potential for carrier improvements. However, a detailed investigation regarding the underlying mechanism of this structure–activity relationship has to be the topic of further studies.

The dendrimeric structures based on the alternating oligoalkylamine motif showed 100-fold lower transfection efficiency *in vivo* compared to the initial carrier C12-(2-3-2). However, it is important to note that the same N/P ratio applied to linear G0 (2-3-2) and branched G1 or G2 leads to smaller total amounts of the lipid with increasing generation (G0 to G2) as the number of potentially protonable amines also increases (from 4 to 14). The low values of encapsulation efficiency of particles comprising C16-G1 and C12-G2 (23% and 49%, respectively) together with negative zeta potential values (-14.8 and -23.5 mV, respectively) suggest that higher amounts of dendrimer-based lipids would be required to obtain particles of desired properties. It has been shown that similar, lipid-derivatized dendrimeric structures possess high potency for siRNA delivery.<sup>[52]</sup> Described there dendrimer to siRNA ratio 5:1 (w/w) would approximately correspond to N/P ratio 10 calculated for

complexation of mRNA. However, such amounts might be insufficient in the case of mRNA due to differences in size of these two nucleic acids.

The investigation of an alkyl chain length in lipidoids showed that neither too short (C5 or C6) nor too long (C16) alkyl chains are able to deliver mRNA with high efficiency, both *in vitro* and *in vivo*. The optimum in the tested cell line was found within C12 and C14, whereas in mice it shifted to C10 and C12. Previously, it has been shown that tails shorter than C12 did not exceed 30% silencing with siRNA.<sup>[44]</sup> Possibly the optimum is shifted to the shorter alkyl chains in the case of mRNA, although it should be acknowledged that an optimized combination of a headgroup and tail might be more critical.

### 4.2 Helper lipids

Not only the lipidoid, but also other components in a lipid delivery system are crucial for its efficiency. The results demonstrated that in the absence of a phospholipid, lipoplexes were completely nonfunctional in mRNA delivery, both *in vitro* as well as *in vivo*. Such outcome supports the theory of the charge mediator role of a phospholipid: forming ion pairs between its phosphate group and lipidoid headgroup, whereas positively charged moiety (e.g. choline in the case of phosphocholines) interacts with nucleic acid phosphates.<sup>[50]</sup> Especially that the activity *in vivo* seemed to be independent on the phospholipid type (1,2-dioleoyl-*sn*-glycero-3-phosphoethanolamine (DOPE) or 1,2-distearoyl-*sn*-glycero-3-phosphocholine (DSPC)). The hypothetical phospholipid role in transfection efficiency has been thoroughly explained on the example of DOPE or DPPE (dipalmitoylphosphatidylethanolamine) lipoplexes for oligonucleotides delivery.<sup>[75]</sup> The authors proposed that helper lipids promoting formation of a hexagonal phase (see Figure 4.2) also enhance transfection efficiency (DOPE in the described experiments). In contrast to lamellar phase, hexagonal conformation is critical for an efficient endosomal escape, mostly in terms of complex translocation across the membrane but also of nucleic acid dissociation from the lipoplexes.

In addition, although some tendencies in phospholipid chain length and saturation could be noted in the *in vitro* experiments, no pronounced effects were observed *in vivo*.

The influence of the second helper lipid, cholesterol, on the transfection efficiency *in vitro* was less evident than in the case of DPPC. Moreover, it could be observed in the formulations with lowered PEG-shielding only. The possible explanation lies in the presumable cholesterol role, namely stabilization of the lipoplexes.<sup>[76,77]</sup> This lipoplex characteristic has a greater impact on *in vivo* application and especially in well shielded particles did not lead to significant differences in transfection efficiency. Moreover, some specific cholesterol-driven effects, e.g. described cholesterol ratio-dependent targeting of liver cells subpopulation shown for gene silencing<sup>[52]</sup> can be observed *in vivo* exclusively.

### 4.3 The importance of a PEG-lipid in lipoplex shielding

Since the role of a PEG-lipid is the most critical for *in vivo* applications as it prolongs the particles circulation in the blood stream and prevents interactions with blood components, it is a challenge to test its influence in cell culture. Yet, an attempt to determine the impact of a PEG-lipid headgroup, anchor length and saturation, PEG length, and PEG-lipid density in the formulation was made. At first, a couple of different backbones were compared in terms of their transfection efficiency. On the contrary to the phospholipid, it does not seem to be critical for complex activity to use a PEG-lipid with a backbone comprising charged moieties (e.g. 1,2-dimyristoyl-*sn*-glycero-3-phosphoethanolamine-N-[methoxy(polyethylene glycol)-2000] (ammonium salt) (DMPE-PEG2k)). On the other hand, since neutral 1,2-dimyristoyl-*sn*-glycerol, methoxypolyethylene glycol (DMG-PEG2k) exhibited a trend towards increased efficiency compared to DMPE-PEG2k but at the same time another neutral PEG-lipid (cholesterol-PEG2k) showed lower activity, the effect of a backbone must be much more complex.

A more distinct effect was observed when the unsaturated and long anchor chain (C18:1) was compared to the saturated and short one (C14:0) in PEGylated glycerol-3-phosphoethanolamine (DOPE-PEG2k vs. DMPE-PEG2k). The results demonstrated higher delivery potential of the first one. However, as both anchor length and saturation varied, the influencing factor could not be identified. Nonetheless, further experiments allowed to attribute a significant impact to the anchor length. Even subtle variations in the anchor chain length (from C14 to C16) showed a drastic im-

impact on the transfection efficiency. As it has been described, the hydrophobicity of the PEG-lipid changes the particle deshielding rate and, hence, carriers activity.<sup>[56]</sup>

The comparison of two different PEG lengths (2,000 and 5,000 Da) *in vitro* showed that the increased PEG chain hampers the transfection process. Such a result could be an indicator of higher shielding (more stealth particles obtained), especially taking into consideration the fact of slower deshielding of the particles in cell culture.<sup>[78]</sup> The longer PEG applied *in vivo* could prolong the blood circulation of the lipoplexes, which would lead to changes in the translation kinetics. Another possible result could be faster recognition by the immune system. It has been shown for the lymph node targeting liposomes that increased PEG length accelerates the vesicle transport.<sup>[79]</sup> Therefore, the impact of the PEG chain length on mRNA delivery should be further investigated in an animal model.

In order to obtain stealth nanoparticles, their surface should be completely covered with a PEG-lipid. Especially with the aim of targeted delivery, stealth particles would be beneficial by reducing any unspecific interactions and, hence, ensuring receptor-mediated uptake mostly. In a series of experiments with pre- and post-assembling of a PEG-lipid up to 40% molar (of all lipids) it was shown that from a certain point saturation on the particle surface is reached. The excessive PEG-lipid cannot be incorporated into lipoplexes anymore, forming PEG-micelles as a separate particle population. When the method of post-assembling was applied, the resulting particles exhibited size and zeta potential increase without changes in PDI. These results suggest that this way of particle formation allows to incorporate larger amounts of a PEG-lipid than the typical one-step, pre-assembling process. The decrease of activity related to higher PEG-lipid content observed *in vivo* is most likely due to obtaining more stealth particles. As it has been shown for lipid nanoparticles for gene silencing, increased PEG density led to reduced efficiency *in vivo* due to inhibited ApoE-mediated delivery mechanism.<sup>[65]</sup> However, the efficacy of lipoplexes with 20% PEG could be rescued by attaching a targeting ligand on the particle surface.

### 4.4 Coupled dependences between the lipids

In some experiments it could be noted that variations in one lipid component have an impact on trends observed for another one, e.g. decreased amount of a PEG-lipid

changes the examined single lipid dependence patterns (Chapter 3.2.3 “Variations in the lipid composition”). Therefore, the outcome of a screening focusing on only one component or moiety can be affected by the remaining lipids or their ratios. For that reason it is important to understand the role and impact of each variable (headgroups, alkyl chain length and saturation, molar ratios, N/P etc.) in the complex “lipoplex equation”. However, it must be noted that these variables are not necessarily independent from each other. In this chapter, an attempt to define some rules in the influence of a lipid alkyl chain length on the transfection efficiency in relation to other lipid components has been made.

Interestingly, in the experiments varying the alkyl chain lengths of the lipidoid and the PEG-lipid at the same time a shift in maximal efficiencies to the higher doses with increasing alkyl length of lipidoid was observed (see Figure 3.23). An explanation could be stronger binding of mRNA with increasing alkyl chain length, which leads to higher effective doses. Moreover, the mutual interactions between the lipids revealed that a factor playing an important role is rather the length difference between alkyl chains of compared lipids. For instance, the highest transfection efficiency for C14-PEG was obtained with C10-(2-3-2) and for C18-PEG with C14-(2-3-2) (in both cases length difference of four carbon atoms). On the other hand, in the experiment investigating the coupled dependences between alkyl chain lengths of the lipidoid and the phospholipid at the same time exhibited rather constant advantage of using C16 PC. Such discrepancies in the observed patterns of the coupled dependences lipidoid/PEG-lipid and lipidoid/phospholipid should not be unexpected when the different role of each lipid is taken into consideration. A variation in alkyl chains of lipidoid/PEG-lipid presumably determines the particles stability and mRNA binding strength, whereas a phospholipid supposedly has an optimal alkyl length for mediating the charge between mRNA and the lipidoid more independently of the lipidoid’s chains. In order to make the influence of varying alkyl lengths in both lipidoid and phospholipid at the same time more transparent, some graphs from performed experiments were gathered together in Figure 4.1. The length difference of four carbon atoms was chosen ( $\Delta C=4$ , e.g. C10-(2-3-2) and C14 PC) as it seemed optimal in some previously tested formulations.

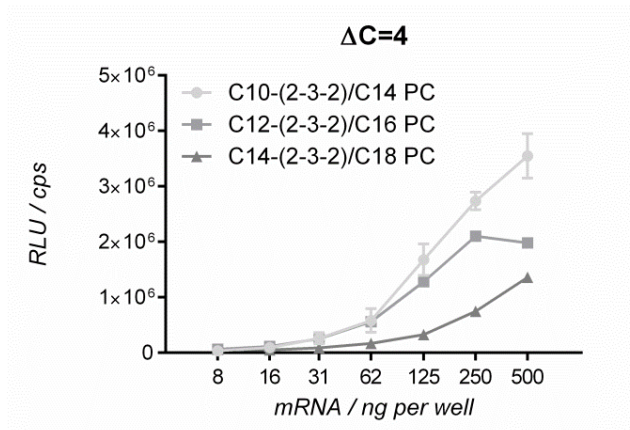


**Figure 4.1.** Transfection efficiency of lipoplexes comprising lipidoids and phospholipids with the length difference in alkyl chain lengths of four carbon atoms.

As shown in Figure 4.1, the transfection efficiency indicated higher complex activity when both chains were shorter (C10-(2-3-2) in combination with C14 PC).

With the addition of the third component in the evaluation of mutual interactions between the lipids the number of possible combinations escalates. Thus, only two components of each lipid type were chosen: C10- and C12-(2-3-2), C14 and C16 PC, as well as C14- and C16-PEG. The transfection efficiency experiment *in vitro* revealed that for both tested lipidoids the highest activity was reached in combination with C16 PC and C16-PEG. In the tested range, the impact of variations in PEG-lipid anchors seemed to have greater impact on C12- than C10-(2-3-2) formulations.

Another tested coupled dependence was the N/P ratio. Since it is determined by the proportion of a lipidoid to mRNA, variations in its value result in a change of the total amount of the lipids to mRNA ratio. It is necessary to find an optimal N/P ratio: sufficient for mRNA complexation and delivery to the cells but with minimized dose of applied carrier. The presented data of bioluminescence in mice after stepwise reduction in the N/P ratio proved that a ratio as low as 4 is sufficient for pronounced reporter protein translation. Previous studies on siRNA delivery have shown that reducing the lipid to siRNA ratio led to only slight decrease in efficiency, while demonstrating significant positive effect on tolerability.<sup>[56]</sup> The optimum was found at lipid to siRNA ratio 7.5 (w/w), which would roughly correspond to N/P 5 in the case of lipid formulation for mRNA described in this work. Other siRNA lipid formulations use lipid to siRNA ratio ranging from 17<sup>[21]</sup> down to as low as 2.6.<sup>[69]</sup>



In conclusion, even very limited number of tested variables and combinations between them clearly showed that in a multicomponent delivery system results of side-by-side comparisons can be affected by other components or ratios in the formulation. Apparently even subtle changes such as two carbon atoms in alkyl chains can drastically influence carriers' activity. On the other hand, the chain saturation has an impact on the lipid transition temperature (the temperature at which lipid bilayers shift from stable lamellar phase to the less stable hexagonal phase, see Figure 4.2), which is hypothesized to enhance lipoplex escape from the endosome.<sup>[80]</sup>

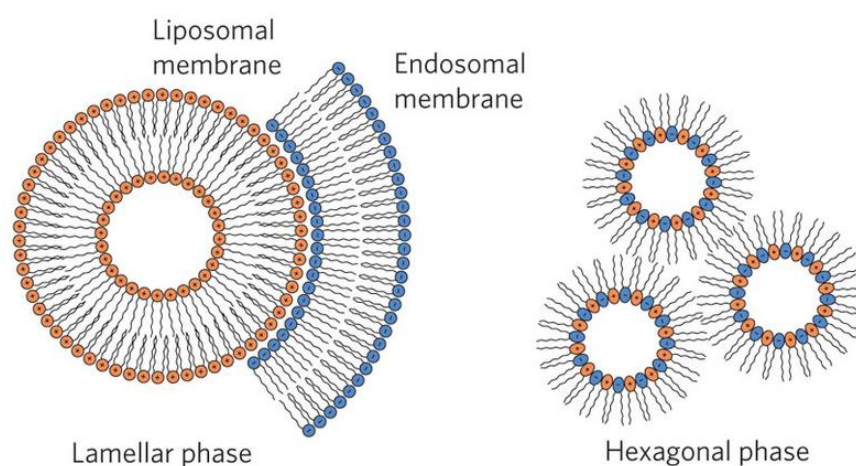


**Figure 4.2.** Lipid structures. The mixing of cationic (orange) and anionic (blue) lipids promotes the transition from the more stable lamellar phase to the less stable hexagonal phase, thus aiding fusion of the liposomal and endosomal membranes.<sup>[80]</sup>

The challenge involves finding an optimum among all possibilities. However, variations in all considered influencing parameters (lipid types, alkyl chain lengths and saturation, linker type, ratios, mixing conditions etc.) gives a number of possible combinations that is unattainable to test. On the other hand, obtained data made it evident that testing only one variable while keeping the remaining ones constant reminds moving along single axis in an n-dimensional matrix: only a surface can be seen and many points inside of it are missed. One solution could be using an orthogonal array optimization, as proposed by Li *et al.*<sup>[81]</sup> Such an experimental design enables a significant efficiency improvement with reduced experimental workload.

### 4.5 Formulation conditions

In order to decrease N/P ratio further without any reduction in delivery capability of lipoplexes, magnesium cations were incorporated as nonlipidic agent stabilizing the mRNA structure. The stabilizing properties were indicated by decreasing tendency in size as well as improved transfection efficiency at N/P 8 and 6 in the presence of  $Mg^{2+}$ . As already proposed by Uchida *et al.*,<sup>[31]</sup> stability of mRNA in the cytoplasm correlates with sustained protein translation. Therefore, developing a system consisting not only of lipids (vital for the cell entry and endosomal escape) but also an inorganic component stabilizing the nucleic acid in the cytoplasm could be a solution for a novel delivery system design.

Next, the importance of the protonation level in nucleic acid binding was shown in an experiment with varying pH of the formulation solution. The acidic pH below or equal to one of the lipidoid's  $pK_a$ 's (5.2) ensured protonation level sufficient for proper complexation (resulting in small, monodisperse particles). Particle formation in solutions of pH 6 or 7 resulted in increase in both hydrodynamic diameter and PDI, indicating either lack or a poor level of protonation, disabling electrostatic interactions with negatively charged mRNA. In the field of siRNA delivery, it is common to use buffers of pH 4 or 5 for the lipid particle formation.<sup>[21,44,45,82]</sup>

### 4.6 mRNA release assay

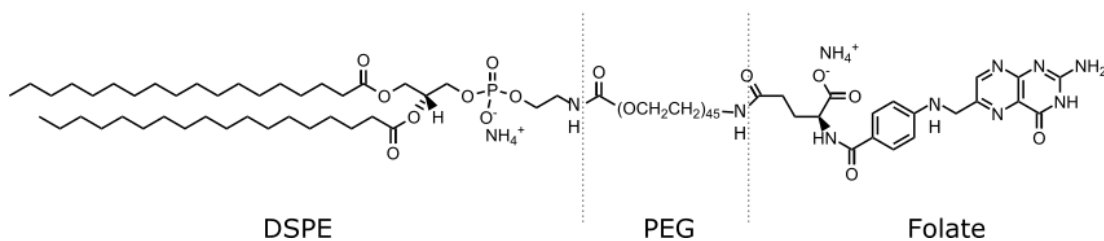
An *in vitro* method based on a model described by Zhang *et al.*<sup>[69]</sup> was supposed to mimic the series of processes that a particle injected intravenously needs to undergo to reach its final destination. The results showed a good correlation between relative mRNA release and bioluminescence in mice, proving that the proposed model covers the most critical steps *in vivo*. The relative mRNA release was defined as the ratio between mRNA release in artificial endosomes (samples treated with blood plasma and anionic liposomes, respectively) to mRNA release in plasma (a control without anionic liposomes). A high value of relative release means that most of the nucleic acid is disassembled from the complexes in the cytosol (related to the mRNA release in artificial endosomes), with only small losses of the cargo in the blood stream (related to the mRNA release in plasma). Importantly, many aspects of the assay should be analysed carefully before drawing conclusions about formula-

tion suitability for *in vivo* applications and its activity. First of all, as shown by the experiments, the comparison of lipoplexes carrying different mRNAs is not possible due to discrepancies in the detected signal coming from different transcripts. Secondly, relative release values of tested lipoplexes should not be compared without prior analysis of the release in artificial endosomes and release in plasma separately. Low values of both releases (in artificial endosomes and plasma) could result in high values of the relative release, although tested complexes are inactive *in vivo* due to the low mRNA amounts dissociated in the cells. Thirdly, especially the plasma-treated sample should be observed cautiously. Particle aggregation in the presence of plasma would exclude them from *in vivo* application even if the relative release value is high. This step could be standardized by introducing an additional absorbance or dynamic light scattering (DLS) measurement in the assay. Such a measurement would allow a quantitative evaluation of particle stability in the blood. Last but not least it has to be emphasized that mRNA release assay *in vitro* remains a model, which is still very simplified compared to the complex *in vivo* system. Thus, it cannot replace testing in animal models.

### 4.7 Targeted delivery with folic acid

The most effective way to ensure high, tissue (or even cell type) specific translation and to minimize the risk of toxic side effects is the use of targeted delivery. In this work, folic acid (FA) was chosen to target tumour cells, which often overexpress the folate receptor on their surface. The successful receptor-specific targeting has been shown previously on the example of FA-PEG-siRNA conjugates,<sup>[83]</sup> multifunctional polyplexes for siRNA delivery with FA coupled to PEG,<sup>[84]</sup> and FA-PEG-linked two-arm oligocation structure for siRNA as well as pDNA delivery,<sup>[85]</sup> among others.

To ensure accessibility of the small molecule for the receptors, it has been attached to the PEG-lipid (N-(Carbonyl-methoxy(polyethylene glycol))-1,2-distearoyl-*sn*-glycero-3-phosphoethanolamine, sodium salt, 2000 Da; DSPE-PEG2k), as shown in Scheme 4.1.



**Scheme 4.1.** Structure of a PEG-lipid and folate conjugate, DSPE-PEG2k-FA.

The experiments performed *in vitro* on human cervix carcinoma cells (KB) showed an evident receptor-mediated uptake of targeted nanoparticles (comprising DSPE-PEG2k-FA). The translation was almost entirely inhibited by competitive binding of free folate added to the cells. The results also revealed that the nontargeted counterpart of the tested PEG-lipid (DSPE-PEG2k) is barely able to transfect these cells, which is another proof of folate receptor uptake of DSPE-PEG2k-FA lipoplexes. The huge discrepancy between translation levels driven by targeted and nontargeted carriers should enable very specific delivery of mRNA *in vivo*, exclusively to the cells possessing the targeted receptor. In addition, the transfection of a control cell line, murine fibroblasts (NIH 3T3) revealed that in this case DMG-PEG2k was significantly more effective than DSPE-PEG2k-FA. Such a result indicates cell type specificity of FA-targeted lipoplexes.

Cancer treatment in an animal model (immunodeficient mice with subcutaneous KB tumours) with lipoplexes comprising mRNA coding for A-chain of the toxin abrin showed a tendency towards tumour growth inhibition compared to the sucrose-treated control. The targeting ability *in vivo* of FA-conjugates was tested in carriers comprising reporter mRNA-FLuc. Interestingly, no significant difference in detected bioluminescence in tumours was noted. The benefits of using FA-targeted delivery were evident *in vitro* and the nontargeted DSPE-PEG2k lipoplexes seemed to be almost nonfunctional, therefore the similar activity pattern *in vivo* was expected. However, a couple of factors should be taken into consideration. Firstly, the targeted delivery plays the most important role *in vivo* when the drugs are applied intravenously and then transported into the tissue of interest by interactions with specific receptors. In this case the transportation step was omitted as the complexes were applied via intratumoural injection, which could be a reason for the diminished FA targeting effect. Secondly, the relatively high activity in tumours of lipoplexes,

which were rather inert *in vitro* could be an indicator of a different deshielding process or rate in the tumour tissue compared to the blood stream, let alone cell culture. Thus, lipid-based systems should be optimized separately for this application.

### 5 Summary

The development of chemically modified mRNA opens a new way towards a novel class of biologic therapeutics. In contrast to gene therapy, mRNA-based drugs do not bear the inherent risk of insertional mutagenesis. Moreover, they provide a transient production platform for *in situ* generation of the therapeutic protein due to the relatively short half-life of mRNA, which enables a well-controlled therapy with repeated dosing. Additionally, chemical modifications of RNA nucleotides have been shown to decrease immune responses and improve the nucleic acid stability. However, the direct delivery of mRNA to cells is hampered by its highly anionic character that prevents a passage across cell membrane unaided and the ubiquitous presence of RNases. Therefore, a delivery system that is designed for the efficient encapsulation of mRNA using carriers that possess effective cell penetrating properties is required.

The aim of the thesis was the development of a lipid-based carrier tailored on the needs of the nucleic acid, which is single-stranded (in contrast to pDNA and siRNA) and relatively large (compared to miRNA). The multicomponent system was supposed to overcome many hurdles met by the drug on its way from the intravenous injection to the protein translation in the target cells, namely liver cells for metabolic diseases and tumour cells for anticancer therapy. By incorporation of various components the goal was to achieve efficient encapsulation of mRNA, protection from degradation and undesired interactions in the blood stream, delivery to the tissue of interest, effective cell penetrating properties, the endosomal escape ability, and the final release of the nucleic acid in the cytoplasm.

At first, a small set of lipidoids was synthesized from a series of oligoalkylamines and subsequently characterized in terms of their buffering capacity in the range of pH 6.2 to 6.5, which is hypothesized to enhance endosomal escape of the carrier complex into the cytoplasm through membrane disruption by positively charged nanoparticle surface. It was found that only the alternating structure of the lipidoid C12-(2-3-2) (ethyl-propyl-ethyl spacers between amines) displayed a peak buffering capacity in the desired range. Even though every tested lipidoid was able to

complex mRNA efficiently and form decent nanoparticles, C12-(2-3-2)-based carriers showed the highest transfection efficiency in different cell lines and in an animal model. Since no correlation between particle uptake or cytotoxicity and their mRNA capability was found, the crucial effect of the buffering capacity was confirmed. Moreover, variation in only one methylene group resulted in enhanced protein translation, which reveals a novel fundamental structure–activity relationship for the delivery of mRNA.

Following experiments have proven the vital role of helper lipids, among others. Phospholipids presumably act as the charge mediators between the lipidoid and mRNA and thus lipoplexes lacking this component are nonfunctional. The investigation of a PEG-lipid headgroup, anchor chain length and saturation, PEG chain length, and PEG-lipid density on the particle surface showed that i) even slight modifications leading to changes in a PEG-lipid hydrophobicity have a huge impact on complex activity, which might be caused by a changed deshielding rate, ii) increased PEG length or PEG-lipid density result in stealth particles, which hamper protein translation or change the translation kinetics, iii) a certain PEG-lipid density on particle surface cannot be exceeded, iv) the method of post-assembling allows to incorporate more PEG-lipid than the typical pre-assembling.

A series of experiments testing some combinations of varying chain lengths in a lipidoid, phospholipid, and a PEG-lipid at the same time revealed mutual interactions between lipids affecting the efficiency of the resulting lipoplexes. The data showed that a choice of the most effective component is mostly dependent on the other lipids or ratios between them used in the formulation.

The developed mRNA release assay proved to be an effective indicator for predicting formulations delivery efficiencies *in vivo*. The ratio of mRNA released in artificial endosomes to mRNA released in serum showed a positive correlation to reporter enzyme activity detected in mice after i.v. administration.

Moreover, the concept of targeted lipid-based delivery with small molecules as ligands was proven on the example of folic acid targeting on folate receptor overexpressing cells. Lipoplexes conjugated with folic acid on the surface performed remarkably efficient *in vitro*, showing a receptor-mediated uptake. Although the benefits of using targeted formulation *in vivo* were not significant, a trend towards in-

creased bioluminescence in mice treated with FA-targeted lipoplexes was observed. Moreover, the lipid nanoparticles successfully delivered the therapeutic mRNA to the tumour tissue, causing toxin-driven tumour growth inhibition.

In conclusion, this thesis demonstrates that the fine-tuning of lipid-based carriers is a key to augmented mRNA delivery capability. Furthermore, it was proven critical to consider the multicomponent system as a complex matrix and to test coupled dependences instead of single lipid components or factors. Since many tested lipoplexes led to high reporter protein translation both *in vitro* as well as *in vivo*, this work provides a foundation to develop mRNA delivery systems that may have future clinical applications.



---

## 6 References

- [1] “National Human Genome Research Institute,” can be found under <https://www.genome.gov/>, **n.d.**
- [2] “Genetics Home Reference,” can be found under <https://ghr.nlm.nih.gov/condition/cystic-fibrosis>, **n.d.**
- [3] M. Edelstein, “Journal of Gene Medicine,” can be found under <http://www.abedia.com/wiley/years.php>, **n.d.**
- [4] S. Clancy, *Nat. Educ.* **2008**, *1*, 125.
- [5] J. Yu, J. E. Russell, *Mol. Cell. Biol.* **2001**, *21*, 5879–88.
- [6] V. F. I. Van Tendeloo, P. Ponsaerts, Z. N. Berneman, *Curr. Opin. Mol. Ther.* **2007**, *9*, 423–31.
- [7] K. Karikó, M. Buckstein, H. Ni, D. Weissman, *Immunity* **2005**, *23*, 165–175.
- [8] B. R. Anderson, H. Muramatsu, S. R. Nallagatla, P. C. Bevilacqua, L. H. Sansing, D. Weissman, K. Karikó, *Nucleic Acids Res.* **2010**, *38*, 5884–5892.
- [9] M. S. D. Kormann, G. Hasenpusch, M. K. Aneja, G. Nica, A. W. Flemmer, S. Herber-Jonat, M. Huppmann, L. E. Mays, M. Illenyi, A. Schams, et al., *Nat. Biotechnol.* **2011**, *29*, 154–157.
- [10] E. R. Balmayor, J. P. Geiger, M. K. Aneja, T. Berezhanysky, M. Utzinger, O. Mykhaylyk, C. Rudolph, C. Plank, *Biomaterials* **2016**, *87*, 131–146.
- [11] D. S. Friend, D. Papahadjopoulos, R. J. Debs, *Biochim. Biophys. Acta - Biomembr.* **1996**, *1278*, 41–50.
- [12] I. S. Zuhorn, R. Kalicharan, D. Hoekstra, *J. Biol. Chem.* **2002**, *277*, 18021–18028.
- [13] I. a Khalil, K. Kogure, H. Akita, H. Harashima, *Pharmacol. Rev.* **2006**, *58*, 32–45.
- [14] C. Lamaze, S. L. Schmid, *Curr. Opin. Cell Biol.* **1995**, *7*, 573–580.
- [15] S. D. Conner, S. L. Schmid, *Nature* **2003**, *422*, 37–44.
- [16] M. B. Bally, P. Harvie, F. M. P. Wong, S. Kong, E. K. Wasan, D. L. Reimer, *Adv. Drug Deliv. Rev.* **1999**, *38*, 291–315.
- [17] C. Plank, B. Oberhauser, K. Mechtler, C. Koch, E. Wagner, *J. Biol. Chem.* **1994**,

- 269, 12918–12924.
- [18] J. Behr, *Int. J. Chem.* **1997**, *2*, 34–36.
- [19] E. Wagner, in *Nonviral Vectors Gene Ther. Lipid- Polym. Gene Transf.* (Eds.: L. Huang, D. Liu, E. Wagner), Academic Press, **2014**, pp. 231–261.
- [20] I. M. Hafez, N. Maurer, P. R. Cullis, *Gene Ther.* **2001**, *8*, 1188–96.
- [21] M. Jayaraman, S. M. Ansell, B. L. Mui, Y. K. Tam, J. Chen, X. Du, D. Butler, L. Eltepu, S. Matsuda, J. K. Narayanannair, et al., *Angew. Chemie - Int. Ed.* **2012**, *51*, 8529–8533.
- [22] A. Yamamoto, M. Kormann, J. Rosenecker, C. Rudolph, *Eur. J. Pharm. Biopharm.* **2009**, *71*, 484–489.
- [23] M. A. Islam, E. K. G. Reesor, Y. Xu, H. R. Zope, B. R. Zetter, J. Shi, *Biomater. Sci.* **2015**, *3*, 1519–33.
- [24] J. H. Strauss, E. G. Strauss, *Microbiol. Rev.* **1994**, *58*, 491–562.
- [25] H. Yin, R. L. Kanasty, A. A. Eltoukhy, A. J. Vegas, J. R. Dorkin, D. G. Anderson, *Nat. Rev. Genet.* **2014**, *15*, 541–555.
- [26] T. Bettinger, R. C. Carlisle, M. L. Read, M. Ogris, L. W. Seymour, *Nucleic Acids Res.* **2001**, *29*, 3882–91.
- [27] M. L. Read, S. Singh, Z. Ahmed, M. Stevenson, S. S. Briggs, D. Oupicky, L. B. Barrett, R. Spice, M. Kendall, M. Berry, et al., *Nucleic Acids Res.* **2005**, *33*, 1–16.
- [28] X. Su, J. Fricke, D. G. Kavanagh, D. J. Irvine, *Mol. Pharm.* **2011**, *8*, 774–787.
- [29] S. Üzgün, G. Nica, C. Pfeifer, M. Bosinco, K. Michaelis, J.-F. Lutz, M. Schneider, J. Rosenecker, C. Rudolph, *Pharm. Res.* **2011**, *28*, 2223–2232.
- [30] C. Cheng, A. J. Convertine, P. S. Stayton, J. D. Bryers, *Biomaterials* **2012**, *33*, 6868–6876.
- [31] H. Uchida, K. Itaka, T. Nomoto, T. Ishii, T. Suma, M. Ikegami, K. Miyata, M. Oba, N. Nishiyama, K. Kataoka, *J. Am. Chem. Soc.* **2014**, *136*, 12396–12405.
- [32] R. W. Malone, P. L. Felgner, I. M. Verma, *Proc. Natl. Acad. Sci. U. S. A.* **1989**, *86*, 6077–81.
- [33] F. T. Zohra, E. H. Chowdhury, S. Tada, T. Hoshiba, T. Akaike, *Biochem. Biophys. Res. Commun.* **2007**, *358*, 373–378.
- [34] D. Lu, R. Benjamin, M. Kim, R. M. Conry, D. T. Curiel, *Cancer Gene Ther.* **1994**,

- 1, 245–52.
- [35] P. Harvie, F. M. P. Wong, M. B. Bally, *J. Pharm. Sci.* **2000**, *89*, 652–663.
- [36] Y. Bao, Y. Jin, P. Chivukula, J. Zhang, Y. Liu, J. Liu, J.-P. Clamme, R. I. Mahato, D. Ng, W. Ying, et al., *Pharm. Res.* **2013**, *30*, 342–351.
- [37] J. Heyes, K. Hall, V. Tailor, R. Lenz, I. MacLachlan, *J. Control. Release* **2006**, *112*, 280–290.
- [38] V. P. Torchilin, *Nat. Rev. Drug Discov.* **2005**, *4*, 145–160.
- [39] H. Hatakeyama, H. Akita, K. Kogure, M. Oishi, Y. Nagasaki, Y. Kihira, M. Ueno, H. Kobayashi, H. Kikuchi, H. Harashima, *Gene Ther.* **2007**, *14*, 68–77.
- [40] L. Y. Song, Q. F. Ahkong, Q. Rong, Z. Wang, S. Ansell, M. J. Hope, B. Mui, *Biochim. Biophys. Acta - Biomembr.* **2002**, *1558*, 1–13.
- [41] K. K. L. Phua, S. K. Nair, K. W. Leong, *Nanoscale* **2014**, *6*, 7715–29.
- [42] P. Midoux, C. Pichon, *Expert Rev. Vaccines* **2015**, *14*, 221–234.
- [43] A. Akinc, A. Zumbuehl, M. Goldberg, E. S. Leshchiner, V. Busini, N. Hossain, S. a Bacallado, D. N. Nguyen, J. Fuller, R. Alvarez, et al., *Nat. Biotechnol.* **2008**, *26*, 561–9.
- [44] K. T. Love, K. P. Mahon, G. Christopher, K. A. Whitehead, W. Querbes, J. Robert, J. Qin, W. Cantley, L. L. Qin, M. Frank-Kamenetsky, et al., *Proc. Natl. Acad. Sci.* **2010**, *107*, 9915–9915.
- [45] S. C. Semple, A. Akinc, J. Chen, A. P. Sandhu, B. L. Mui, C. K. Cho, D. W. Y. Sah, D. Stebbing, E. J. Crosley, E. Yaworski, et al., *Nat. Biotechnol.* **2010**, *28*, 172–176.
- [46] K. a Whitehead, J. R. Dorkin, A. J. Vegas, P. H. Chang, O. Veiseh, J. Matthews, O. S. Fenton, Y. Zhang, K. T. Olejnik, V. Yesilyurt, et al., *Nat. Commun.* **2014**, *5*, 4277.
- [47] L. B. Jeffs, L. R. Palmer, E. G. Ambegia, C. Giesbrecht, S. Ewanick, I. MacLachlan, *Pharm. Res.* **2005**, *22*, 362–372.
- [48] R. Crawford, B. Dogdas, E. Keough, R. M. Haas, W. Wepukhulu, S. Krotzer, P. A. Burke, L. Sepp-Lorenzino, A. Bagchi, B. J. Howell, *Int. J. Pharm.* **2011**, *403*, 237–244.
- [49] I. V. Zhigaltsev, N. Maurer, K. Edwards, G. Karlsson, P. R. Cullis, *J. Control. Release* **2006**, *110*, 378–386.

- [50] A. K. K. Leung, I. M. Hafez, S. Baoukina, N. M. Belliveau, I. V. Zhigaltsev, E. Afshinmanesh, D. P. Tieleman, C. L. Hansen, M. J. Hope, P. R. Cullis, *J. Phys. Chem. C* **2012**, *116*, 18440–18450.
- [51] Y. Y. C. Tam, S. Chen, P. R. Cullis, *Pharmaceutics* **2013**, *5*, 498–507.
- [52] O. F. Khan, E. W. Zaia, H. Yin, R. L. Bogorad, J. M. Pelet, M. J. Webber, I. Zhuang, J. E. Dahlman, R. Langer, D. G. Anderson, *Angew. Chemie - Int. Ed.* **2014**, *53*, 14397–14401.
- [53] M. A. Monck, A. Mori, D. Lee, P. Tam, J. J. Wheeler, P. R. Cullis, P. Scherrer, *J. Drug Target.* **2000**, *7*, 439–452.
- [54] A. Judge, K. McClintock, J. R. Phelps, I. MacLachlan, *Mol. Ther.* **2006**, *13*, 328–337.
- [55] S. C. Semple, T. O. Harasym, K. a Clow, S. M. Ansell, S. K. Klimuk, M. J. Hope, *J. Pharmacol. Exp. Ther.* **2005**, *312*, 1020–1026.
- [56] A. Akinc, M. Goldberg, J. Qin, J. R. Dorkin, C. Gamba-Vitalo, M. Maier, K. N. Jayaprakash, M. Jayaraman, K. G. Rajeev, M. Manoharan, et al., *Mol. Ther.* **2009**, *17*, 872–9.
- [57] P. C. Rensen, R. M. Schiffelers, a J. Versluis, M. K. Bijsterbosch, M. E. Van Kuijk-Meuwissen, T. J. Van Berkel, *Mol. Pharmacol.* **1997**, *52*, 445–455.
- [58] X. Yan, F. Kuipers, L. M. Havekes, R. Havinga, B. Dontje, K. Poelstra, G. L. Scherphof, J. A. A. M. Kamps, *Biochem. Biophys. Res. Commun.* **2005**, *328*, 57–62.
- [59] A. Akinc, W. Querbes, S. De, J. Qin, M. Frank-Kamenetsky, K. N. Jayaprakash, M. Jayaraman, K. G. Rajeev, W. L. Cantley, J. R. Dorkin, et al., *Mol. Ther.* **2010**, *18*, 1357–1364.
- [60] Y. Y. C. Tam, S. Chen, J. Zaifman, Y. K. Tam, P. J. C. Lin, S. Ansell, M. Roberge, M. A. Ciufolini, P. R. Cullis, *Nanomedicine Nanotechnology, Biol. Med.* **2013**, *9*, 665–674.
- [61] S.-D. Li, L. Huang, *Mol. Pharm.* **2006**, *3*, 579–588.
- [62] S. Ahn, E. Seo, K. Kim, S. J. Lee, *Sci. Rep.* **2013**, *3*, 1997.
- [63] N. S. Templeton, D. D. Lasic, P. M. Frederik, H. H. Strey, D. D. Roberts, G. N. Pavlakis, *Nat. Biotechnol.* **1997**, *15*, 647–52.
- [64] L. J. Cruz, P. J. Tacke, R. Fokkink, C. G. Figdor, *Biomaterials* **2011**, *32*, 6791–

- 6803.
- [65] V. Kumar, J. Qin, Y. Jiang, R. G. Duncan, B. Brigham, S. Fishman, J. K. Nair, A. Akinc, S. a Barros, P. V Kasperkovitz, *Mol. Ther. Nucleic Acids* **2014**, *3*, e210.
- [66] A. M. I. Lam, P. R. Cullis, *Biochim. Biophys. Acta - Biomembr.* **2000**, *1463*, 279–290.
- [67] D. E. Draper, *Rna* **2004**, *10*, 335–343.
- [68] U. Kaukinen, S. Lyytikäinen, S. Mikkola, H. Lönnberg, *Nucleic Acids Res.* **2002**, *30*, 468–474.
- [69] Y. Zhang, L. Arrington, D. Boardman, J. Davis, Y. Xu, K. Difelice, S. Stirdivant, W. Wang, B. Budzik, J. Bawiec, et al., *J. Control. Release* **2014**, *174*, 7–14.
- [70] T. H. Tahirov, T.-H. Lu, Y.-C. Liaw, Y.-L. Chen, J.-Y. Lin, *J. Mol. Biol.* **1995**, *250*, 354–367.
- [71] Y. Endo, K. Tsurugi, *J. Biol. Chem.* **1987**, *262*, 8128–8130.
- [72] E. J. Wawrzynczak, U. Zangemeister-Wittke, R. Waibel, R. V Henry, G. D. Parnell, a J. Cumber, M. Jones, R. a Stahel, *Br. J. Cancer* **1992**, *66*, 361–366.
- [73] D. Gill, in *Bact. Toxins Cell Membr.*, Academic Press London, **1978**, pp. 291–322.
- [74] O. Harush-Frenkel, N. Debotton, S. Benita, Y. Altschuler, *Biochem. Biophys. Res. Commun.* **2007**, *353*, 26–32.
- [75] I. S. Zuhorn, U. Bakowsky, E. Polushkin, W. H. Visser, M. C. A. Stuart, J. B. F. N. Engberts, D. Hoekstra, *Mol. Ther.* **2005**, *11*, 801–810.
- [76] K. Maruyama, T. Yuda, A. Okamoto, S. Kojima, A. Suginaka, M. Iwatsuru, *Biochim. Biophys. Acta (BBA)/Lipids Lipid Metab.* **1992**, *1128*, 44–49.
- [77] D. Liu, L. Huang, *BBA - Biomembr.* **1989**, *981*, 254–260.
- [78] J. Gilleron, W. Querbes, A. Zeigerer, A. Borodovsky, G. Marsico, U. Schubert, K. Manygoats, S. Seifert, C. Andree, M. Stöter, et al., *Nat. Biotechnol.* **2013**, *31*, 638–46.
- [79] S. M. Moghimi, *Biomaterials* **2006**, *27*, 136–144.
- [80] R. Kanasty, J. R. Dorkin, A. Vegas, D. Anderson, *Nat. Mater.* **2013**, *12*, 967–977.
- [81] B. Li, X. Luo, B. Deng, J. Wang, D. W. McComb, Y. Shi, K. M. L. Gaensler, X. Tan, A. L. Dunn, B. A. Kerlin, et al., *Nano Lett.* **2015**, *15*, 8099–8107.

- [82] M. T. Abrams, M. L. Koser, J. Seitzer, S. C. Williams, M. a DiPietro, W. Wang, A. W. Shaw, X. Mao, V. Jadhav, J. P. Davide, et al., *Mol. Ther.* **2010**, *18*, 171–180.
- [83] C. Dohmen, T. Fröhlich, U. Lächelt, I. Röhl, H.-P. Vornlocher, P. Hadwiger, E. Wagner, *Mol. Ther. — Nucleic Acids* **2012**, *1*, 1–6.
- [84] C. Dohmen, D. Edinger, T. Fröhlich, L. Schreiner, U. Lächelt, C. Troiber, J. Rädler, P. Hadwiger, H. P. Vornlocher, E. Wagner, *ACS Nano* **2012**, *6*, 5198–5208.
- [85] D. He, K. Müller, A. K. Levacic, P. Kos, U. Lächelt, E. Wagner, *Bioconjug. Chem.* **2016**, DOI 10.1021/acs.bioconjchem.5b00649.

## 7 Appendix

### 7.1 Abbreviations

AA	A-chain of the toxin abrin
Apo	apolipoprotein
AL	anionic liposomes
ASGPR	asialoglycoprotein receptor
BMA	butyl methacrylate
cdNA	complementary deoxyribonucleic acid
CFTR	Cystic Fibrosis Transmembrane Regulator
cmRNA	chemically modified ribonucleic acid
cps	counts per second
DEAEMA	diethylaminoethyl methacrylate
DePC	1,2-di-O-hexadecyl- <i>sn</i> -glycero-3-phosphocholine
DLPC	1,2-dilauroyl- <i>sn</i> -glycero-3-phosphocholine
DLS	dynamic light scattering
DMAEMA	dimethylaminoethyl methacrylate
DMG-PEG2k/5k	1,2-Dimyristoyl- <i>sn</i> -glycerol-methoxy(polyethylene glycol), 2000/5000 Da
DMPC	1,2-dimyristoyl- <i>sn</i> -glycero-3-phosphocholine
DMPE-PEG2k	1,2-dimyristoyl- <i>sn</i> -glycero-3-phosphoethanolamine-N- methoxy(polyethylene glycol) (ammonium salt), 2000 Da
DNA	deoxyribonucleic acid
DOPS	1,2-dioleoyl- <i>sn</i> -glycero-3-phospho-L-serine (sodium salt)
DOPC	1,2-dioleoyl- <i>sn</i> -glycero-3-phosphocholine
DOPE	1,2-dioleoyl- <i>sn</i> -glycero-3-phosphoethanolamine
DOPE-PEG2k	1,2-dioleoyl- <i>sn</i> -glycero-3-phosphoethanolamine-N- methoxy(polyethylene glycol) (ammonium salt), 2000 Da
DOTAP	1,2-dioleoyl-3-trimethylammonium-propane (chloride salt)
DOTMA	N-[1-(2,3-dioleoyloxy)propyl]-N,N,N-trimethylammonium chloride

DPG-PEG2k/5k	1,2-Dipalmitoyl- <i>sn</i> -glycerol-methoxy(polyethylene glycol), 2000/5000 Da
DPPC	1,2-dipalmitoyl- <i>sn</i> -glycero-3-phosphocholine
DPPE	dipalmitoylphosphatidylethanolamine
DSG-PEG2k	1,2-distearoyl- <i>sn</i> -glycerol-methoxy(polyethylene glycol), 2000 Da
DSPC	1,2-distearoyl- <i>sn</i> -glycero-3-phosphocholine
DSPE-PEG2k	N-(Carbonyl-methoxy(polyethylene glycol))-1,2-distearoyl- <i>sn</i> -glycero-3-phosphoethanolamine, sodium salt, 2000 Da
EDTA	ethylenediaminetetraacetic acid
FA	folic acid
FBS	fetal bovine serum
FR	folate receptor
GalNAc	N-Acetylgalactosamine
GFP	green fluorescent protein
hBMP-2	human bone morphogenetic protein 2
hEpo	human erythropoietin
IFN	interferon
IL	interleukin
i.v.	intravenous
LNP	lipid nanoparticle
mEpo	mouse erythropoietin
mRNA	messenger ribonucleic acid
N/P (ratio)	nitrogen to phosphate (ratio)
PA-Es	polyplexes with even number repeats
PA-Os	polyplexes with odd number repeats
PBS	phosphate-based saline
PC	phosphocholine
PDI	polydispersity
pDNA	plasmid deoxyribonucleic acid
PEG	polyethylene glycol
PEGMA	poly(ethylene glycol) methyl ether methacrylate
PEI	polyethylenimine



PLL	poly(L-lysine)
P/S	penicillin/streptomycin
qPCR	real-time polymerase chain reaction
RLU	relative light units
rRNA	ribosomal ribonucleic acid
RT	room temperature
SEM	standard error of the mean
siRNA	small interfering ribonucleic acid
SPB	surfactant protein B
TNF	tumour necrosis factor
tRNA	transfer ribonucleic acid

## 7.2 List of lipid-based formulations

*Table 7.1. List of all formulations described in experimental part.*

Fig.	Formulation name	Lipidoid		Helper lipid #1 (Phospholipid)		Helper lipid #2 (Cholesterol)		PEG-lipid		N/P ratio
		Type	Molar ratio	Type	Molar ratio	Type	Molar ratio	Type	Molar ratio	
3.1 3.3 3.4 3.5 3.6 3.7	C12-(2-2)	C12-(2-2)	8	DOPE	5.29	Chol	4.41	DMPE-PEG2k	0.88	17
	C12-(3-3)	C12-(3-3)	8	DOPE	5.29	Chol	4.41	DMPE-PEG2k	0.88	17
	C12-(2-2-2)	C12-(2-2-2)	8	DOPE	5.29	Chol	4.41	DMPE-PEG2k	0.88	17
	C12-(3-3-3)	C12-(3-3-3)	8	DOPE	5.29	Chol	4.41	DMPE-PEG2k	0.88	17
	C12-(2-3-2)	C12-(2-3-2)	8	DOPE	5.29	Chol	4.41	DMPE-PEG2k	0.88	17
3.2	C12-(2-3-2)	C12-(2-3-2)	8	DOPE	5.29	Chol	4.41	DMPE-PEG2k	0.88	17
3.8	C8-G1	C8-G1	8	DPPC	5.29	Chol	4.41	DMG-PEG2k	0.88	10
	C12-G1	C12-G1	8	DPPC	5.29	Chol	4.41	DMG-PEG2k	0.88	10
	C16-G1	C16-G1	8	DPPC	5.29	Chol	4.41	DMG-PEG2k	0.88	10
	C8-G2	C8-G2	8	DPPC	5.29	Chol	4.41	DMG-PEG2k	0.88	10

	C12-G2	C12-G2	8	DPPC	5.29	Chol	4.41	DMG-PEG2k	0.88	10	
	C16-G2	C16-G2	8	DPPC	5.29	Chol	4.41	DMG-PEG2k	0.88	10	
3.9	Cx-(2-3-2)	C5-(2-3-2)	8	DOPE	5.29	Chol	4.41	DMG-PEG2k	0.88	8	
		C6-(2-3-2)	8	DOPE	5.29	Chol	4.41	DMG-PEG2k	0.88	8	
		C8-(2-3-2)	8	DOPE	5.29	Chol	4.41	DMG-PEG2k	0.88	8	
		C10-(2-3-2)	8	DOPE	5.29	Chol	4.41	DMG-PEG2k	0.88	8	
		C12-(2-3-2)	8	DOPE	5.29	Chol	4.41	DMG-PEG2k	0.88	8	
		C14-(2-3-2)	8	DOPE	5.29	Chol	4.41	DMG-PEG2k	0.88	8	
3.10	Cx-(2-3-2)	C16-(2-3-2)	8	DOPE	5.29	Chol	4.41	DMG-PEG2k	0.88	8	
		C8-(2-3-2)	8	DOPE	5.29	Chol	4.41	DMG-PEG2k	0.88	8	
		C10-(2-3-2)	8	DOPE	5.29	Chol	4.41	DMG-PEG2k	0.88	8	
		C12-(2-3-2)	8	DOPE	5.29	Chol	4.41	DMG-PEG2k	0.88	17	
		C14-(2-3-2)	8	DOPE	5.29	Chol	4.41	DMG-PEG2k	0.88	17	
3.11	Cx-(2-3-2)	C16-(2-3-2)	8	DOPE	5.29	Chol	4.41	DMG-PEG2k	0.88	17	
		DOPE	C12-(2-3-2)	8	DOPE	5.29	Chol	4.41	DMPE-PEG2k	0.88	17
		DSPC	C12-(2-3-2)	8	DSPC	5.29	Chol	4.41	DMPE-PEG2k	0.88	17
3.12	Cx-(2-3-2)	Cholesterol	C12-(2-3-2)	8	Chol	5.29	Chol	4.41	DMG-PEG2k	0.88	7.5
		16:0	C12-(2-3-2)	8	DPPC	5.29	Chol	4.41	DMG-PEG2k	0.88	8
		14:0	C12-(2-3-2)	8	DMPC	5.29	Chol	4.41	DMG-PEG2k	0.88	8
		12:0	C12-(2-3-2)	8	DLPC	5.29	Chol	4.41	DMG-PEG2k	0.88	8
		Diether 16:0	C12-(2-3-2)	8	DePC	5.29	Chol	4.41	DMG-PEG2k	0.88	8
3.13 1 <sup>st</sup> set	Standard formulation	18:1	C12-(2-3-2)	8	DOPC	5.29	Chol	4.41	DMG-PEG2k	0.88	8
			C12-(2-3-2)	8	DPPC	5.29	Chol	4.41	DMG-PEG2k	0.88	8

	No helper lipids	C12-(2-3-2)	8	-	-	-	-	DMG-PEG2k	0.88	8
	Cholesterol low	C12-(2-3-2)	8	-	-	Chol	2	DMG-PEG2k	0.88	8
	Cholesterol mid	C12-(2-3-2)	8	-	-	Chol	4.41	DMG-PEG2k	0.88	8
	Cholesterol high	C12-(2-3-2)	8	-	-	Chol	6	DMG-PEG2k	0.88	8
	DPPC low	C12-(2-3-2)	8	DPPC	3	-	-	DMG-PEG2k	0.88	8
	DPPC mid	C12-(2-3-2)	8	DPPC	5.29	-	-	DMG-PEG2k	0.88	8
	DPPC high	C12-(2-3-2)	8	DPPC	7	-	-	DMG-PEG2k	0.88	8
3.13 2 <sup>nd</sup> set	Cholesterol low	C12-(2-3-2)	8	DPPC	0.8	Chol	2	DMG-PEG2k	0.88	8
	Cholesterol mid	C12-(2-3-2)	8	DPPC	0.8	Chol	4.41	DMG-PEG2k	0.88	8
	Cholesterol high	C12-(2-3-2)	8	DPPC	0.8	Chol	6	DMG-PEG2k	0.88	8
	DPPC low	C12-(2-3-2)	8	DPPC	3	Chol	0.8	DMG-PEG2k	0.88	8
	DPPC mid	C12-(2-3-2)	8	DPPC	5.29	Chol	0.8	DMG-PEG2k	0.88	8
	DPPC high	C12-(2-3-2)	8	DPPC	7	Chol	0.8	DMG-PEG2k	0.88	8
3.13 3 <sup>rd</sup> set	Cholesterol low	C12-(2-3-2)	8	DPPC	0.8	Chol	2	DMG-PEG2k	0.24	8
	Cholesterol mid	C12-(2-3-2)	8	DPPC	0.8	Chol	4.41	DMG-PEG2k	0.24	8
	Cholesterol high	C12-(2-3-2)	8	DPPC	0.8	Chol	6	DMG-PEG2k	0.24	8
	DPPC low	C12-(2-3-2)	8	DPPC	3	Chol	0.8	DMG-PEG2k	0.24	8
	DPPC mid	C12-(2-3-2)	8	DPPC	5.29	Chol	0.8	DMG-PEG2k	0.24	8
	DPPC high	C12-(2-3-2)	8	DPPC	7	Chol	0.8	DMG-PEG2k	0.24	8
3.14	DMPE-PEG2k	C12-(2-3-2)	8	DSPC	5.29	Chol	4.41	DMPE-PEG2k	0.88	17
	DMG-PEG2k	C12-(2-3-2)	8	DSPC	5.29	Chol	4.41	DMPE-PEG2k	0.88	17
3.15	Cholesterol-PEG2k	C12-(2-3-2)	8	DOPE	5.29	Chol	4.41	Chol-PEG2k	0.88	17
	DMG-PEG2k	C12-(2-3-2)	8	DOPE	5.29	Chol	4.41	DMG-PEG2k	0.88	17

	DOPE-PEG2k	C12-(2-3-2)	8	DSPC	5.29	Chol	4.41	DOPE-PEG2k	0.88	17
	DMPE-PEG2k	C12-(2-3-2)	8	DSPC	5.29	Chol	4.41	DMPE-PEG2k	0.88	17
3.16	C14-PEG2k	C12-(2-3-2)	8	DOPE	5.29	Chol	4.41	DMG-PEG2k	0.88	17
	C16-PEG2k	C12-(2-3-2)	8	DOPE	5.29	Chol	4.41	DPG-PEG2k	0.88	17
	C18-PEG2k	C12-(2-3-2)	8	DOPE	5.29	Chol	4.41	DSG-PEG2k	0.88	17
3.17	DMG-PEG2k	C12-(2-3-2)	8	DPPC	5.29	Chol	4.41	DMG-PEG2k	0.88	8
	DPG-PEG2k	C12-(2-3-2)	8	DPPC	5.29	Chol	4.41	DPG-PEG2k	0.88	8
	DMG-PEG5k	C12-(2-3-2)	8	DPPC	5.29	Chol	4.41	DMG-PEG5k	0.88	8
	DPG-PEG5k	C12-(2-3-2)	8	DPPC	5.29	Chol	4.41	DPG-PEG5k	0.88	8
3.18	5%	C12-(2-3-2)	8	DPPC	5.29	Chol	4.41	DMG-PEG2k	0.88	8
	10%	C12-(2-3-2)	8	DPPC	5.29	Chol	4.41	DMG-PEG2k	1.97	8
	20%	C12-(2-3-2)	8	DPPC	5.29	Chol	4.41	DMG-PEG2k	4.42	8
3.19	5%	C12-(2-3-2)	8	DOPE	5.29	Chol	4.41	DMG-PEG2k	0.88	8
	20%	C12-(2-3-2)	8	DOPE	5.29	Chol	4.41	DMG-PEG2k	4.42	8
3.20	10% DMG-PEG2k	C12-(2-3-2)	8	DPPC	5.29	Chol	4.41	DMG-PEG2k	1.97	8
	20% DMG-PEG2k	C12-(2-3-2)	8	DPPC	5.29	Chol	4.41	DMG-PEG2k	4.42	8
	40% DMG-PEG2k	C12-(2-3-2)	8	DPPC	5.29	Chol	4.41	DMG-PEG2k	11.8	8
	10% DPG-PEG2k	C12-(2-3-2)	8	DPPC	5.29	Chol	4.41	DPG-PEG2k	1.97	8
	20% DPG-PEG2k	C12-(2-3-2)	8	DPPC	5.29	Chol	4.41	DPG-PEG2k	4.42	8
	40% DPG-PEG2k	C12-(2-3-2)	8	DPPC	5.29	Chol	4.41	DPG-PEG2k	11.8	8
3.22	Standard formulation	C12-(2-3-2)	8	DPPC	5.29	Chol	4.41	DMG-PEG2k	0.88	8
3.23	C14-PEG2k C10-(2-3-2)	C10-(2-3-2)	8	DOPE	5.29	Chol	4.41	DMG-PEG2k	0.88	8
	C14-PEG2k C12-(2-3-2)	C12-(2-3-2)	8	DOPE	5.29	Chol	4.41	DMG-PEG2k	0.88	8

	C14-PEG2k C14-(2-3-2)	C14-(2-3-2)	8	DOPE	5.29	Chol	4.41	DMG- PEG2k	0.88	8
	C14-PEG2k C16-(2-3-2)	C16-(2-3-2)	8	DOPE	5.29	Chol	4.41	DMG- PEG2k	0.88	8
	C16-PEG2k C10-(2-3-2)	C10-(2-3-2)	8	DOPE	5.29	Chol	4.41	DPG- PEG2k	0.88	8
	C16-PEG2k C12-(2-3-2)	C12-(2-3-2)	8	DOPE	5.29	Chol	4.41	DPG- PEG2k	0.88	8
	C16-PEG2k C14-(2-3-2)	C14-(2-3-2)	8	DOPE	5.29	Chol	4.41	DPG- PEG2k	0.88	8
	C16-PEG2k C16-(2-3-2)	C16-(2-3-2)	8	DOPE	5.29	Chol	4.41	DPG- PEG2k	0.88	8
	C18-PEG2k C10-(2-3-2)	C10-(2-3-2)	8	DOPE	5.29	Chol	4.41	DSG- PEG2k	0.88	8
	C18-PEG2k C12-(2-3-2)	C12-(2-3-2)	8	DOPE	5.29	Chol	4.41	DSG- PEG2k	0.88	8
	C18-PEG2k C14-(2-3-2)	C14-(2-3-2)	8	DOPE	5.29	Chol	4.41	DSG- PEG2k	0.88	8
	C18-PEG2k C16-(2-3-2)	C16-(2-3-2)	8	DOPE	5.29	Chol	4.41	DSG- PEG2k	0.88	8
3.24	C8-(2-3-2) C12 PC	C8-(2-3-2)	8	DLPC	5.29	Chol	4.41	DMG- PEG2k	0.88	8
	C8-(2-3-2) C14 PC	C8-(2-3-2)	8	DMPC	5.29	Chol	4.41	DMG- PEG2k	0.88	8
	C8-(2-3-2) C16 PC	C8-(2-3-2)	8	DPPC	5.29	Chol	4.41	DMG- PEG2k	0.88	8
	C10-(2-3-2) C12 PC	C10-(2-3-2)	8	DLPC	5.29	Chol	4.41	DMG- PEG2k	0.88	8
	C10-(2-3-2) C14 PC	C10-(2-3-2)	8	DMPC	5.29	Chol	4.41	DMG- PEG2k	0.88	8
	C10-(2-3-2) C16 PC	C10-(2-3-2)	8	DPPC	5.29	Chol	4.41	DMG- PEG2k	0.88	8
	C12-(2-3-2) C12 PC	C12-(2-3-2)	8	DLPC	5.29	Chol	4.41	DMG- PEG2k	0.88	8
	C12-(2-3-2) C14 PC	C12-(2-3-2)	8	DMPC	5.29	Chol	4.41	DMG- PEG2k	0.88	8
	C12-(2-3-2) C16 PC	C12-(2-3-2)	8	DPPC	5.29	Chol	4.41	DMG- PEG2k	0.88	8
	C16-(2-3-2) C12 PC	C16-(2-3-2)	8	DLPC	5.29	Chol	4.41	DMG- PEG2k	0.88	8
	C16-(2-3-2) C14 PC	C16-(2-3-2)	8	DMPC	5.29	Chol	4.41	DMG- PEG2k	0.88	8
	C16-(2-3-2) C14 PC	C16-(2-3-2)	8	DPPC	5.29	Chol	4.41	DMG- PEG2k	0.88	8
3.25	C16 PC C8-(2-3-2)	C8-(2-3-2)	8	DPPC	5.29	Chol	4.41	DMG- PEG2k	0.88	8

## 7 Appendix

	C16 PC C10-(2-3-2)	C10-(2-3-2)	8	DPPC	5.29	Chol	4.41	DMG- PEG2k	0.88	8
	C16 PC C12-(2-3-2)	C12-(2-3-2)	8	DPPC	5.29	Chol	4.41	DMG- PEG2k	0.88	8
	C16 PC C16-(2-3-2)	C16-(2-3-2)	8	DPPC	5.29	Chol	4.41	DMG- PEG2k	0.88	8
3.26	10-14-14	C10-(2-3-2)	8	DMPC	5.29	Chol	4.41	DMG- PEG2k	0.88	8
	10-16-14	C10-(2-3-2)	8	DPPC	5.29	Chol	4.41	DMG- PEG2k	0.88	8
	10-14-16	C10-(2-3-2)	8	DMPC	5.29	Chol	4.41	DPG- PEG2k	0.88	8
	10-16-16	C10-(2-3-2)	8	DPPC	5.29	Chol	4.41	DPG- PEG2k	0.88	8
	12-14-14	C12-(2-3-2)	8	DMPC	5.29	Chol	4.41	DMG- PEG2k	0.88	8
	12-16-14	C12-(2-3-2)	8	DPPC	5.29	Chol	4.41	DMG- PEG2k	0.88	8
	12-14-16	C12-(2-3-2)	8	DMPC	5.29	Chol	4.41	DPG- PEG2k	0.88	8
	12-16-16	C12-(2-3-2)	8	DPPC	5.29	Chol	4.41	DPG- PEG2k	0.88	8
3.27	N/P 5-17	C12-(2-3-2)	8	DOPE	5.29	Chol	4.41	DMG- PEG2k	0.88	5-17
3.28a	N/P 17 or 8	C12-(2-3-2)	8	DOPE	5.29	Chol	4.41	DMG- PEG2k	0.88	17 or 8
3.28b	N/P 8 or 4	C12-(2-3-2)	8	DPPC	5.29	Chol	4.41	DMG- PEG2k	0.88	8 or 4
3.29	N/P 2-8 + or - Mg <sup>2+</sup>	C12-(2-3-2)	8	DPPC	5.29	Chol	4.41	DMG- PEG2k	0.88	2-8
3.30	pH 2.0 - 7.0	C12-(2-3-2)	8	DPPC	5.29	Chol	4.41	DMG- PEG2k	0.88	8
3.33	Standard ratios	C12-(2-3-2)	8	DPPC	5.29	Chol	4.41	DMG- PEG2k	0.88	8
	Different ratios	C12-(2-3-2)	50	DPPC	10	Chol	38.5	DMG- PEG2k	1.5	8
	DPPC low	C12-(2-3-2)	8	DPPC	3	Chol	0.8	DMG- PEG2k	0.24	8
	DPPC mid	C12-(2-3-2)	8	DPPC	5.29	Chol	0.8	DMG- PEG2k	0.24	8
	DPPC high	C12-(2-3-2)	8	DPPC	7	Chol	0.8	DMG- PEG2k	0.24	8
3.34	DPPC	C12-(2-3-2)	8	DPPC	5.29	Chol	4.41	DMG- PEG2k	0.88	8
	16:0 TAP	C12-(2-3-2)	8	16:0 TAP	5.29	Chol	4.41	DMG- PEG2k	0.88	8

	16:0 DG	C12-(2-3-2)	8	16:0 DG	5.29	Chol	4.41	DMG-PEG2k	0.88	8
	16:0 EPC	C12-(2-3-2)	8	16:0 EPC	5.29	Chol	4.41	DMG-PEG2k	0.88	8
	16:0 DAP	C12-(2-3-2)	8	16:0 DAP	5.29	Chol	4.41	DMG-PEG2k	0.88	8
3.35	16:1(cis)PC	C12-(2-3-2)	8	16:1(cis)PC	5.29	Chol	4.41	DMG-PEG2k	0.88	8
	16:1(trans)PC	C12-(2-3-2)	8	16:1(trans)PC	5.29	Chol	4.41	DMG-PEG2k	0.88	8
	18:2(cis)PC	C12-(2-3-2)	8	18:2(cis)PC	5.29	Chol	4.41	DMG-PEG2k	0.88	8
	C12-(2-3-2)	C12-(2-3-2)	8	DPPC	5.29	Chol	4.41	DMG-PEG2k	0.88	8
	C12-200	C12-200	40	DOPE	30	Chol	25	DMG-PEG2k	5	15
	MC3	MC3	50	DSPC	10	Chol	38.5	DMG-PEG2k	1.5	10
3.36 3.38	DMG-PEG2k	C12-(2-3-2)	8	DPPC	5.29	Chol	4.41	DMG-PEG2k	0.88	8
	DSPE-PEG2k	C12-(2-3-2)	8	DPPC	5.29	Chol	4.41	DSPE-PEG2k	0.88	8
	DSPE-PEG2k-FA	C12-(2-3-2)	8	DPPC	5.29	Chol	4.41	DSPE-PEG2k-FA	0.88	8
3.37	FA-Tox(AA)	C12-(2-3-2)	8	DPPC	5.29	Chol	4.41	DSPE-PEG2k-FA	0.88	8

### 7.3 Publications

1. Jarzebińska, A., Pasewald, T., Lambrecht, J., Mykhaylyk, O., Kümmerling, L., Beck, P., Hasenpusch, G., Rudolph, C., Plank, C., and Dohmen, C. (2016). A Single Methylene Group in Oligoalkylamine-Based Cationic Polymers and Lipids Promotes Enhanced mRNA Delivery. *Angewandte Chemie - International Edition* 55, 9591-9595
2. Utzinger M., Jarzebinska A., Haag N., Schweizer M., Winter G., Dohmen C., Rudolph C., and Plank C. (pending). cmRNA/lipoplex encapsulation in PLGA microspheres enables transfection via calcium phosphate cement (CPC)/PLGA composites

### 8 Acknowledgements

Many people supported and helped me during last 3.5 years and therefore deserve my heartfelt thanks.

First of all, I would like to thank Prof. Dr. Christian Plank and PD Dr. Carsten Rudolph for giving me the possibility to work in an exceptional environment. A great scientific progress and industrial experience gained in a friendly atmosphere would not be possible without their encouragement and faith in me, which I am very grateful for.

Furthermore, I thank Prof. Dr. Ernst Wagner for his support and trust. It was an honour to be a member of his chair.

The person who contributed most to my work is definitely Dr. Christian Dohmen. I highly appreciate his patient supervision, sacrificed time, helpful advice, and constant support. All of that from a great person, whom it was a pleasure to meet on my way.

Dr. Ulrich Lächelt deserves my special acknowledgement for his help in pH titration experiments, which played an important role in my work.

For creating this unique atmosphere I would like to thank the whole Ethris team. Thanks to them it was a pleasure to work, I got inspired and motivated.

Especially, I am very thankful to my wonderful team: Dr. Philipp Beck, Laura Mac-carrone, Linda Kümmerling, and Dr. Martin Schweizer for successful scientific cooperation in many projects, enormous help, and making my everyday work easier and funnier.

During all this time, it was a pleasure to be a member of the Dream Team. Kristina Kragh, Simone Poll, and Dr. Mehrije Ferizi were always there to help and always able to cheer me up.

I also would like to thank Maximilian Utzinger, my companion, lab and office mate, with whom I had very productive discussions about science, with whom I shared my joy, who listened to my complains, and with whom I fooled around so many times.

A very special “thank you” I owe to my dear colleague and friend, Dr. Tamara Pasewald. I could count on her no matter what, no matter when.



## **8 Acknowledgements**

---

Szczególne podziękowania należą się mojej Rodzinie. Bez wsparcia moich Rodziców i Rodzeństwa nie byłoby mnie tutaj, gdzie jestem.